ENEA
ITALIAN NATIONAL AGENCY FOR NEW TECHNOLOGIES, ENERGY AND SUSTAINABLE ECONOMIC DEVELOPMENT

Introduction to X-ray based methods

X-ray scattering techniques - powerful tools for the microstructural characterization of (nano)materials

Leander Tapfer
ENEA, Brindisi Research Centre

Nanoinnovation
Rome, September 20, 2016

Characterization: role and importance

characterization

it is an integral part of all activities

we use analytical methods to assess structure

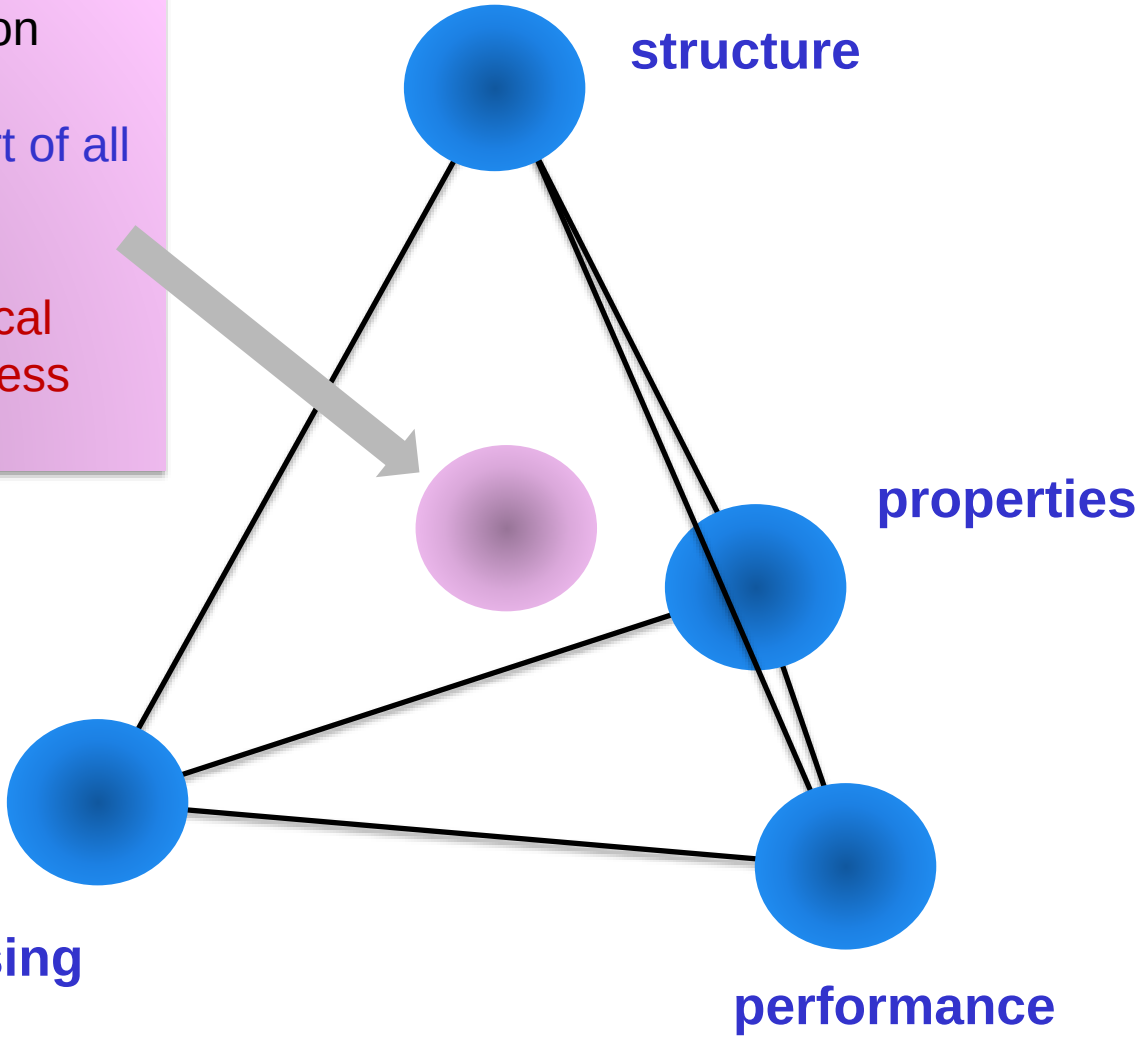

microstructural features and characterization techniques

The scale of «microstructural features», the magnification required to reveal the feature, and some common techniques available for studying the microstructure

Scale	Macrostructure	Mesostructure	Microstructure	Nanostructure
Typical magnification	x1	x 100 - 1 000	x 10 000	x 1 000 000
Common experimental techniques	Visual inspection	light optical microscopy	Scanning and transmission EM	**X-ray diffraction**
	X-Ray radiography	Scanning electron microscopy	Atomic force microscopy	Scanning tunneling microscopy
	Ultrasonic inspection	X-ray topography	X-ray tomography	High-resolution transmission EM
Characteristic microstructural features	Production defects	Grain and particle sizes	Dislocation substructure	Crystal and interface structure
	Porosity, cracks and inclusions	Phase morphology and anisotropy	Grain and phase boundaries	Point defects and point-defects clusters
			Precipitation phenomena	

X-ray interactions with matter

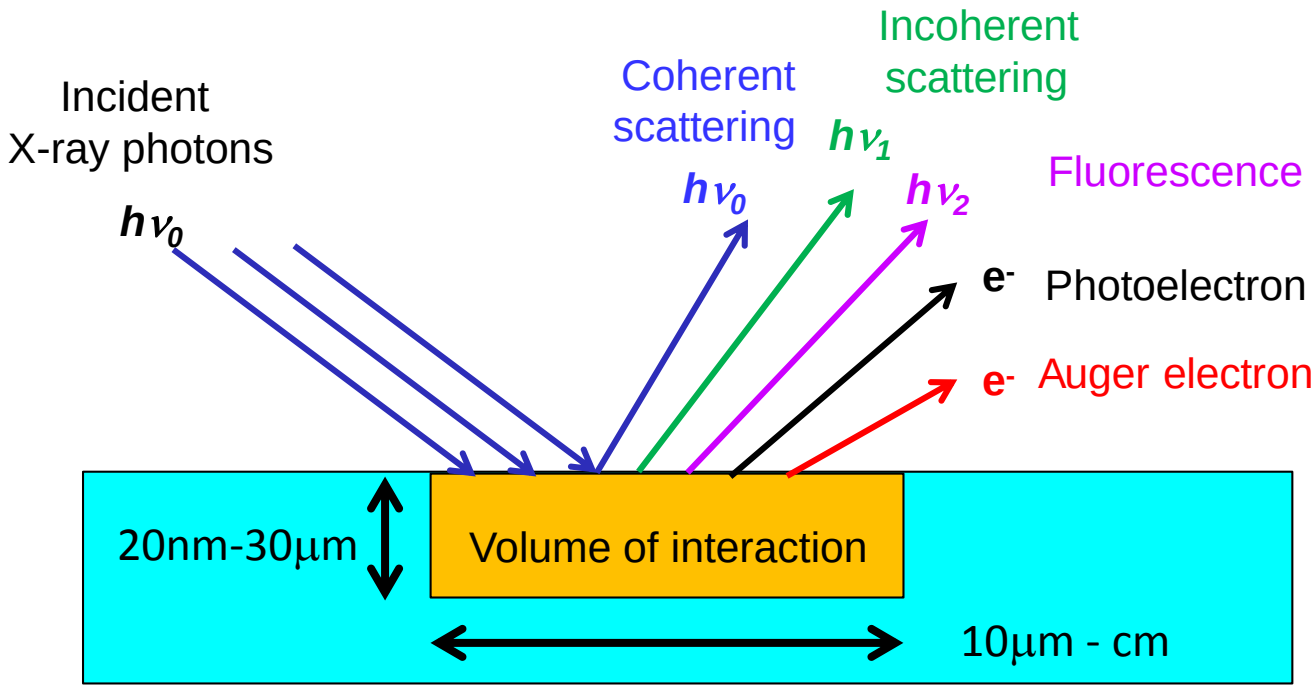

$h\nu$: photon
e^-: electron

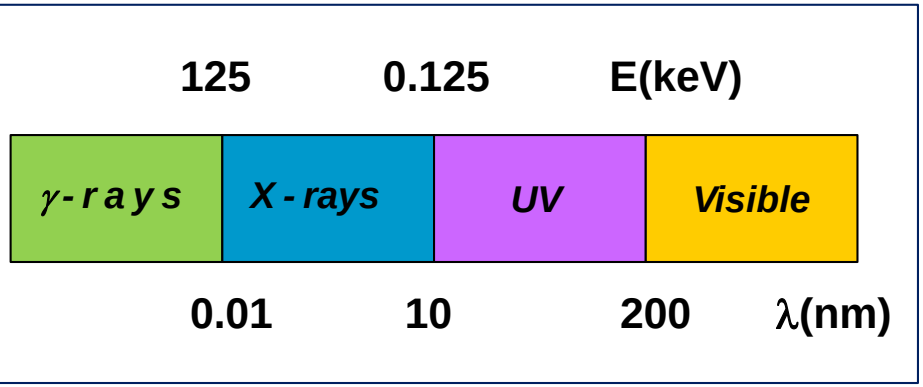

X-ray radiation mostly used in lab instruments: *Cu* radiation

- *Cu* Kα: λ= 0.15418 nm (8.05 keV, conventional resolution)
- *Cu* $K\alpha_1$: (λ= 0.15056 nm (high resolution)

X-ray scattering/diffraction methods (some….)

X-ray powder diffraction

Pair distribution function analysis (total X-ray scattering)

Glancing incidence diffraction

Texture analysis

Residual stress measurements

X-ray reflectivity

Diffuse scattering

Anomalous X-ray scattering

SAXS/WAXS

Grazing incidence small angle scattering/diffraction (non coplanar)

High-resolution X-ray diffraction

Reciprocal space mapping

X-ray fluorescence

Standing wave analysis

X-ray interferometry

X-ray topography

X-ray tomography

Outline for the present lecture

- Introduction
- Basic concepts (fundamentals)
- X-ray powder diffraction
- Glancing incidence diffraction
- X-ray reflectivity
- SAXS/WAXS
- High-resolution X-ray diffraction
- Reciprocal space mapping

Basic concepts - introduction

Coherence Length of the X-ray Radiation

Longitudinal (temporal) Coherence Length

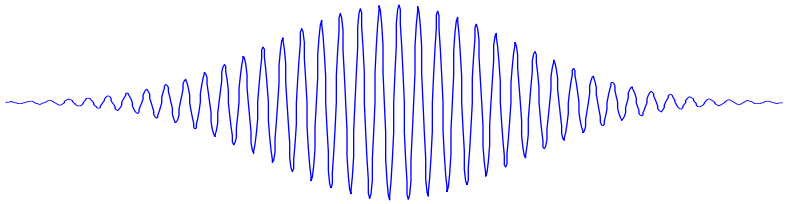

$$L_T = \frac{\lambda^2}{2\Delta\lambda}$$ …. from the Heisenberg's principle

Transverse (spatial) Coherence Length

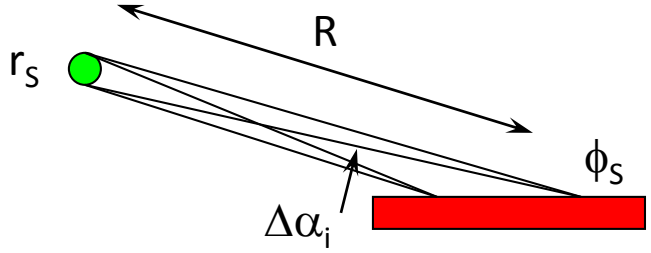

$$L_S = \lambda \frac{R}{2r_S} \approx \frac{\lambda}{2\phi_S} \approx \frac{\lambda}{\Delta\alpha_i}$$

Typical Values (for CuKa$_1$):

l = 1.54056 Å,

Dl = 3.615x10^{-4} Å

L_T > 1 mm

Lateral Coherence Length

$$L_S = \lambda \frac{R}{2r_S} \approx \frac{\lambda}{2\phi_S} \approx \frac{\lambda}{\Delta\alpha_i}$$

conventional X-ray tube

focus size 0.1×10 mm²

λ = 1.5418 Å

R = 30 cm

r_S = 0.1 mm

L_S ≈ 15 µm

synchrotron radiation

λ = 1.5418 Å

R = 40 m

r_S = 40 µm

L_S ≈ 80 µm (up to 1mm)

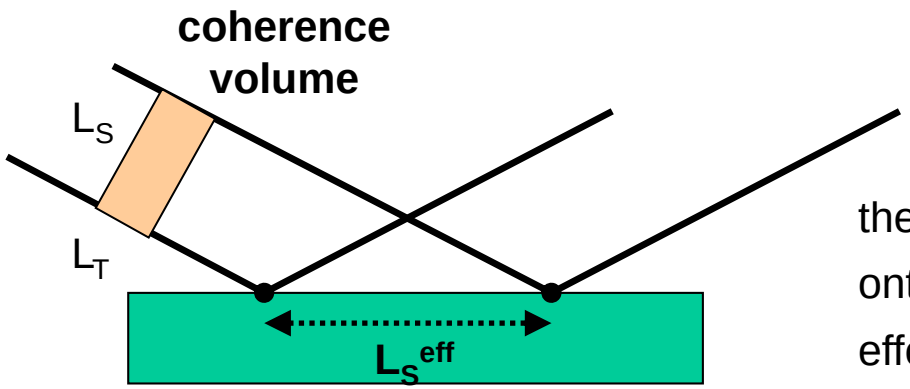

the projection of the coherence volume onto the sample surface defines the effective coherence length L_S^{eff}

Lateral Coherence Length at Glancing Incidence

definition of the parameters used to estimate the coherence lengths

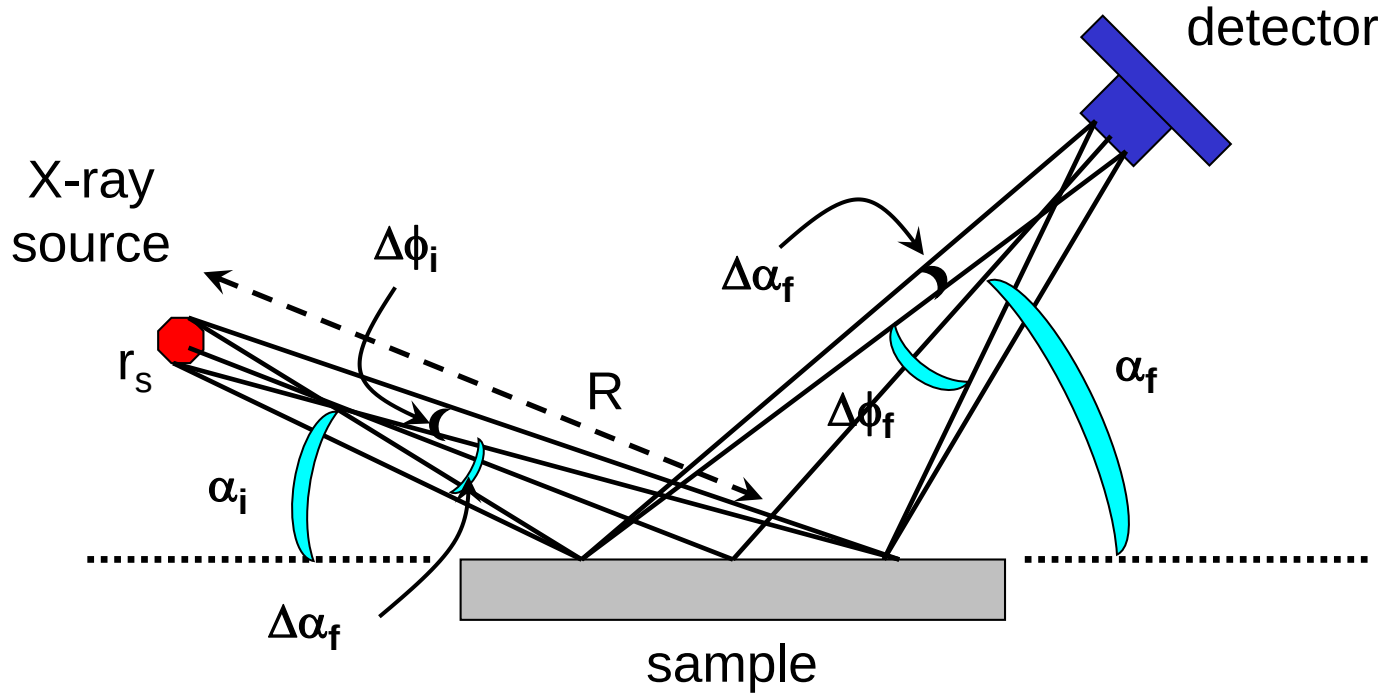

<u>conventional X-ray tube</u>

$L_S \geq 10$ µm

<u>synchrotron radiation</u>

$L_S \geq 1$ mm

Fundamentals of diffraction – reciprocal lattice

"Real" space

Reciprocal space

Set of planes

$\mathcal{F}$

Point

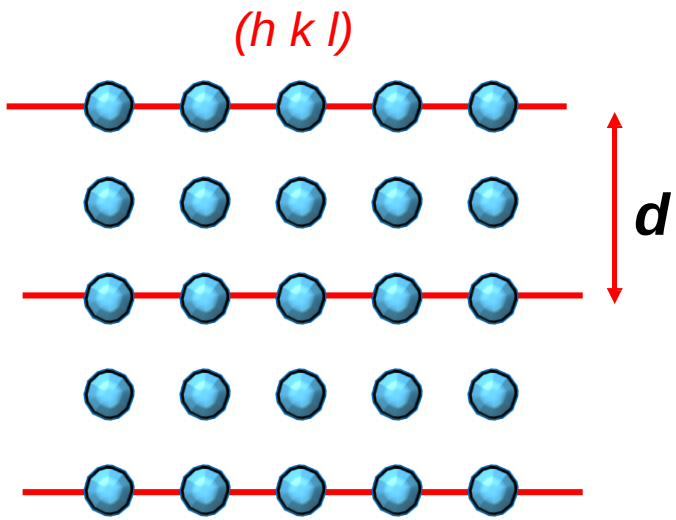

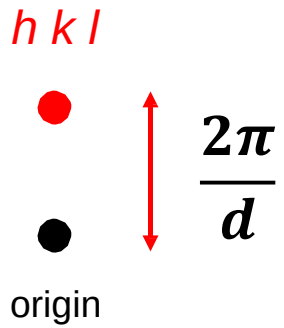

Fundamentals of diffraction – reciprocal lattice

"Real" space

Set of planes

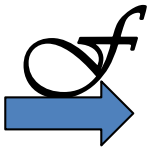

Reciprocal space

Point

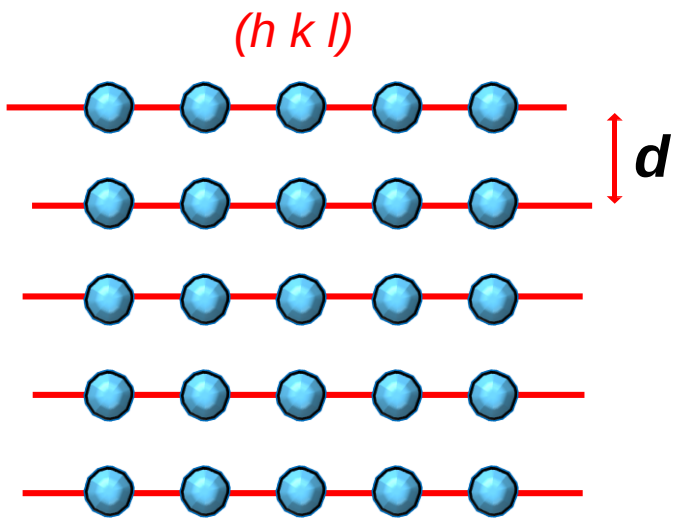

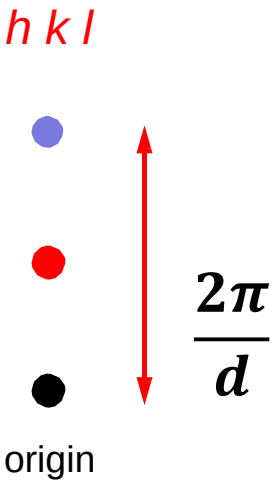

Fundamentals of diffraction – reciprocal lattice

"Real" space

Set of planes

$\mathcal{F}$

Reciprocal space

Point

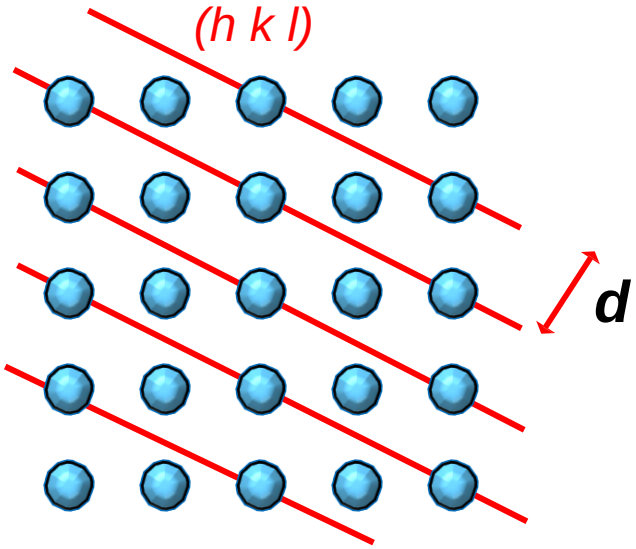

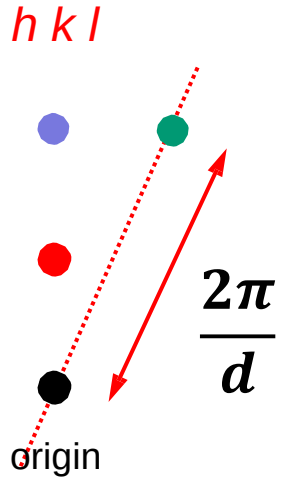

Fundamentals of diffraction - Bragg's law - Ewald's sphere

"Real" space

$\mathscr{F}$

Reciprocal space

Bragg's law

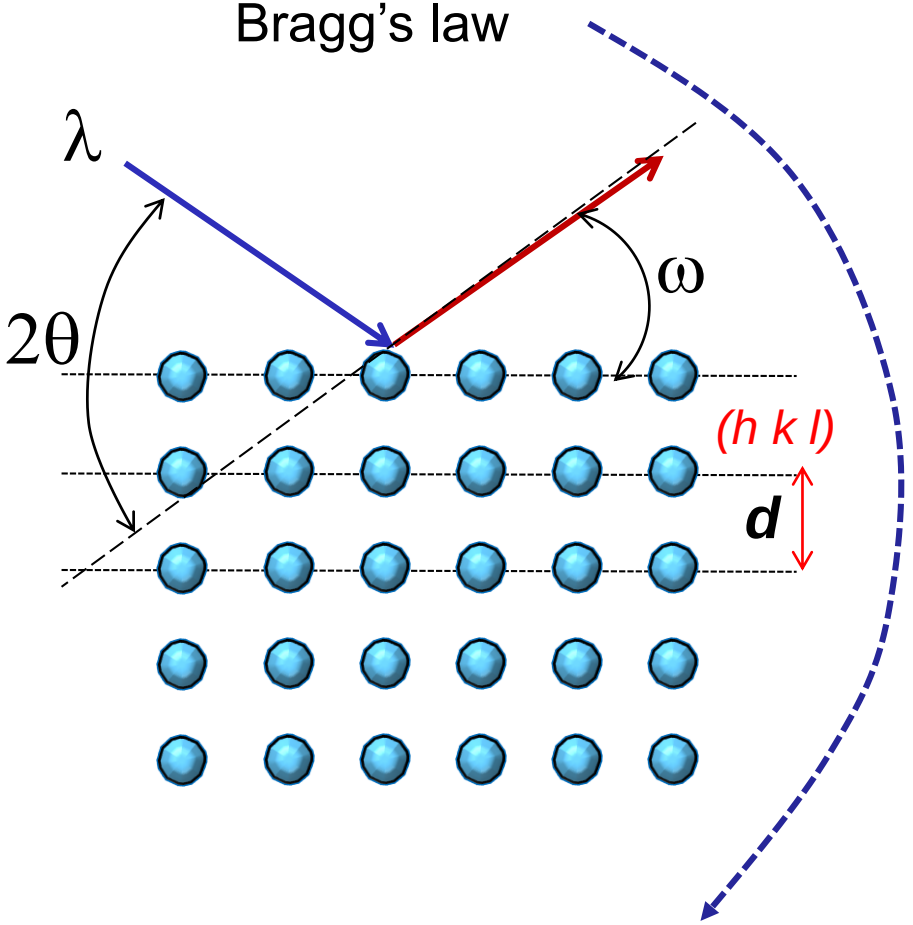

Ewald's sphere

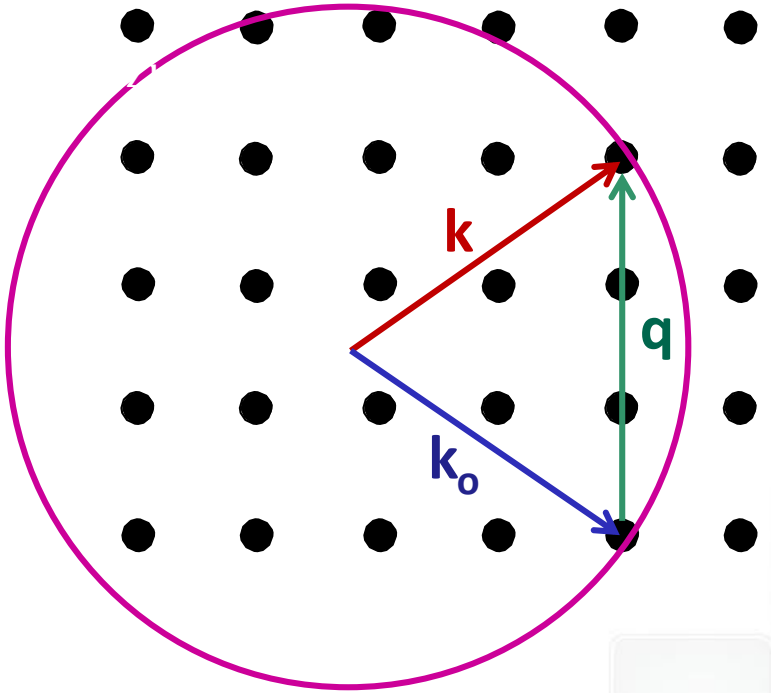

$$2 \cdot d \cdot \sin\theta = n \cdot \lambda$$

$$\mathbf{q} = \mathbf{k} - \mathbf{k_o} \qquad q = \frac{4 \cdot \pi}{\lambda} \cdot \sin\theta$$

Three-dimensional lattice (real space – reciprocal space)

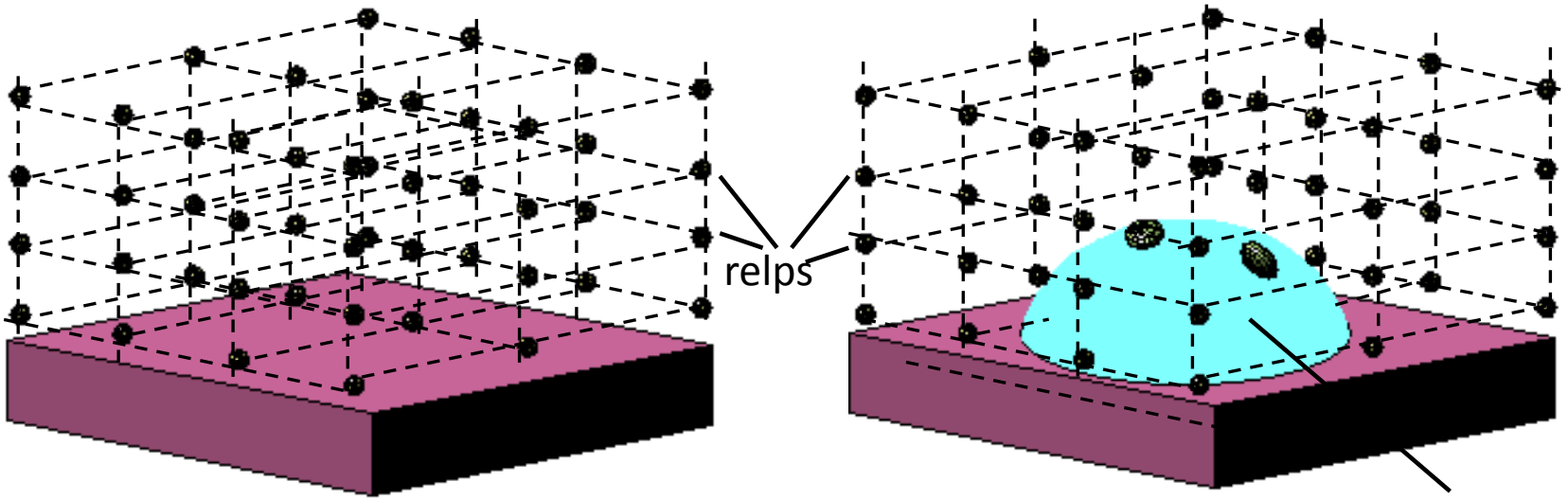

some reciprocal lattice points are contained entirely within the *Ewald* sphere and some are entirely outside. These will not be observed

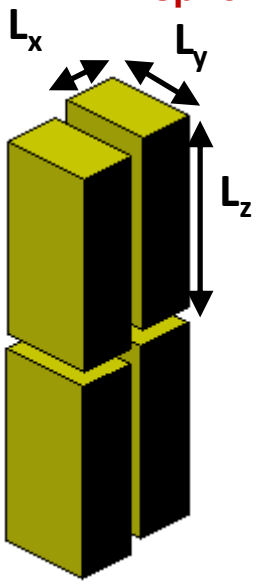

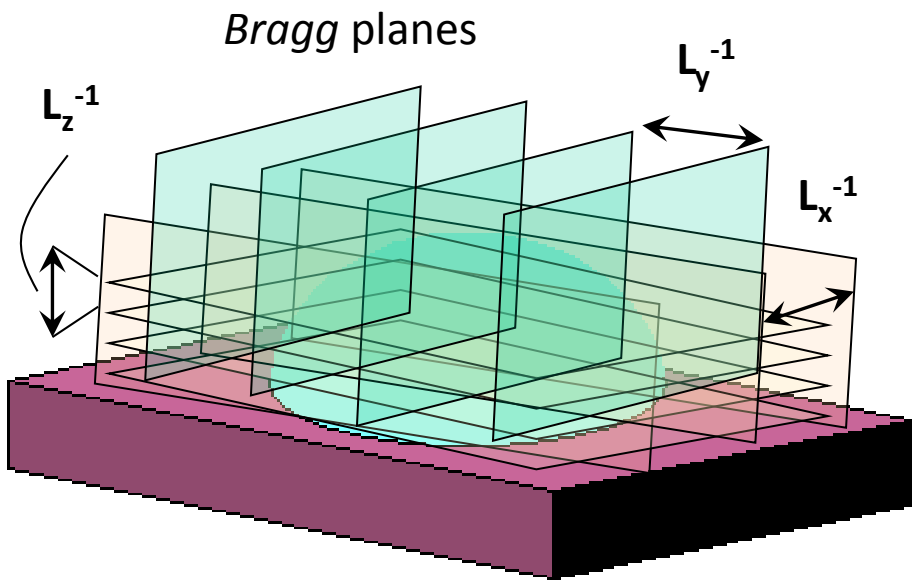

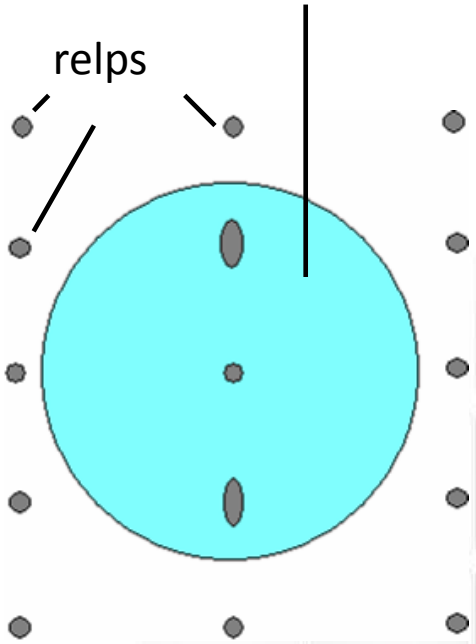

Fundamentals of diffraction – reciprocal lattice

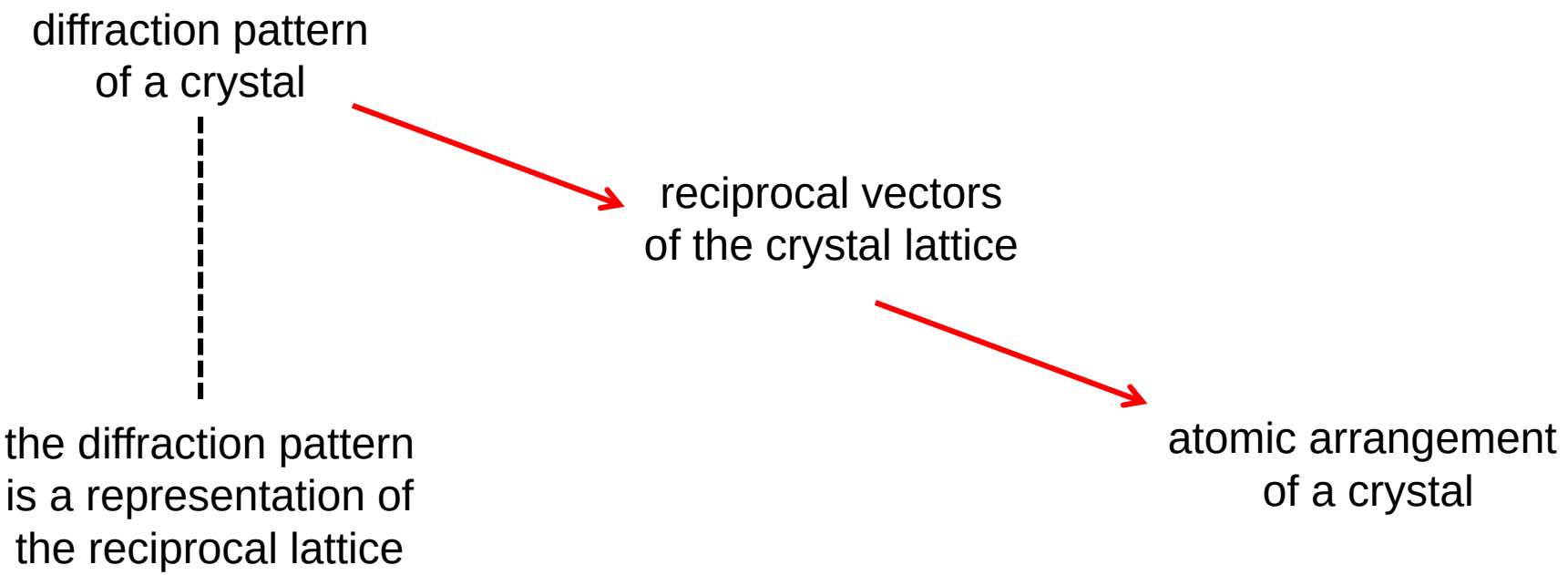

The diffraction pattern of a crystal can be used to determine the reciprocal vectors of the lattice, and by using this process, the atomic arrangement of a crystal can be determined

Diffraction on single and polycrystalline materials

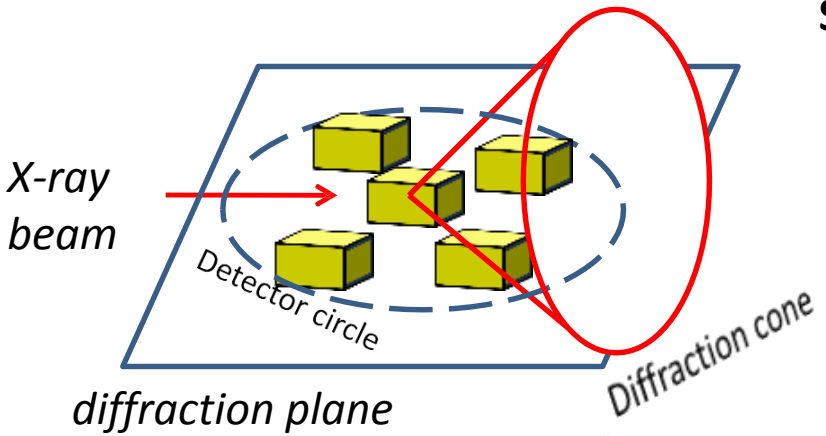

Single crystal

Point detector scan

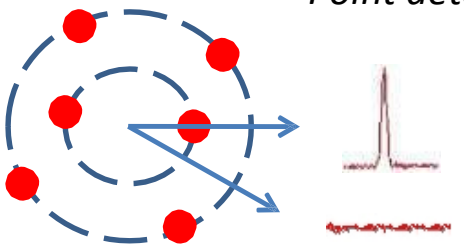

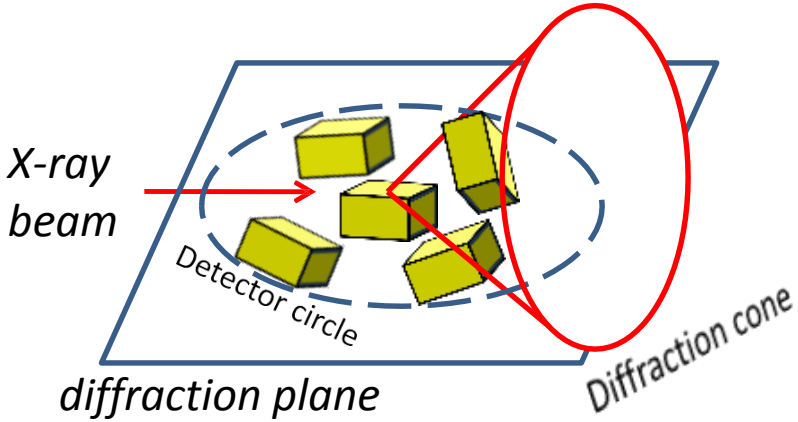

Poly crystal (random)

Point detector scan

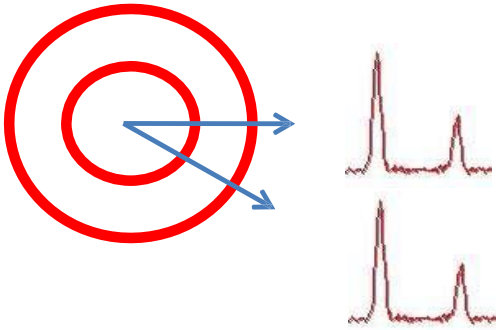

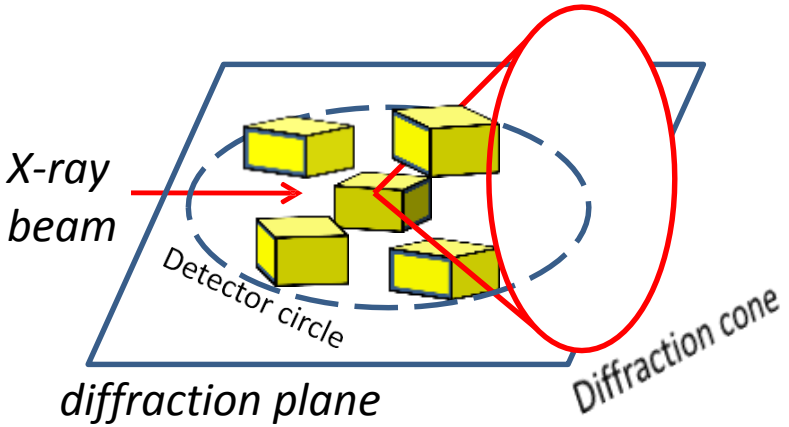

Poly crystal (texture)

Point detector scan

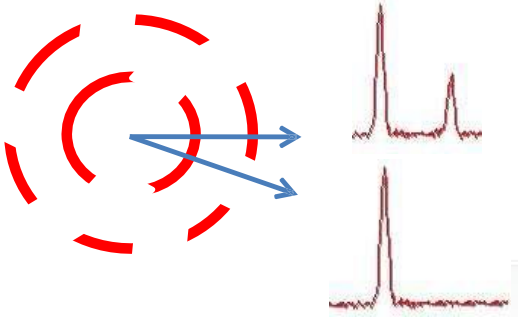

adapted from M. Sardela

Powder diffraction

Experimental configuration powder diffraction (Bragg-Brentano)

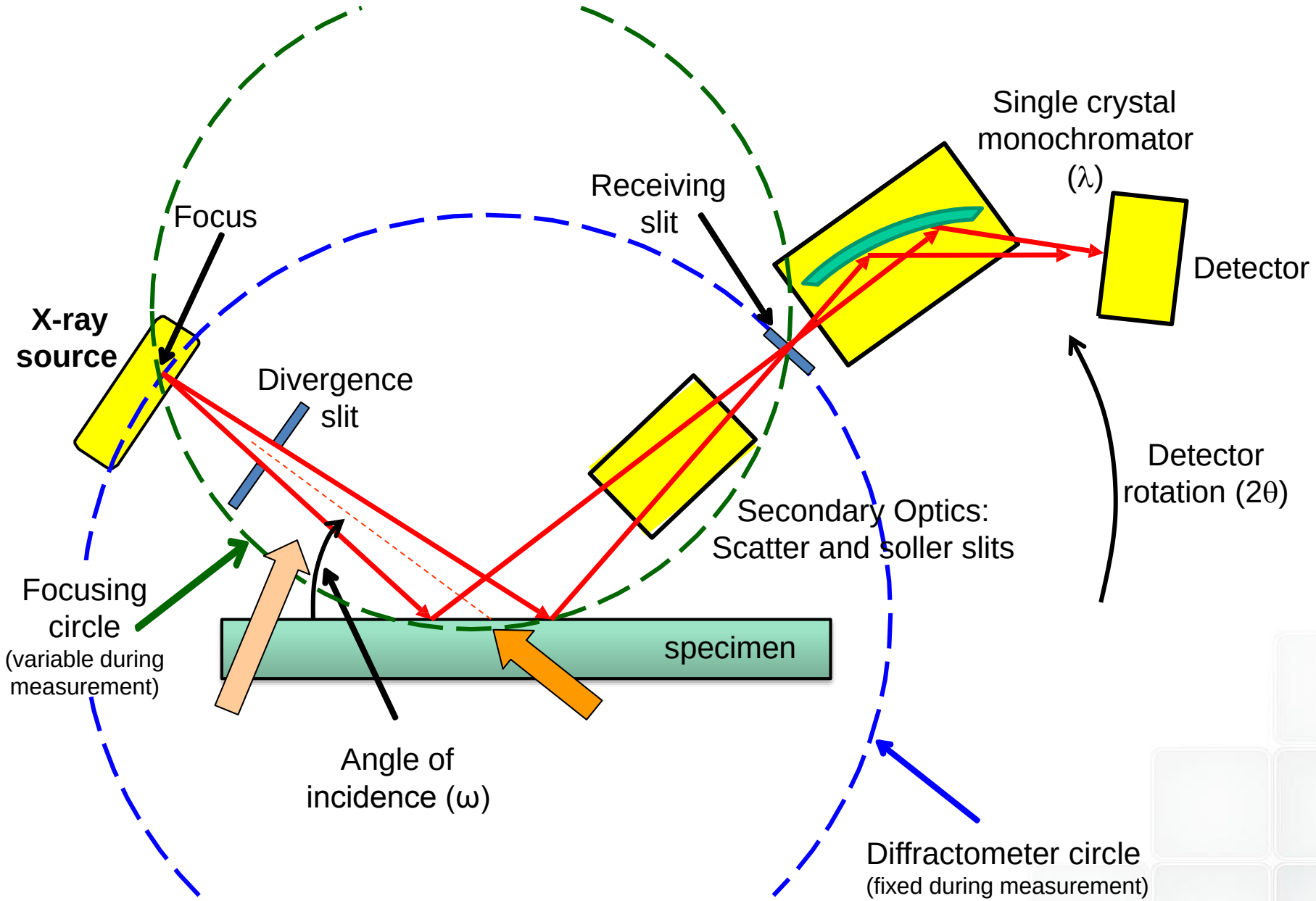

Powder diffraction for the characterization and analysis of:

microcrystalline and nanocrystalline materials

- Crystalline? Amorphous?
- What elements, compounds, phases are present?
- Structure? Lattice constants?
- Strain?
- Grain sizes? Grain orientations? Is there a mixture? What fraction (%)?
- Powders, bulk materials, thin films, nanoparticles, soft materials.

Which Information does a Powder Pattern offer?

- peak position ⇒ dimension of the elementary cell
- peak intensity ⇒ content of the elementary cell
- peak broadening ⇒ strain/crystallite size
- scaling factor amount ⇒ quantitative phase
- diffuse background ⇒ false order
- modulated background ⇒ close order

Powder pattern analysis

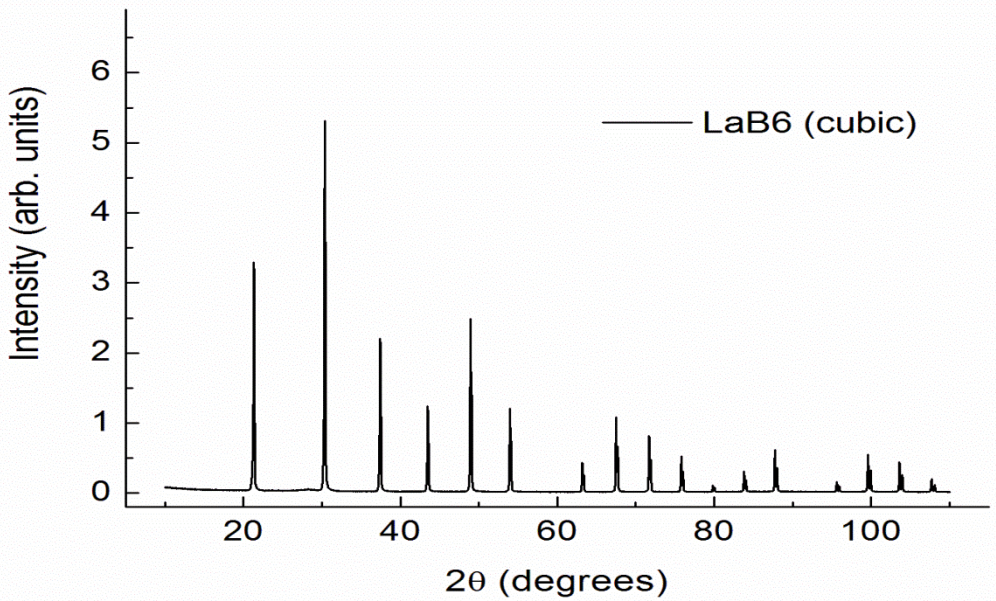

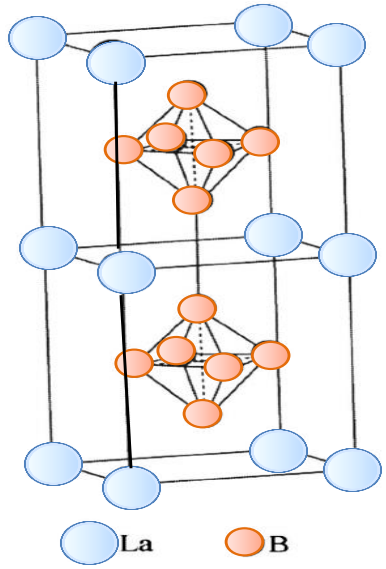

- The d-spacings of lattice planes depend on the size of the elementary cell and determine the position of the peaks.
- The intensity of each peak is caused by the crystallographic structure, the position of the atoms within the elementary cell and their thermal vibration.
- The line width and shape of the peaks may be derived from conditions of measuring and properties - like particle size - of the sample material.

Powder Pattern – Phase analysis – Powder Diffraction File (PDF)

Quantitative phase analysis through powder diffraction file (PDF) of the ICDD (International Centre for Diffraction data)

Bragg equation $2\theta_{hkl} \rightarrow d_{hkl}=\lambda/(2 \sin \theta_{hkl})$ $I_{hkl} \sim |F_{hkl}|^2$

34-0427 Wavelength= 1.5405981

LaB6

Boron Lanthanum

Rad.: CuKa1 λ: 1.540598 Filter: Mono d-sp: Diff.

Cut off: 22.1 Int.: Diffract. I/Icor.:

Ref: Natl. Bur. Stand. (U.S.) Monogr. 25, 20, 62 (1983)

Sys.: Cubic S.G.: Pm3m (221)

a: 4.15690(5) b: c: A: C:

α: β: γ: Z: 1 mp:

Ref: Ibid.

Dx: 4.711 Dm: SS/FOM: F_{24} = 179(.0056 , 24)

Color: Violet-black
The sample was obtained from Koch-Light Laboratories, Colnbrook Bucks, England, UK, and donated by Gobel, H., Munich, Germany. CAS #: 12008-21-8. σ(I_{obs})= ±0.05. The structure was determined by von Stackelburg and Neumann (1932). B6 Ca type. Fluorophlogopite, silver used as an internal stands. PSC: cP7. To replace 6-401. Mwt: 203.77. Volume[CD]: 71.83.

2θ	Int	h	k	l
21.354	54	1	0	0
30.387	100	1	1	0
37.445	41	1	1	1
43.517	22	2	0	0
48.969	46	2	1	0
53.995	24	2	1	1
63.218	8	2	2	0
67.564	23	3	0	0
71.757	16	3	1	0
75.849	10	3	1	1
79.869	2	2	2	2
83.849	6	3	2	0
87.793	13	3	2	1
95.665	2	4	0	0
99.640	8	4	1	0
103.656	7	4	1	1
107.755	3	3	3	1
111.940	4	4	2	0
116.250	9	4	2	1
120.725	3	3	3	2
130.416	3	4	2	2
135.794	3	5	0	0
141.773	10	5	1	0
148.670	6	5	1	1

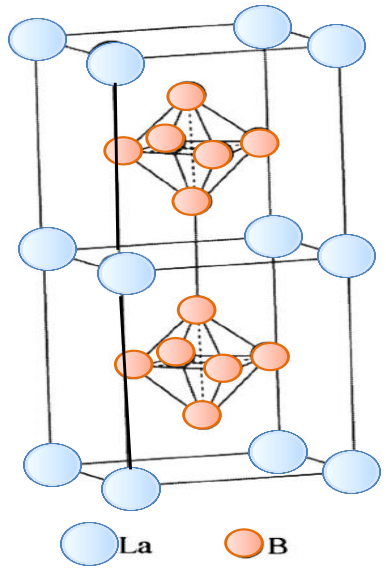

Principles of the Rietveld method

- the Rietveld method (Hugo M. Rietveld, 1967/1969) allows the optimization of a certain amount of model parameters (structure & instrument), to get a best fit between a measured and a calculated powder diagram.
- the parameter will be varied with a non-linear least-squares algorithm, that the difference will be minimized between the measured and the calculated pattern:

$$S = \sum_i w_i \left[y_i(obs) - y_i(calc) \right]^2 \quad \rightarrow \quad \min$$

Basis formula of the Rietveld method

Parameters in Rietveld method

$$y_i(calc) = \sum_k SF \cdot M_k \cdot P_k \cdot F_k^2 \cdot LP(2\Theta_k) \cdot \Phi_k(2\Theta_i - 2\Theta_k) + yb_i(obs)$$

- *SF* : Scaling factor
- M_k : Multiplicity of the reflections ***k***
- P_k : Value of a preferred orientation function for the reflections ***k***
- F_k^2 : Structure factor of the reflections ***k***
- *LP* : Value of the Lorentz-Polarizations function for the reflections ***k***
- Φ_k : Peak profile function for the reflections k on the position ***i***
- yb_i : Value of the background at the position ***i***
- *k* : Index over all reflexes with intensity on the position ***i***

Profile-Functions

- Gaussian

$$G = \frac{\sqrt{C_0}}{\Gamma_k \sqrt{\pi}} \exp\left[-\frac{C_0}{\Gamma_k^2} \left(2\theta_i - 2\theta_k\right)^2 \right]; \quad C_0 = 4 \ln 2$$

- Lorentzian (Cauchy)

$$L = \frac{2\sqrt{C_0}}{\pi \Gamma_k} \frac{1}{1 + \frac{C_0}{\Gamma_k^2} \left(2\theta_i - 2\theta_k\right)^2}; \quad C_0 = 4$$

- Pearson VII

$$P_{VII} = \frac{C_0}{\Gamma_k} \left[1 + \frac{4\left(\sqrt[m]{2} - 1\right)}{\Gamma_k^2} \left(2\theta_i - 2\theta_k\right)^2 \right]^{-m}; \quad C_0 = \frac{2\sqrt{m}\left(\sqrt[m]{2} - 1\right)^{\frac{1}{2}}}{\sqrt{\pi\left(m - 0.5\right)}}$$

- Pseudo-Voigt

$$pV = \eta L + \left(1 - \eta\right) G$$

- Definition of the linewidth

$$\Gamma_k^2 = U \tan^2 \theta_k + V \tan \theta_k + W$$

Background

- subtraction of the background, if the background (without sample) can be measured
- interpolation of the background intensity (with some problems if there are many lines in the diffraction pattern: in the case of more phases, low symmetry or large unit cell)
- Polynom Function (6 Parameters)
- a special function for amorphous components

$$y_{ib} = B_0 + B_1 Q + \sum_{m=1}^{n} B_{2m} \frac{\sin\left(B_{2m+1} Q\right)}{B_{2m+1} Q}$$

Hints and Tricks - how to get good experimental data

- **With a good adjusted diffractometer**
  - Bad adjustment causes a line-displacement and -broadening
  - Line-displacement can be corrected (correlated with the lattice parameters), the line-broadening not
- **With substances of fine grains**
  - Coarse grains are the source for „random“ Integral-Intensities
  - Coarse grains cause problems with the surface absorption
- **Sufficient measurement time**
  - The absolute error in the Intensity-measurement is proportional to $\sqrt{(N)}$ (Poisson-distribution)
  - The relative error is proportional to $1/\sqrt{(N)}$

Structure Refinement (Rietveld Method)

- The parameters, that define the crystal structure cannot be refined (lattice parameter, fractional coordinates, anisotropic temperature vibrations)
- Only the necessary parameter should be refined (the convergence is better for few parameters)
- The quality of powder data are rarely so good that the anisotropic temperature factors can be calculated
- The measured data should be registered in a possibly wide angular range (structural and instrumental parameters depend differently on the diffraction angle)

Microabsorption

- flat sample in reflection mode – microabsorption

Porous sample, the density is independent of the distance from the surface

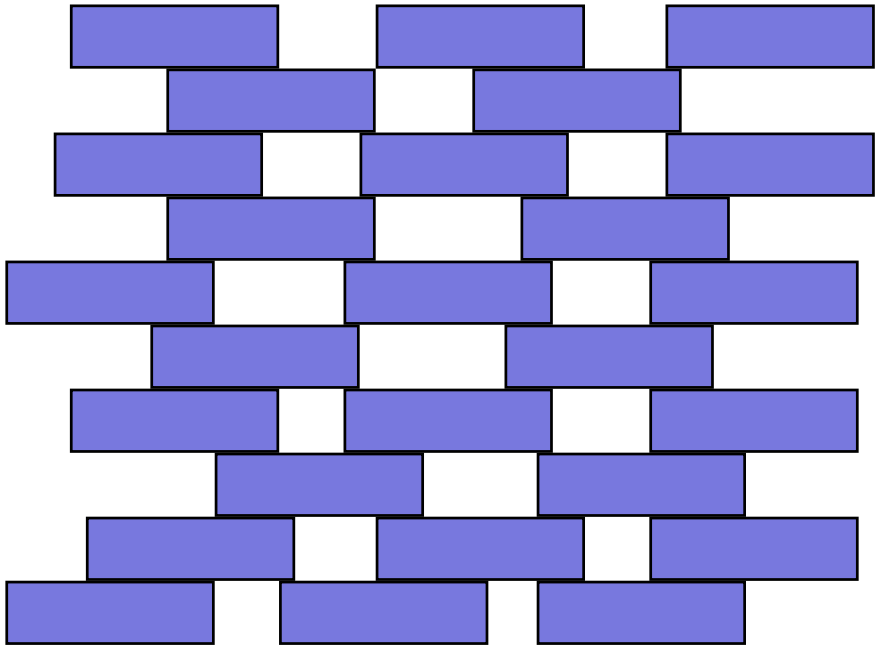

the porosity is described by a smaller linear attenuation coefficient

$$\mu \rightarrow \mu'$$

$$\mu' \leq \mu$$

however, the absorption-term does not depend on the diffraction angle

problems in the quantitative phase analysis

Surface porosity and/or density gradient

- flat sample in reflection mode – surface absorption

gradient of the density

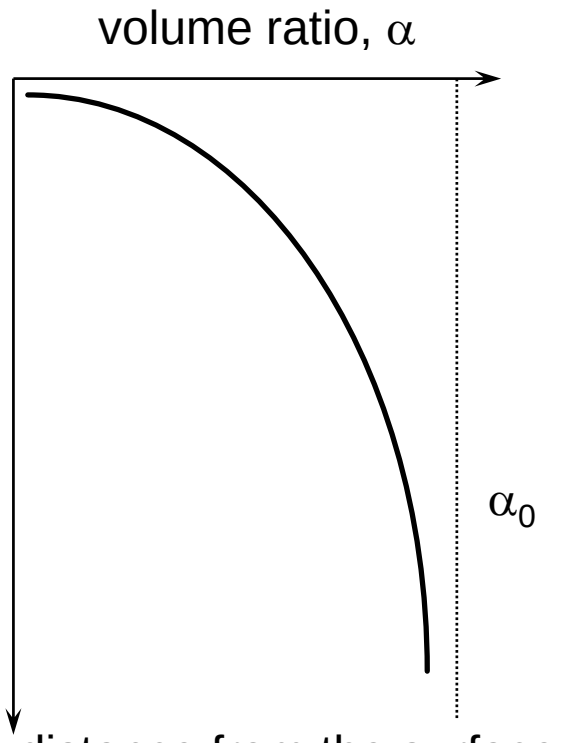

Porous sample, mainly on the surface

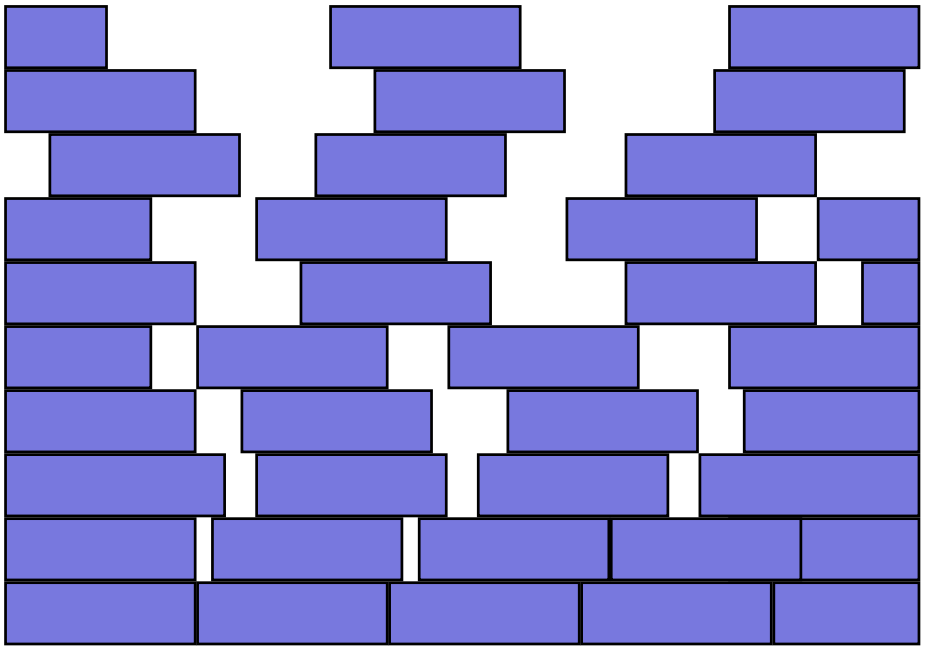

Crystallite size analysis

Scherrer's equation – gran size analysis

Scherrer's equation $$D = \frac{k \cdot \lambda}{\Delta\omega \cdot \cos\theta}$$

k shape factor (= 0.8 - 1.2)

$\Delta\omega$ X-ray wavelength *FWHM* (in radians)

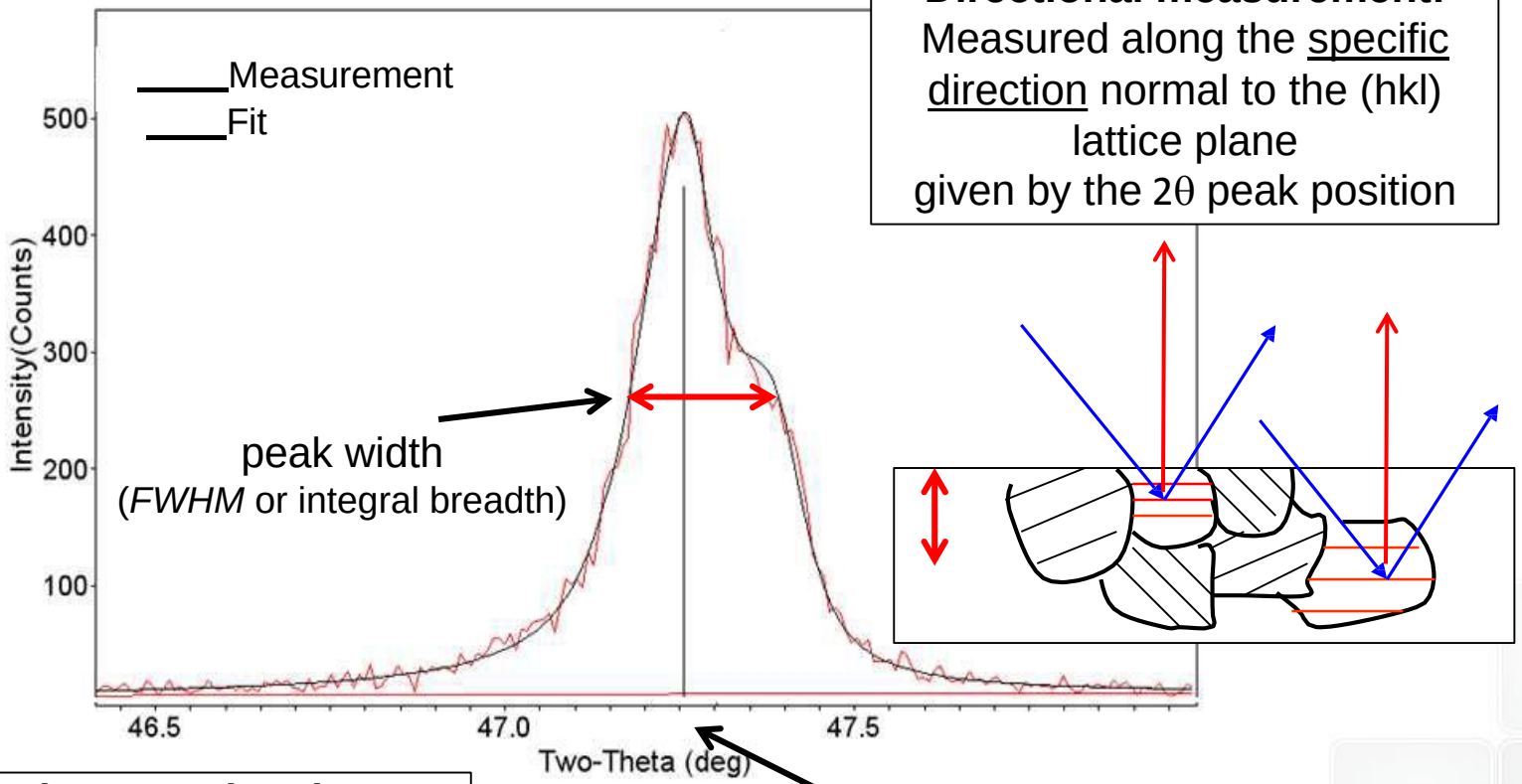

Directional measurement!
Measured along the specific direction normal to the (hkl) lattice plane
given by the 2θ peak position

Simplistic approximation!
Not accounting for peak broadening from strain and defects

Strain effects in diffraction lines

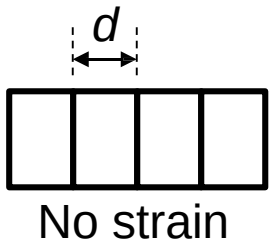

No strain

Macrostrain
uniform tensile or
compressive stress
(lattice expansion or
contraction)

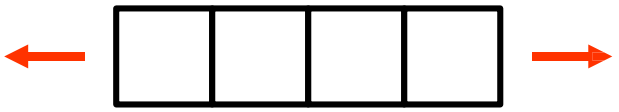

Uniform strain

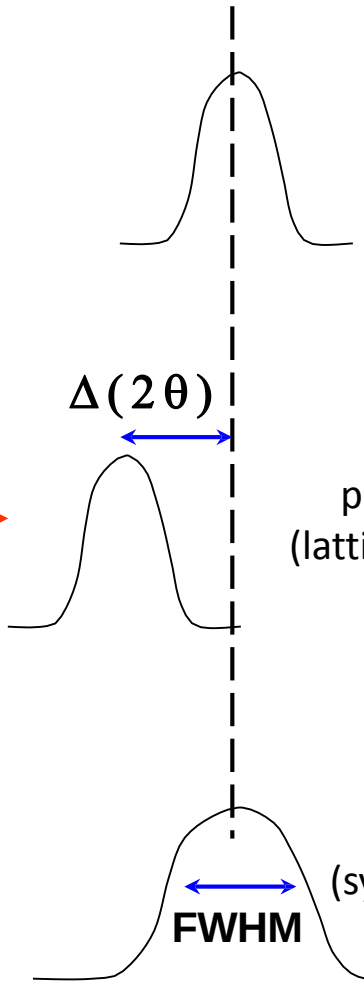

peak **position** shift
(lattice constant change)

peak **width** change
(symmetric broadening)

Micro-strain non-uniform
strain (both tensile and
compressive stresses)
(lattice distortion).
Dislocations, vacancies,
defects, thermal effects.

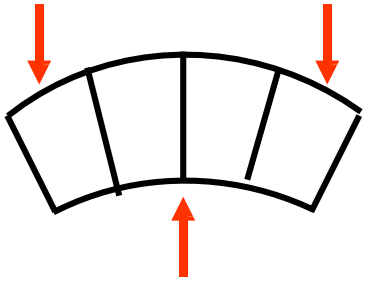

Nonuniform strain

Line Broadening

parameters of the diffraction lines:

Position (2θ), Maximum Intensity (I_{max}), Full-Width-at-Half-maximum (FWHM), Integral Intensity (I_{int}), Integral Breadth (β)

size effect

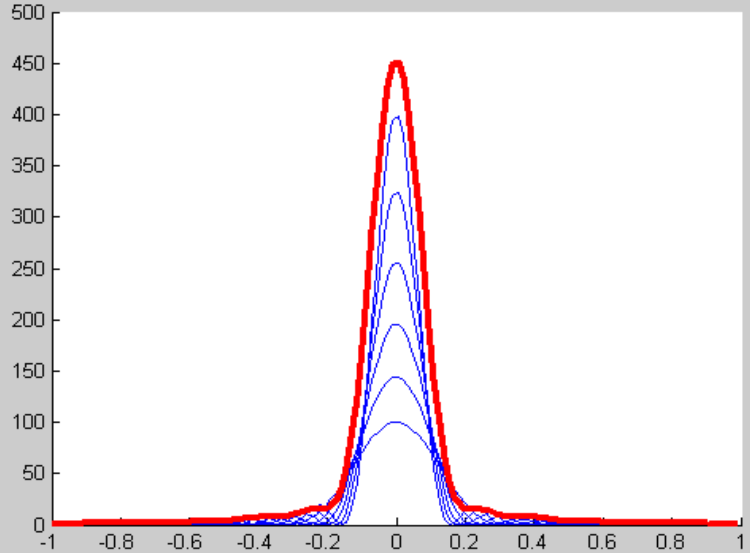

strain effect

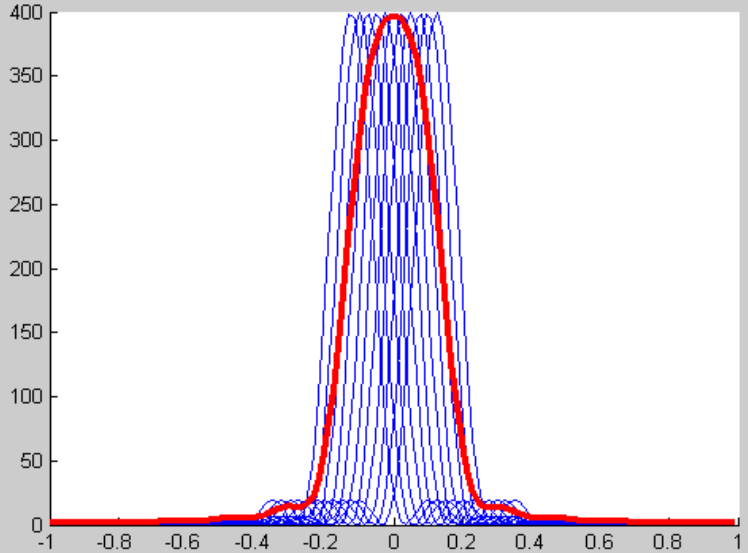

Cauchy $$y = \frac{I_0}{\frac{(x - x_0)^2}{w} + 1}$$

$$y = I_0 \exp\left(- \frac{(x - x_0)^2}{w} \right)$$ Gaussian

X-ray diffraction of nanowires (nanorods) on surfaces

Nanorods and cluster

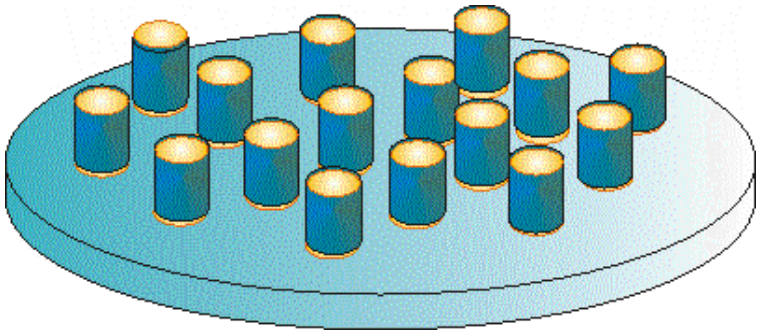

highly ordered – the growth axis of ZnO-wires are ⊥ to the surface

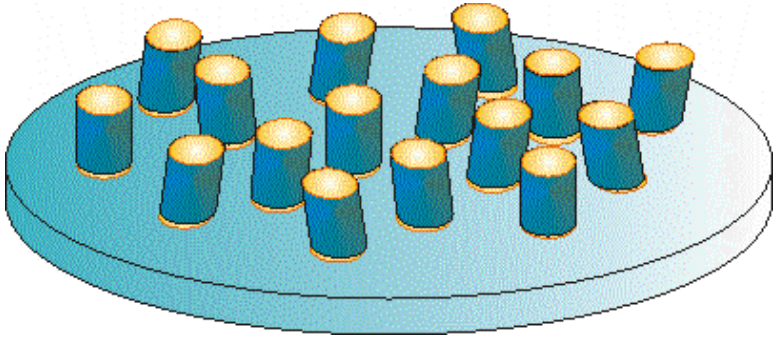

almost ordered – there is preferred growth axis direction of the ZnO-wires (“highly-textured”)

ZnO wires on Si substrate
(Au islands on top of the ZnO wires)

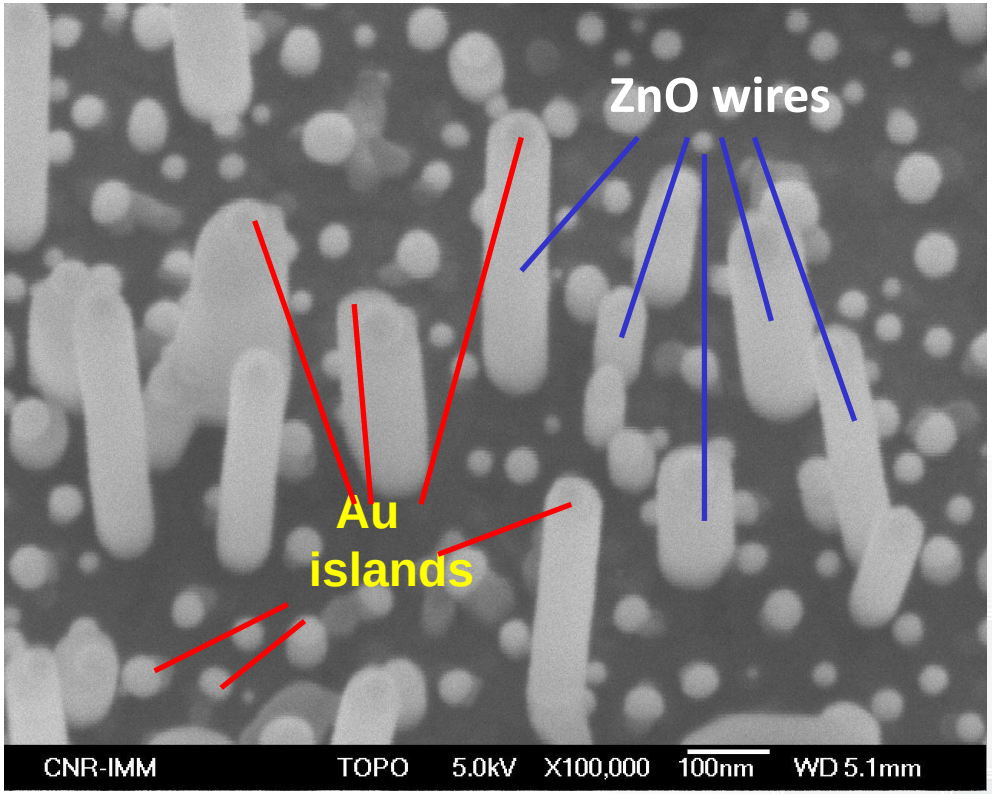

Peak profile analysis and size determination

$$FWHM = \left(\frac{\ln 2}{\pi}\right)^{1/2} \frac{\lambda}{D\cos\theta}$$

$$\frac{\beta\cos\theta}{\lambda} \propto \frac{1}{D}$$

(111)Au

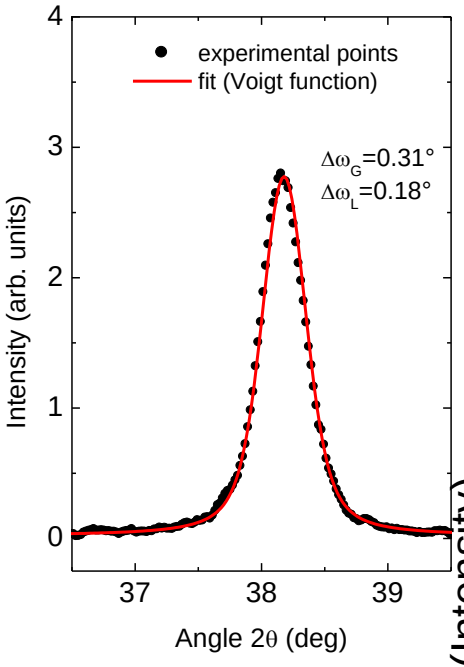

(002)ZnO

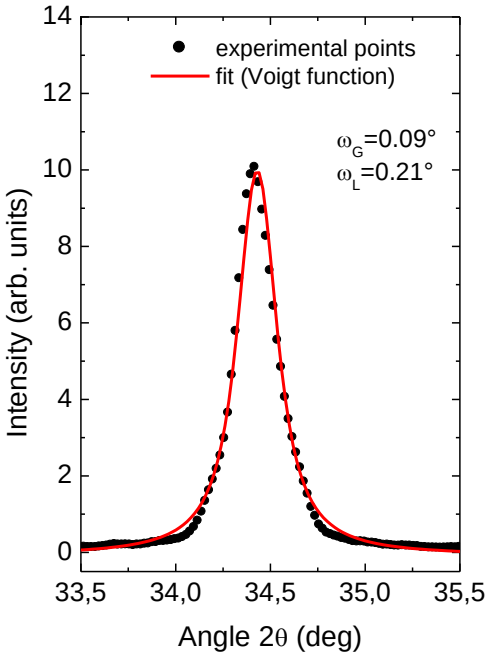

(111)Au and (002)ZnO peak fitting by Voigt function

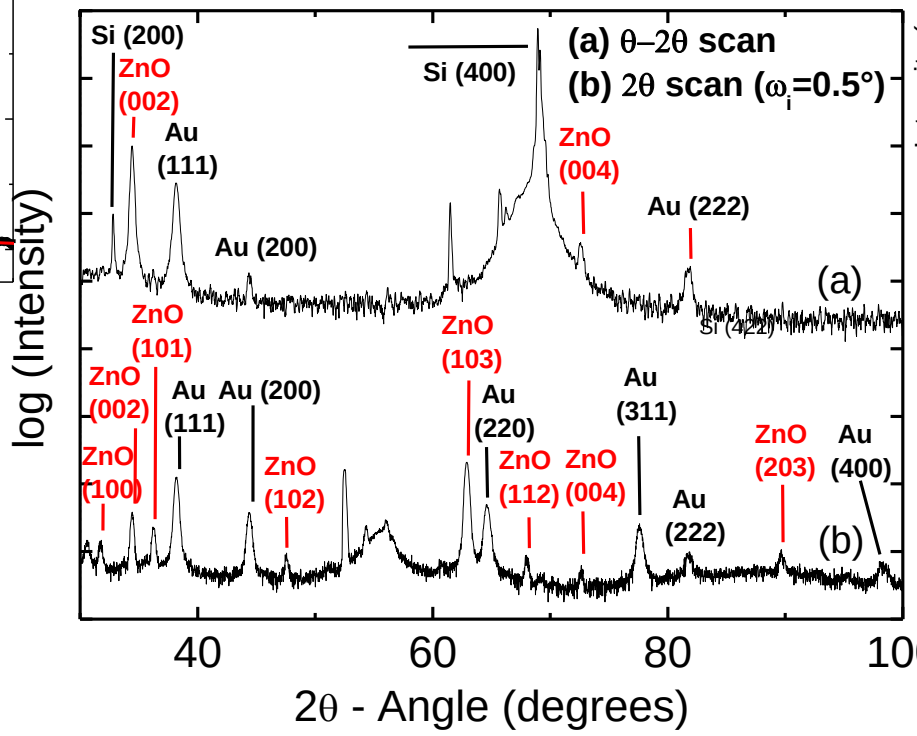

<D> ≈ 25nm

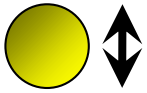

spherical shaped

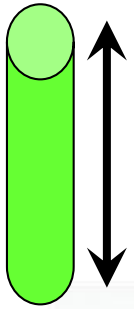

<D> ≈ 92nm

rod height

X-ray diffraction (powder diffraction) analysis of nanocrystals

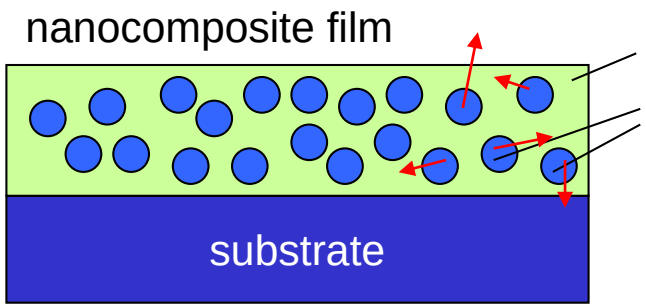

the nanocrystals are randomly distributed in the polymer matrix and the crystallographic orientation too (powder-like).

effect of the crystallite size (spherical shape): $\frac{\beta \cos\theta}{\lambda} \propto \frac{1}{D}$

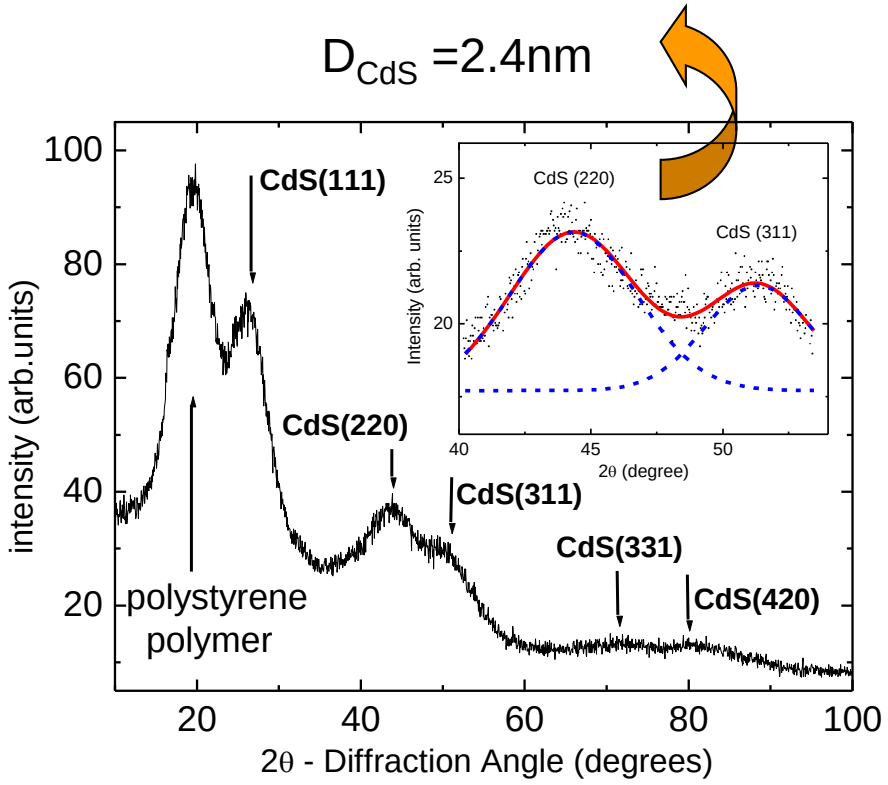

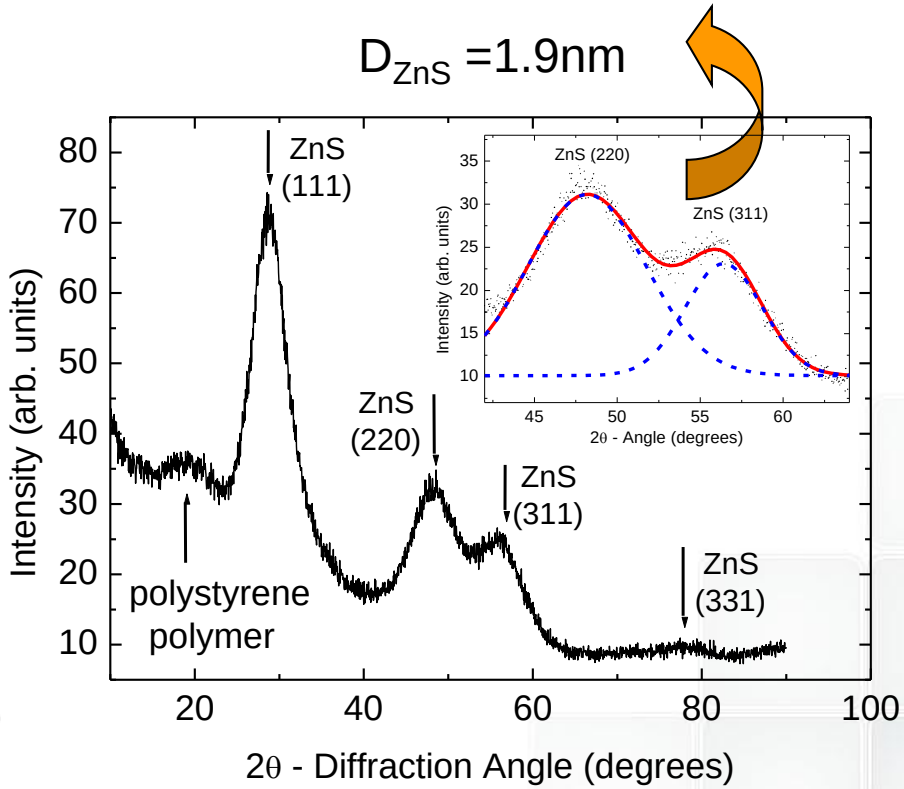

X-ray diffraction (powder diffraction) analysis by Debye formula

If the nanocrystals are very small (size < 5nm) the Debye formula should be used for the diffraction pattern analysis and the size and “internal” strain determination

particle (small crystal of any shape) made by **N** atoms,
x_{ij} is the distance between atoms ***i*** and ***j***,
f_i and f_j are the atomic scattering factors of atom ***i*** and ***j***, respectively.

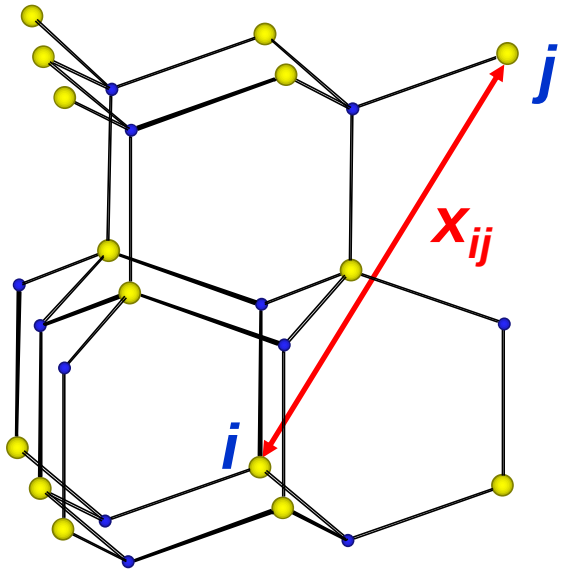

Debye formula for the intensity:

$$I_N(s) = \sum_{i=1}^{N}\sum_{j=1}^{N} f_i \cdot f_j \cdot \frac{\sin(2 \cdot \pi \cdot s \cdot x_{ij})}{2 \cdot \pi \cdot s \cdot x_{ij}}$$

small crystal of
wurtzite structure

see for instance
B. Palosz
A. Cervellino

Debye formula: calculation method

Zincblende
ABCABCABC…

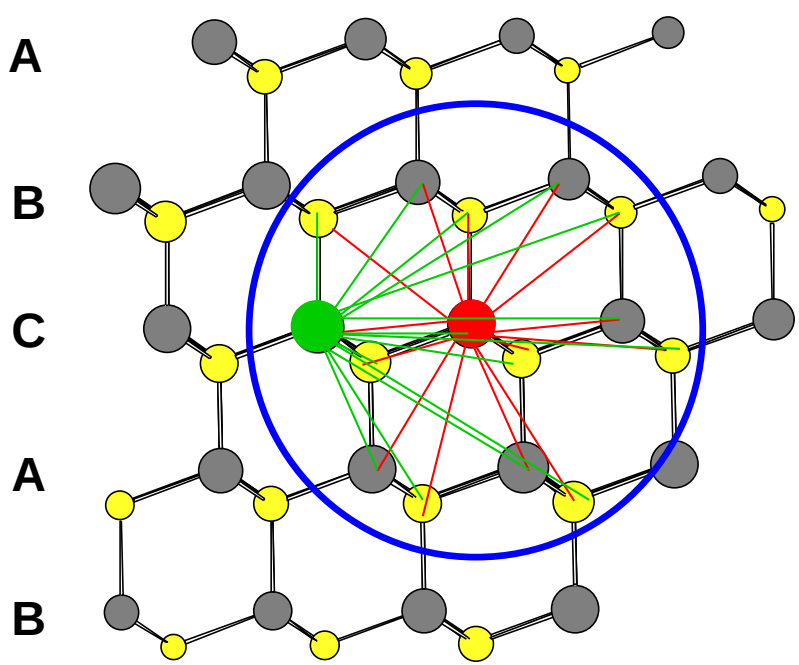

Wurtzite
ABABABAB

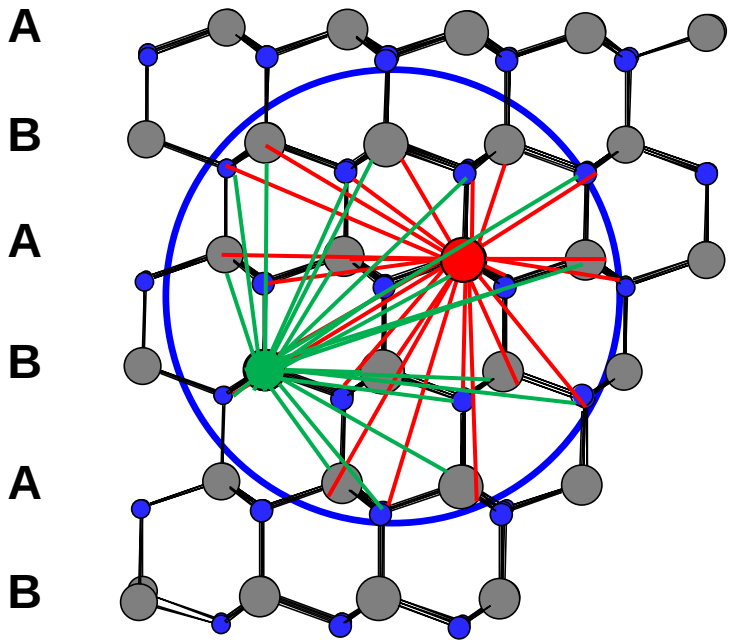

Example: structure of gold clusters (nanocrystals)

Structure of Gold Nanoparticles

CUBOCTAHEDRAL

ICOSAHEDRAL

DECAHEDRAL

Metal nanoparticles may crystallize in a crystallographic and also in a non-crystallographic structure with very small cluster size.

Noble metals with f.c.c. structure are known to form particles having non-crystallographic symmetry (decahedral and icosahedral), resulting from a very complex twinning.

Appearance of nanoclusters of different structure types.

Structure Analysis by a full-pattern X-ray powder diffraction analysis (Rietveld-like approach)

see for instance A. Cervellino et al., (2003) and (2004)

Experimental data and simulation results

1-phase synthesized dodecanethiol-AuNPs

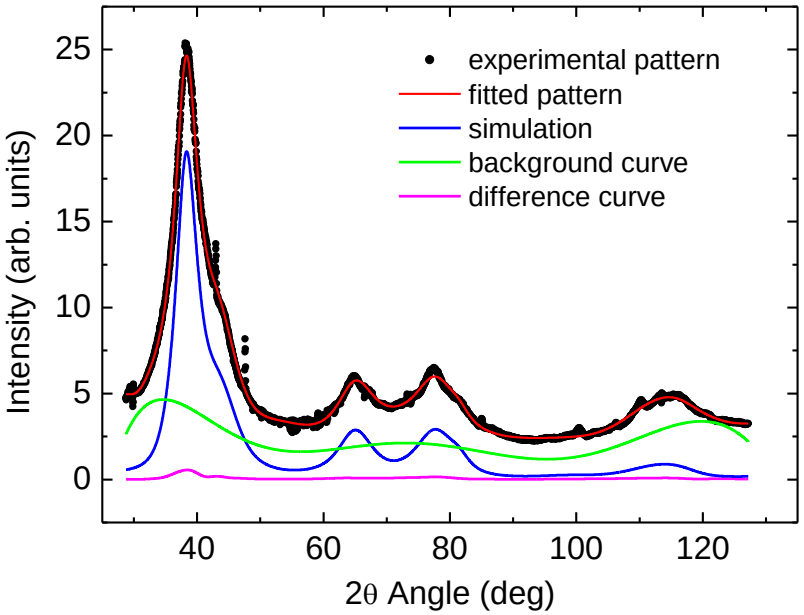

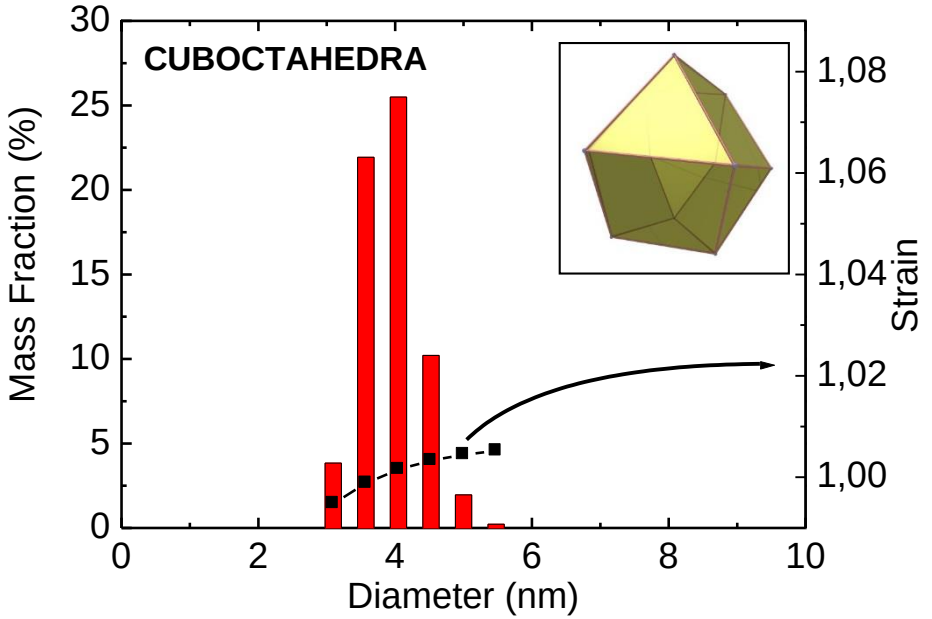

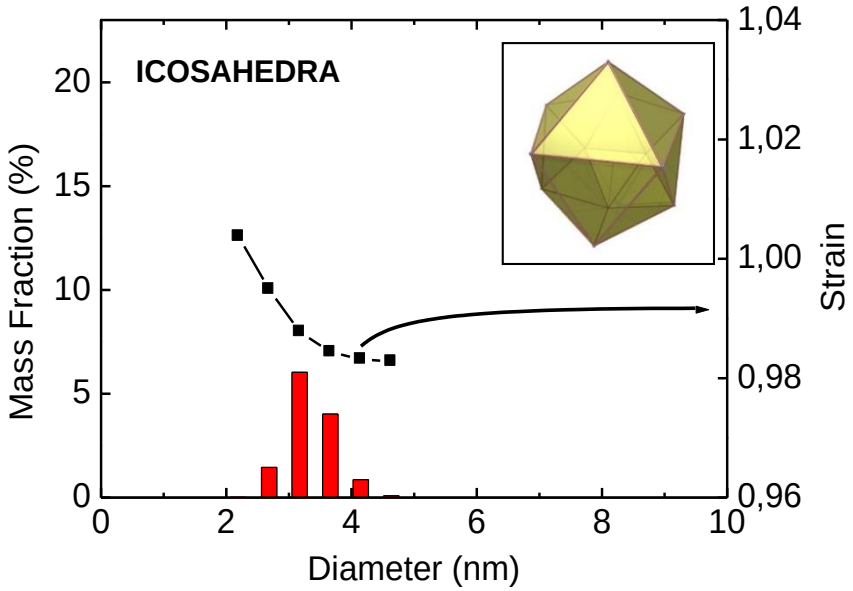

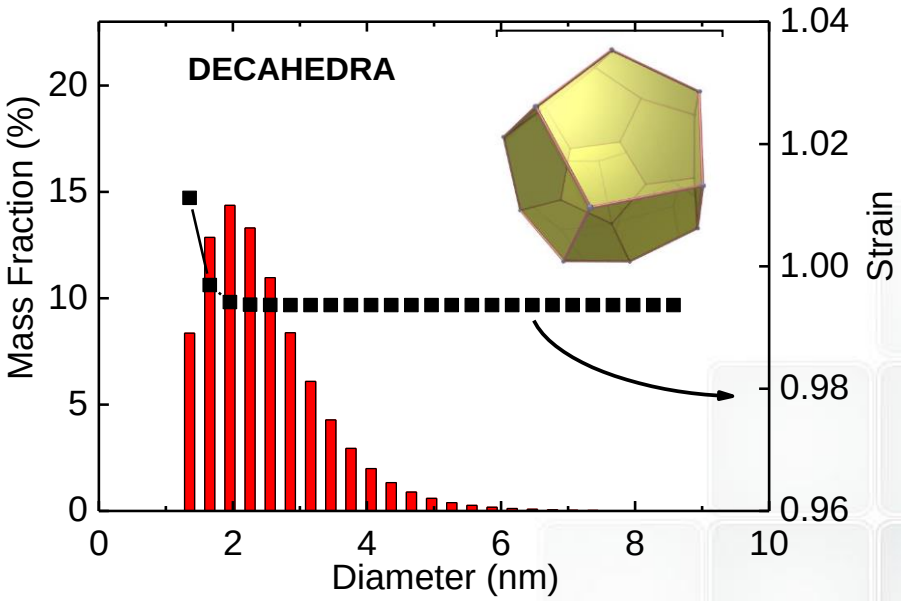

Thin film analysis

Parallel beam configuration

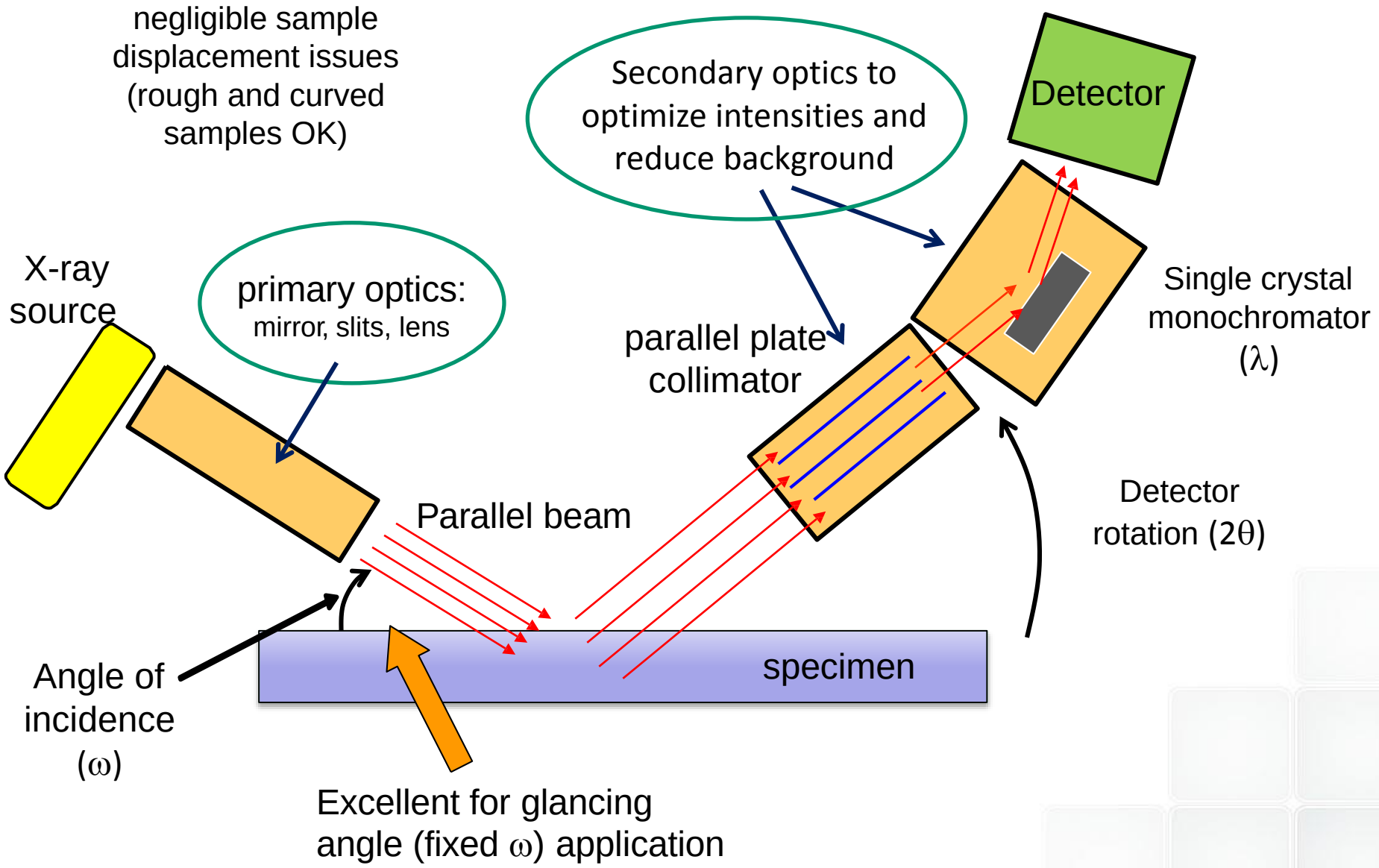

Glancing incidence X-ray diffraction analysis (GID, GIXD)

Glancing incidence configuration

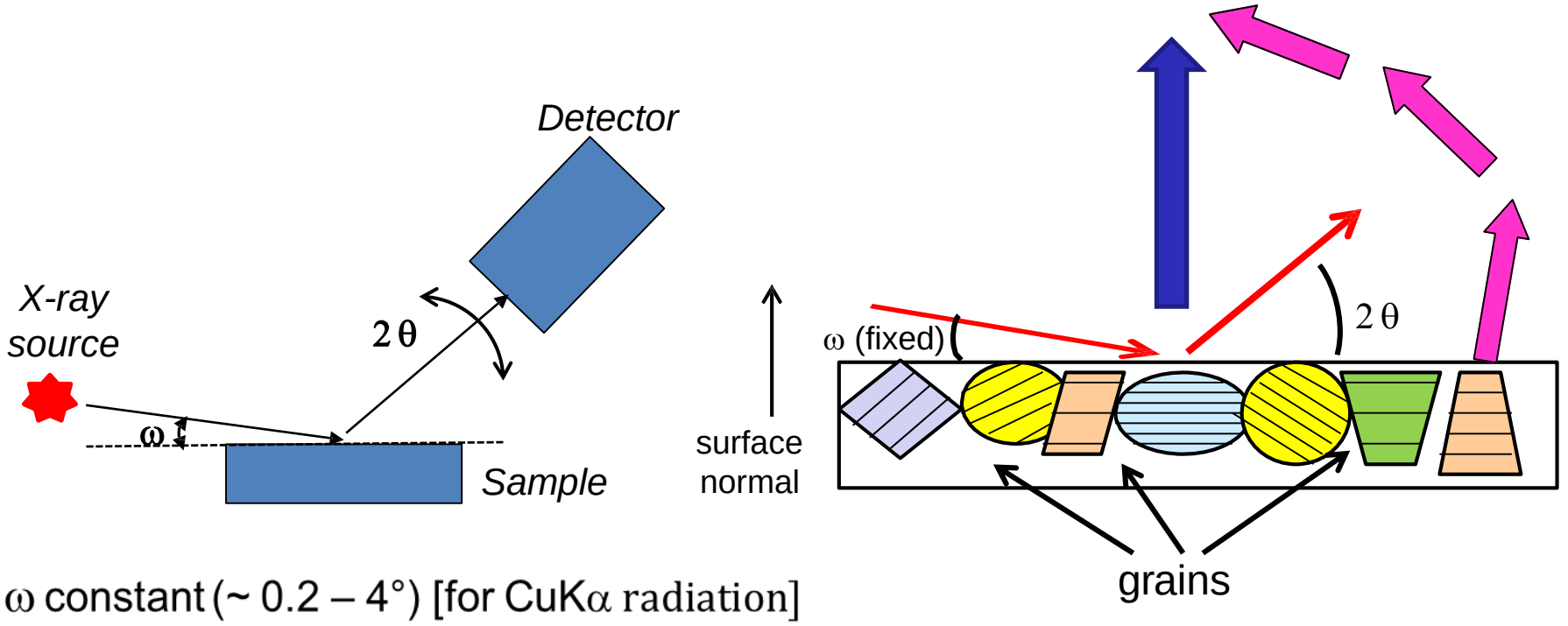

ω constant (~ 0.2 – 4°) [for CuKα radiation]

conventional Bragg-Brentano configuration
2θ-ω scans probe only grains with (hkl) planes aligned parallel to the surface

\+

parallel-beam **glancing incidence** configuration
2θ - scans probe grains with (hkl) planes oriented in all directions

X-ray penetration depth vs. angle of incidence

X-ray penetration depth depends on:

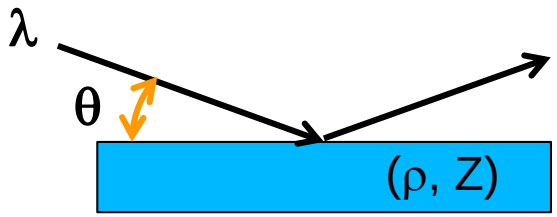

- materials parameter (atomic Z number, mass density ρ)
- X-ray wavelength (λ)
- incidence angle (θ)

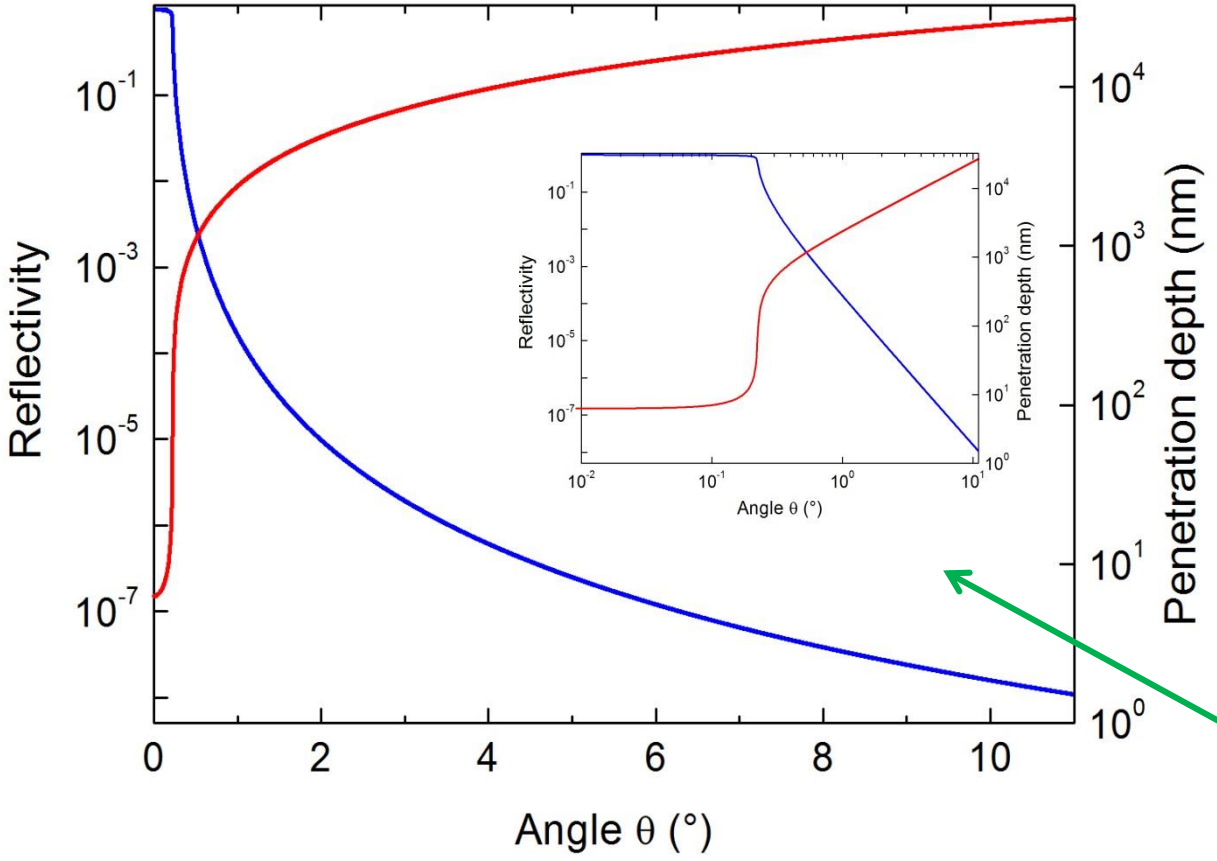

for small incidence angles θ< 10°:
nm - μm

at high incidence angles θ>10°:
μm - mm

Silicon
Cukα-radiation (λ=0.154nm)

Parallel beam configuration - applications

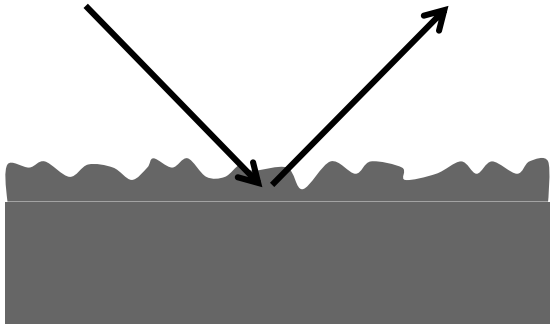

rough or irregular surface

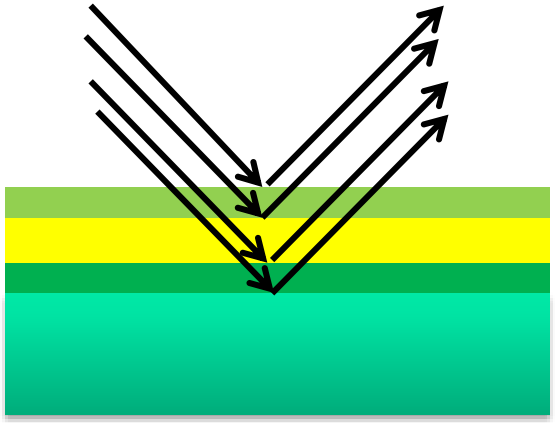

film/substrate systems,
multilayers, superlattices

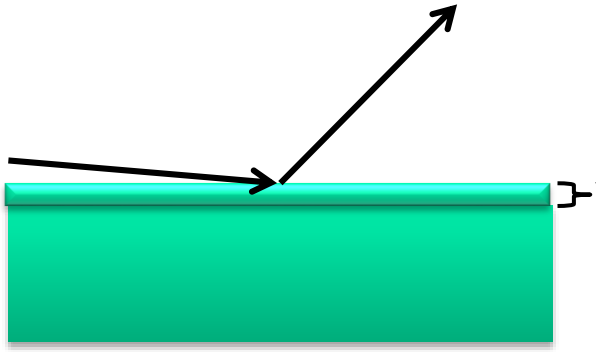

glancing / grazing incidence
angle applications; phase and/or
stress gradient (depth profiling)

Differences and peculiarities: ω-2θ scan *vs* glancing incidence 2θ scan

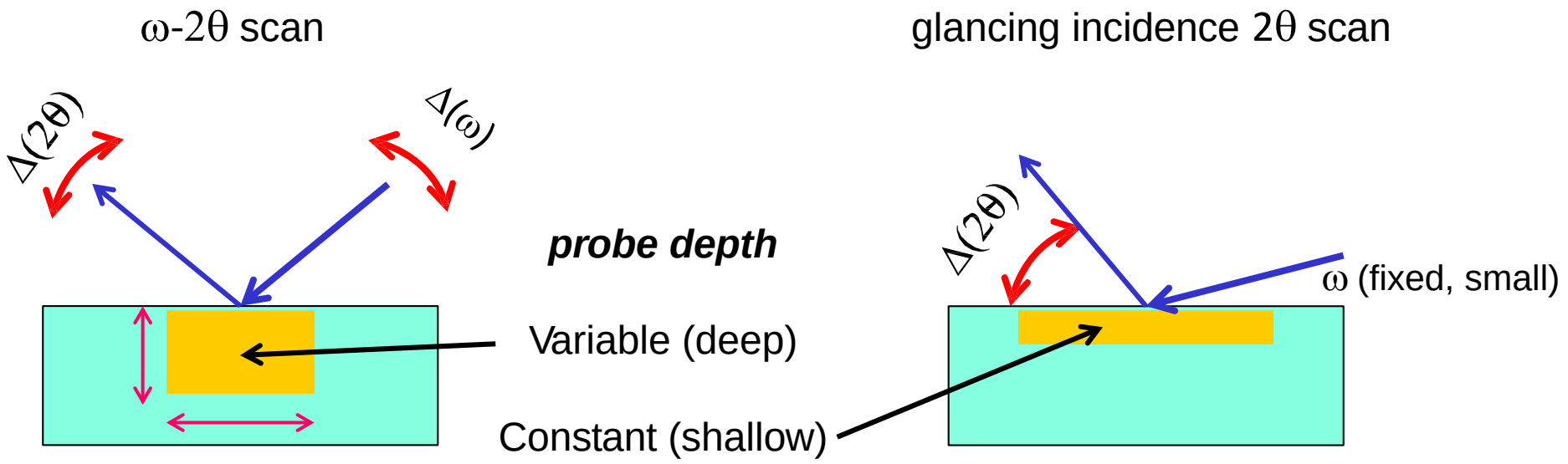

	ω-2θ scan	glancing incidence 2θ scan
grain orientations	directions ⊥ to surface	various directions
depth resolution	constant, up to mm	• from few nm up to mm; depth profiling possible by varying incidence angle • sensitive to surface • ideal for ultrathin layers
best configuration	Bragg-Brentano parallel beam	parallel beam (less sensitive to sample displacement)

glancing incidence diffraction (GID, GIXD)

Example:

GID 2θ scans of Thin oxide films deposited on substrate (Si, SiO_2)

GID scan of Gd_2O_3 sol-gel thin films annealed at 500°C for 16h on different substrates

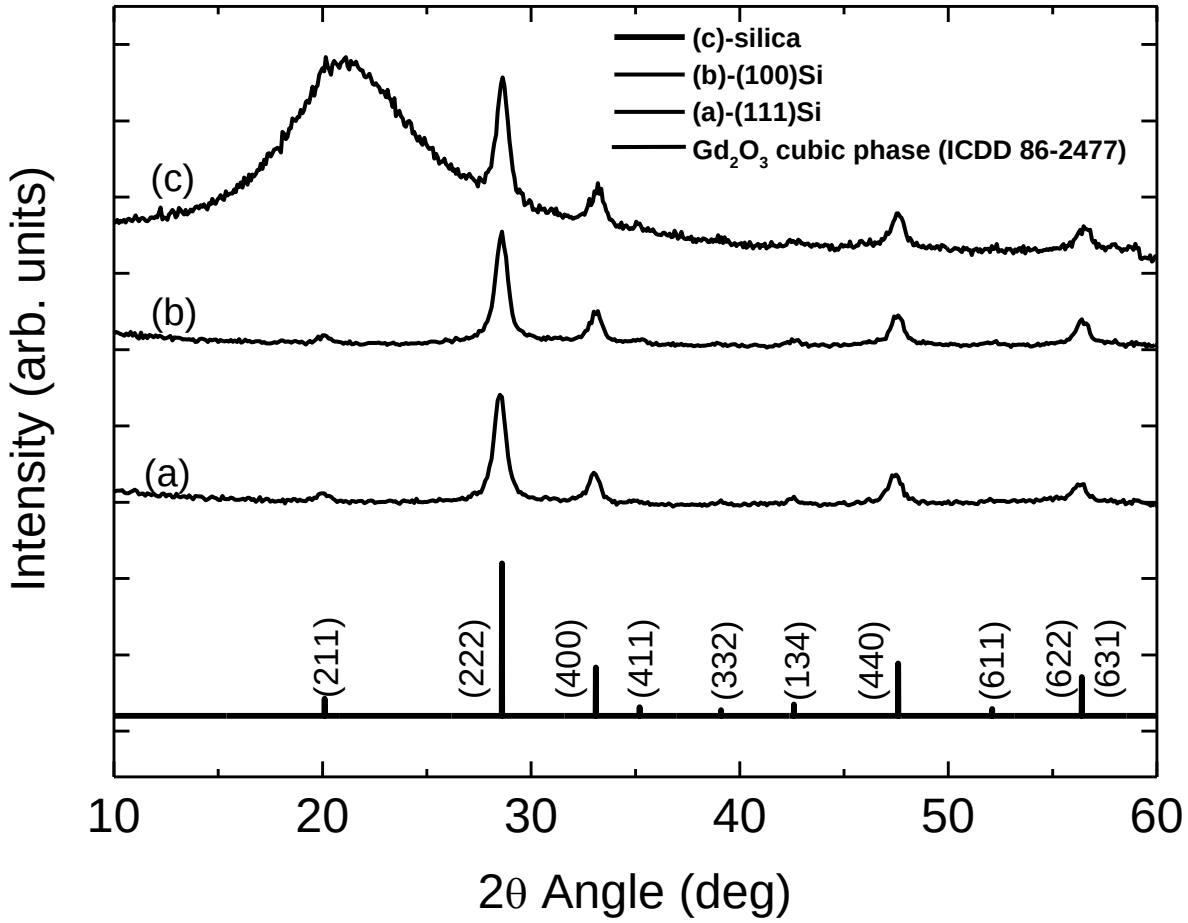

silica substrate

111-Si wafer

100-Si wafer

pattern of Gd_2O_3 (cubic phase) [ICDD Card Nr. 88-2477]

glancing incidence diffraction (GID, GIXD)

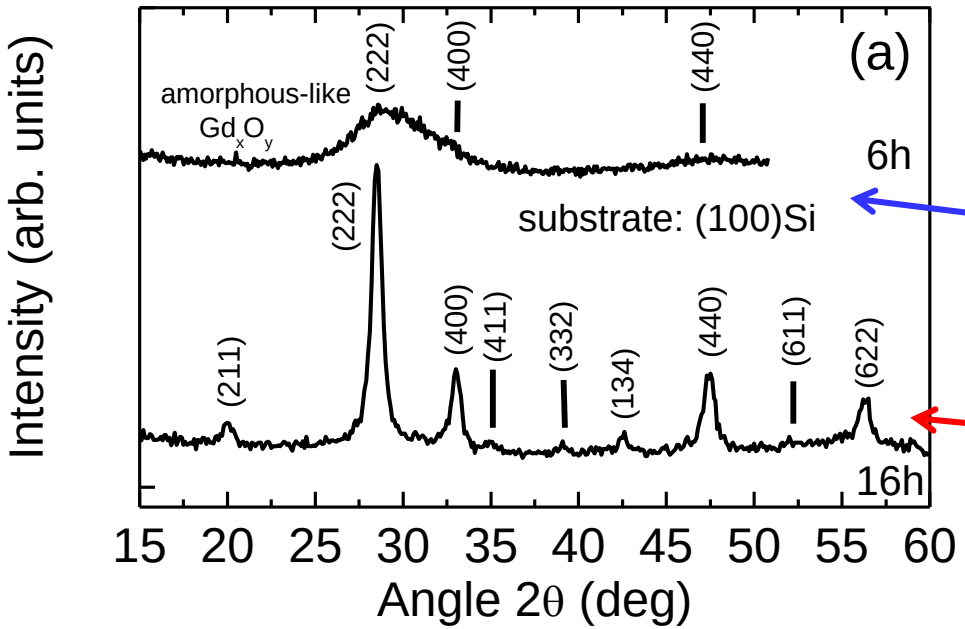

Gd_2O_3 sol-gel films on Si wafer (annealing temperature 500°C).

annealing time: 6h

annealing time: 16h

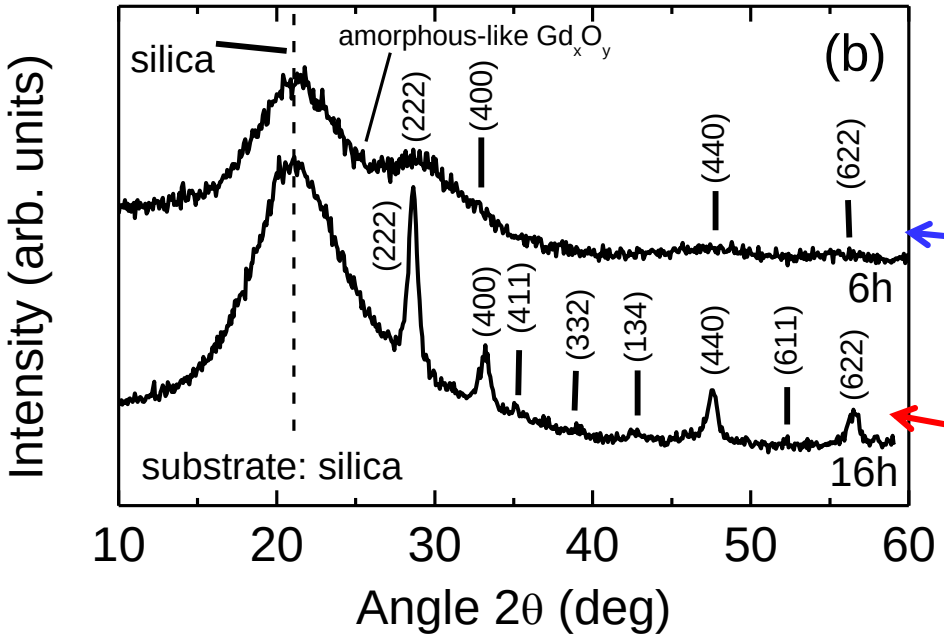

Gd_2O_3 sol-gel films on silica substrate (annealing temperature 500°C).

annealing time: 6h

annealing time: 16h

glancing incidence diffraction – crystallite size

Peak (most intense) profile analysis and application of Scherrer's relation for crystallite size determination

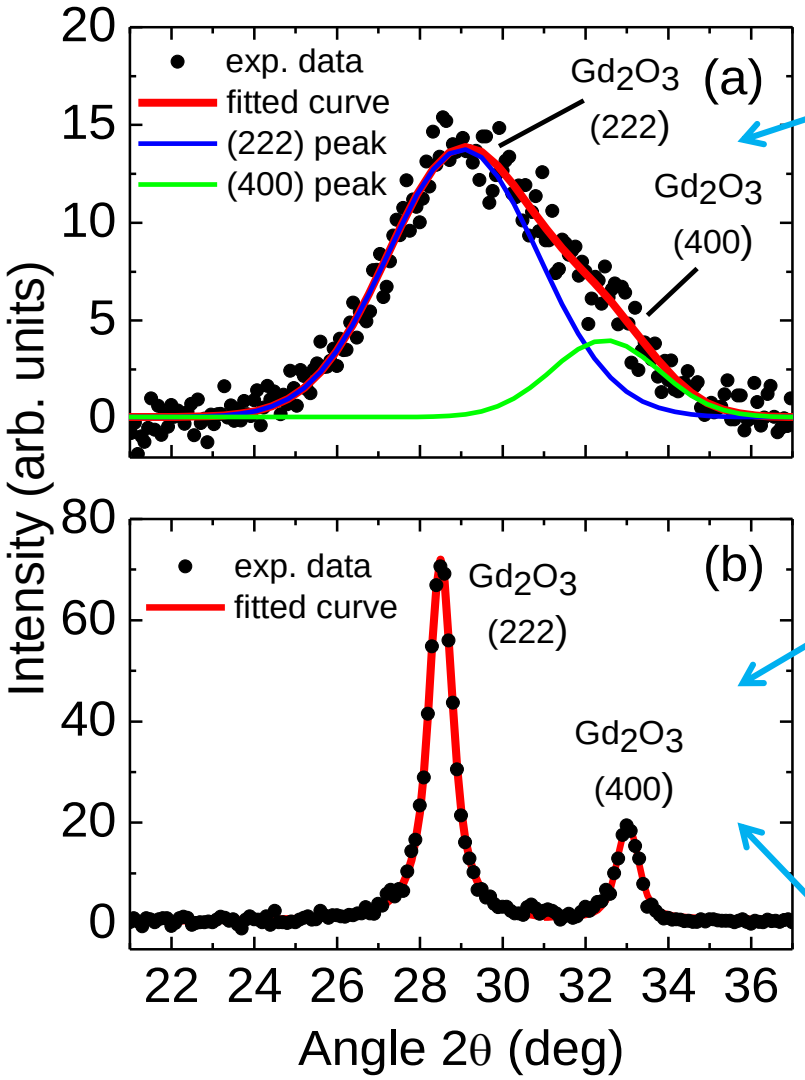

crystalline domains of the films annealed for 6h are about Ø=2-3 nm

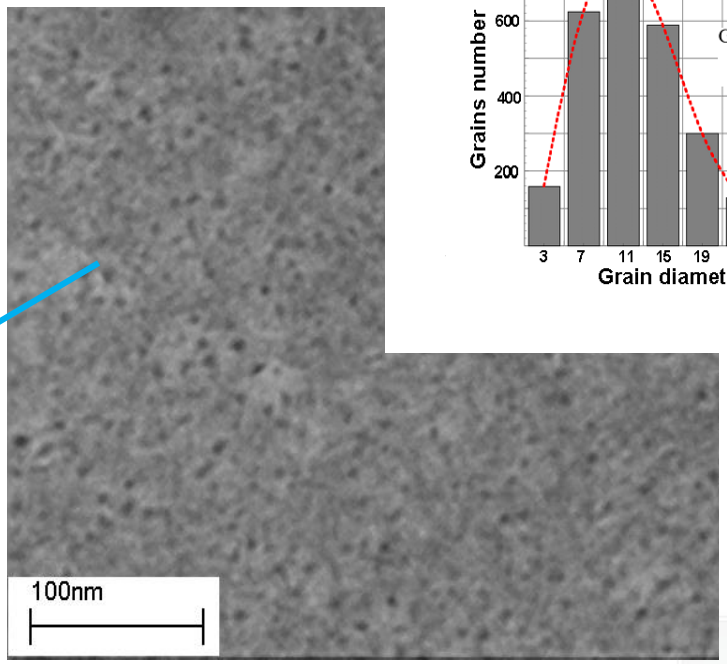

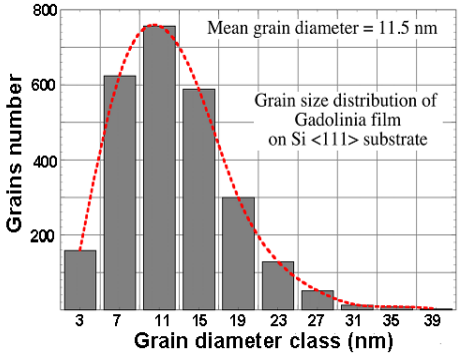

grain size (11±3)nm

crystalline domains of the films annealed for 26h are about ø = 10-12 nm

Nanoparticles on surface – application of parallel beam GID measurements

Deposition of ultrathin gold films (**2 nm**) on Si (or SiO_2) and formation of Au nanoparticles by thermal annealing in inert atmosphere

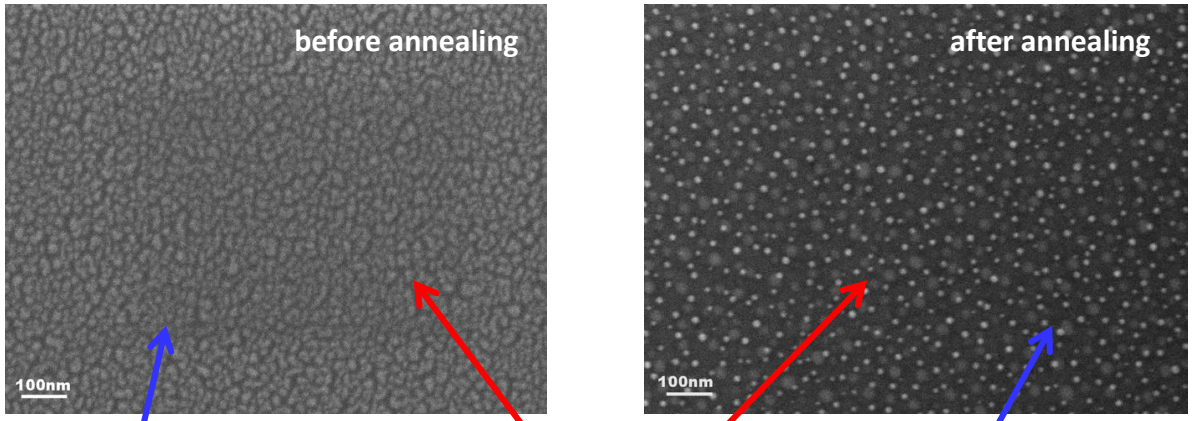

SEM micrographs **before** and **after** thermal annealing

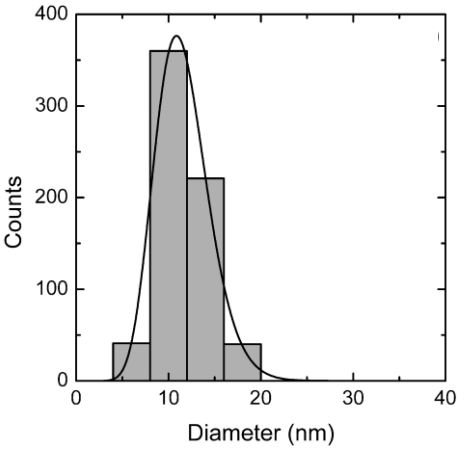

Histogram of surface particle diameter

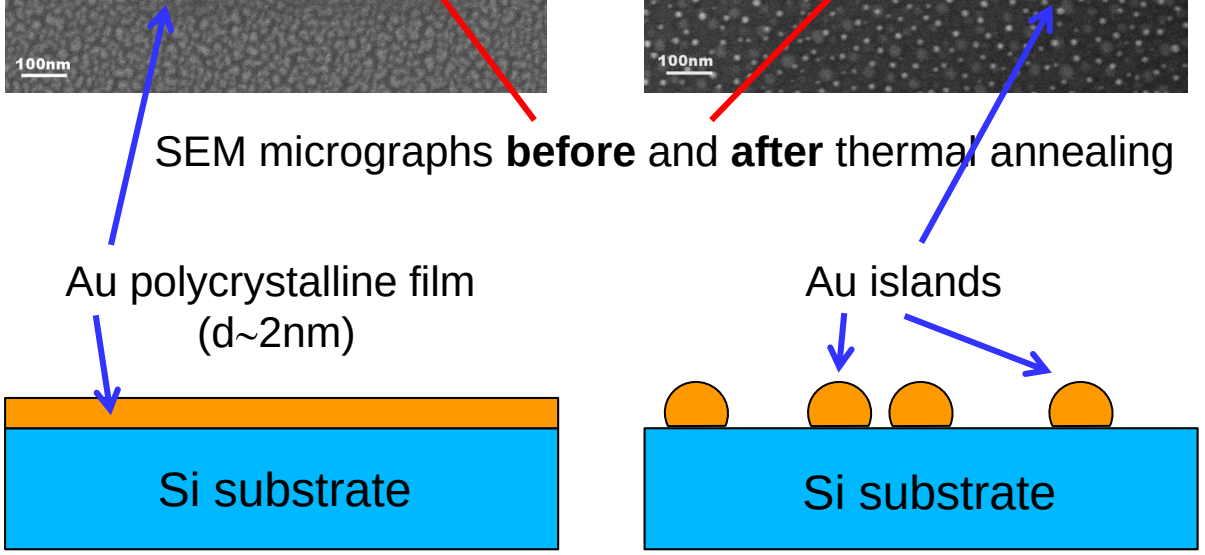

glancing-incidence X-ray diffraction (GID) in parallel beam configuration

measurement scheme

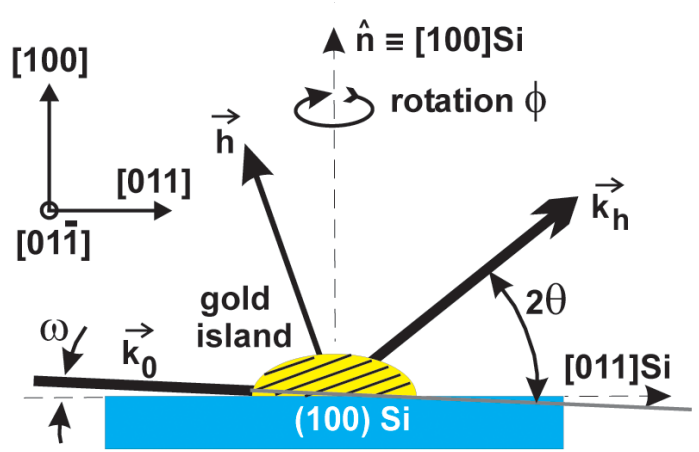

GID patterns for different annealing temperatures

polycrystalline structure (Au Bragg peaks)

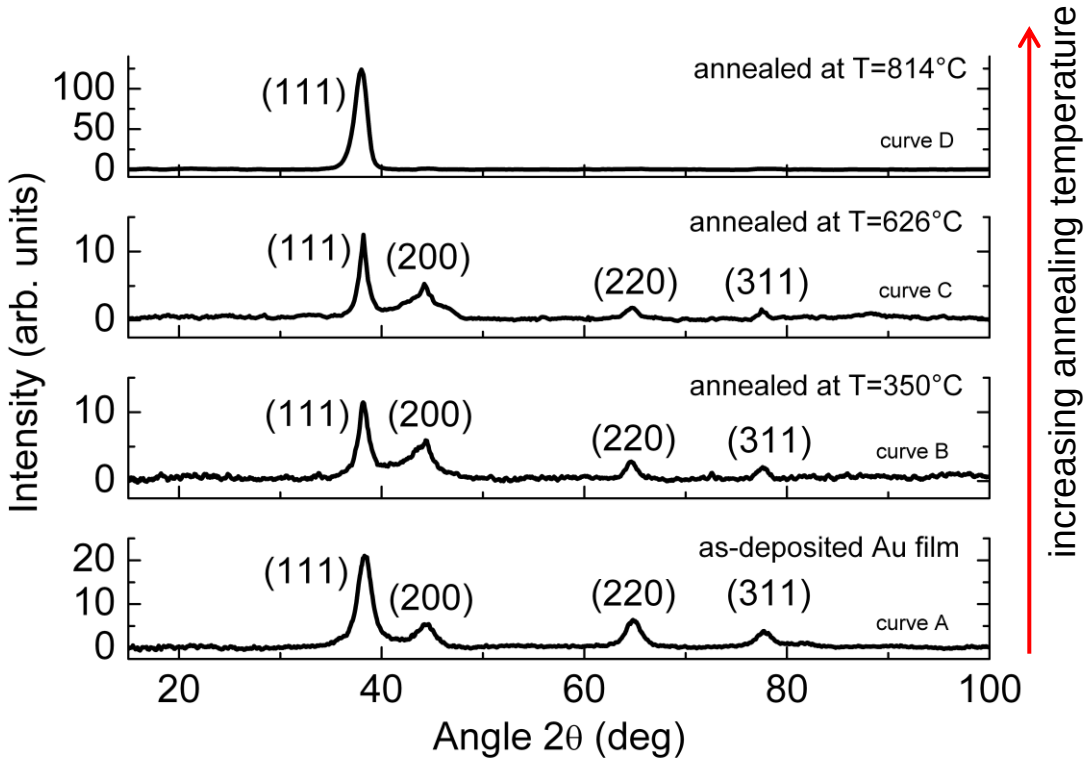

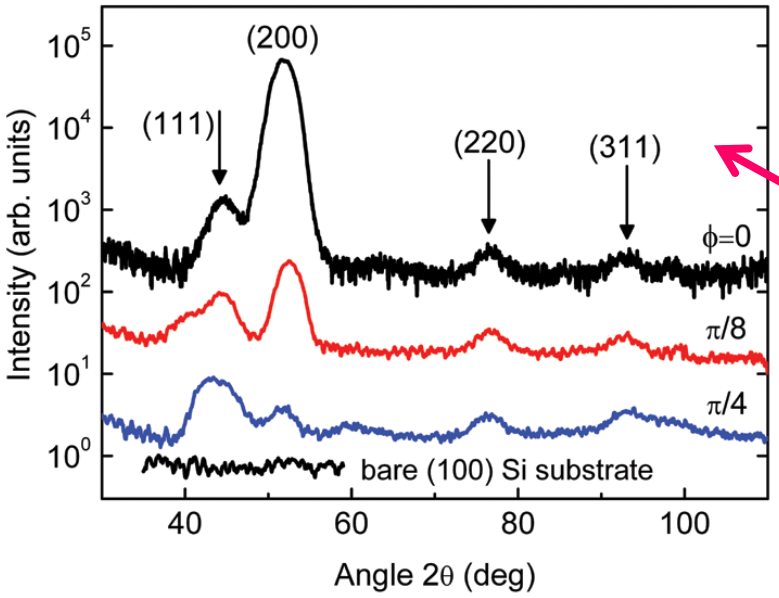

GID for different azimuthal angles for texture analysis

- how are the Au islands placed on Si (crystallographic)?
- how is the Au lattice accommodated with respect to the Si lattice?

Modelling of the lattice accommodation of the Au and Si lattices

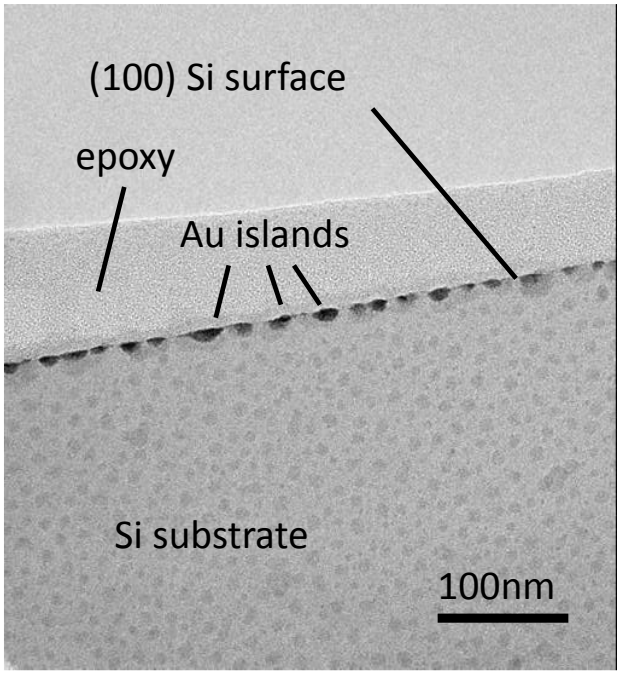

low resolution

TEM analysis

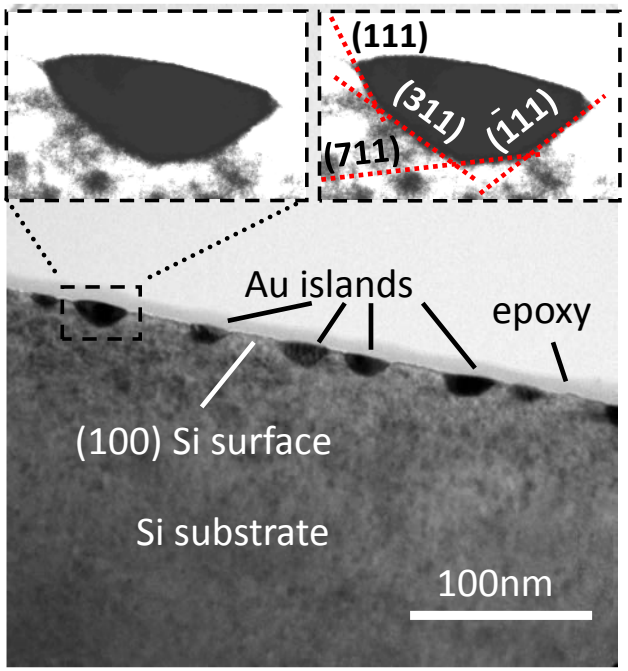

high resolution

From GID and TEM analysis:

modelling of the Au island on/in Si lattice

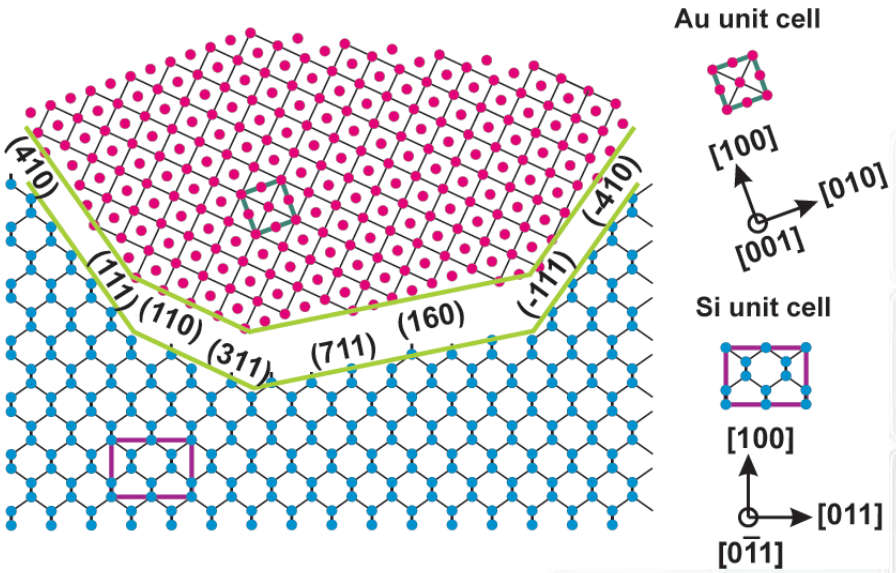

High-resolution X-ray diffraction (HRXRD) and Reciprocal space mapping (RSM)

diffractometer configuration for:

- high resolution X-ray diffraction (HRXRD)
- reciprocal space mapping (RSM)

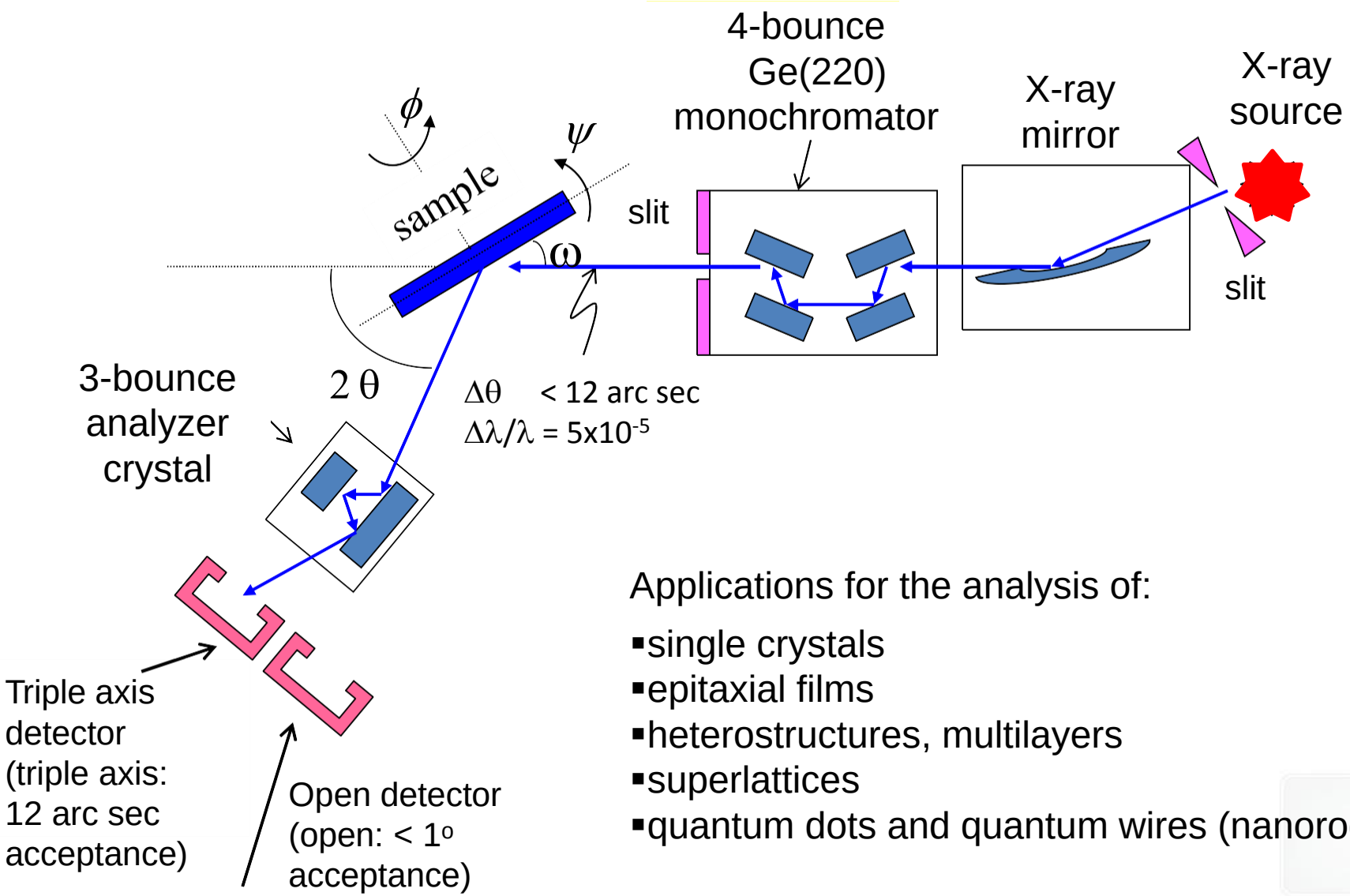

Applications for the analysis of:

- single crystals
- epitaxial films
- heterostructures, multilayers
- superlattices
- quantum dots and quantum wires (nanorods)

Analysis and determination of parameters by HRXRD and RSM

High resolution rocking curves

- lattice distortions within 10^{-5}
- lattice parameter measurements
- layer thickness (high precision)
- superlattice periods
- lattice strain relaxation
- alloy composition
- interface smearing / roughness

(some data analysis requires dynamical simulation).

Reciprocal space mapping

- 2D analysis (in-plane and out of plane)
- lattice strain relaxation
- diffuse scattering analysis for lattice defect analysis (clusters, stacking faults, dislocations)
- mosaicity
- lattice coherence

lattice strain and strain relief (relaxation)

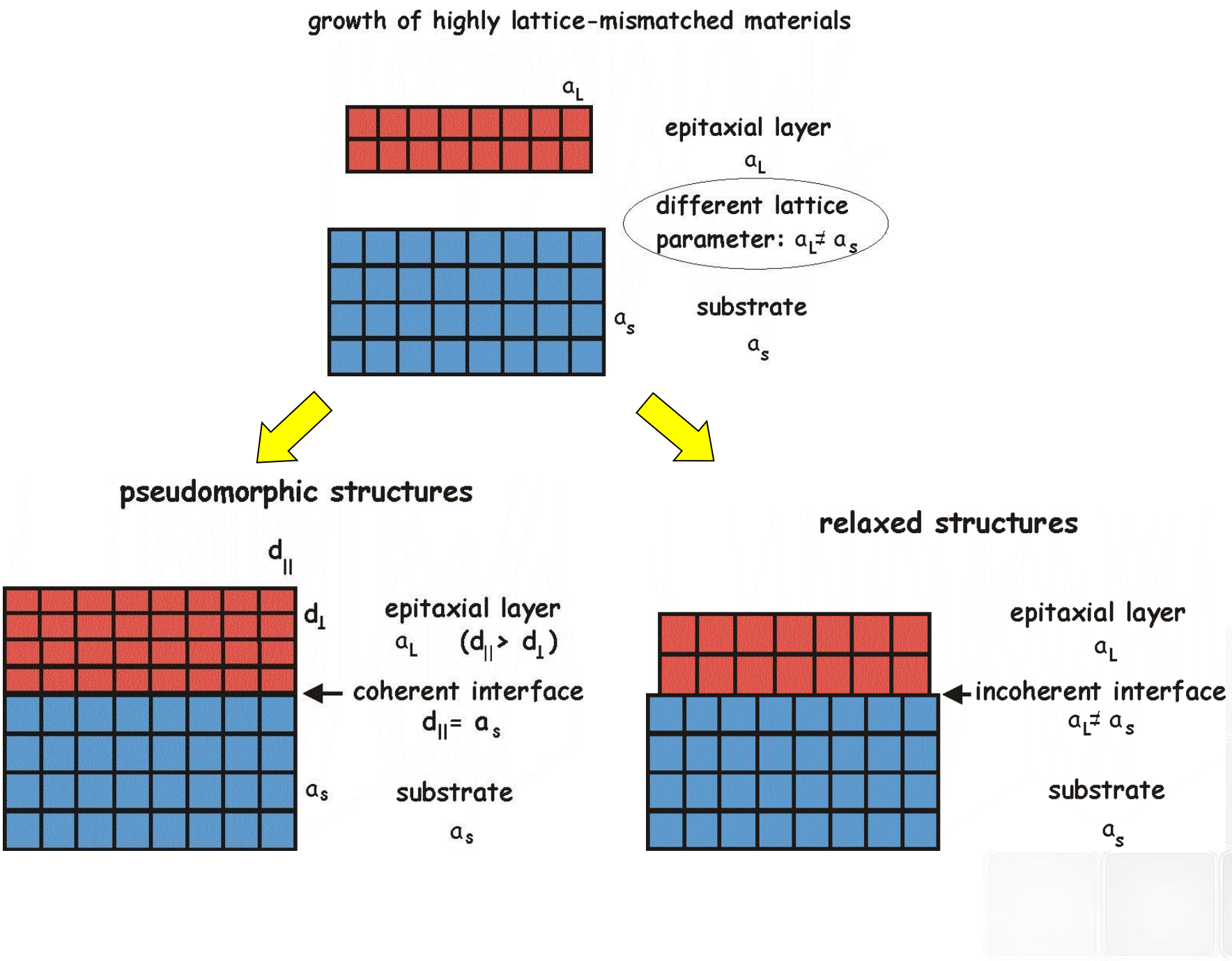

High-resolution X-ray diffraction measurements

Measurement of thin layers (multilayers) and of (even small!!) lattice mismatch

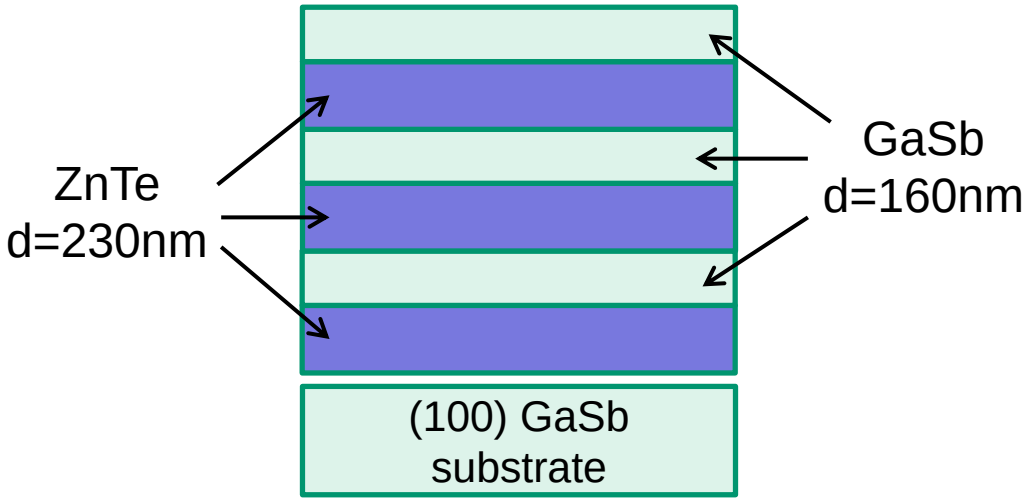

almost the same lattice constant
a(GaSb) = 6.096 Å
a(ZnTe) = 6.101Å

small lattice mismatch
~ 0.0008

HRXRD curve around the (400) reflection

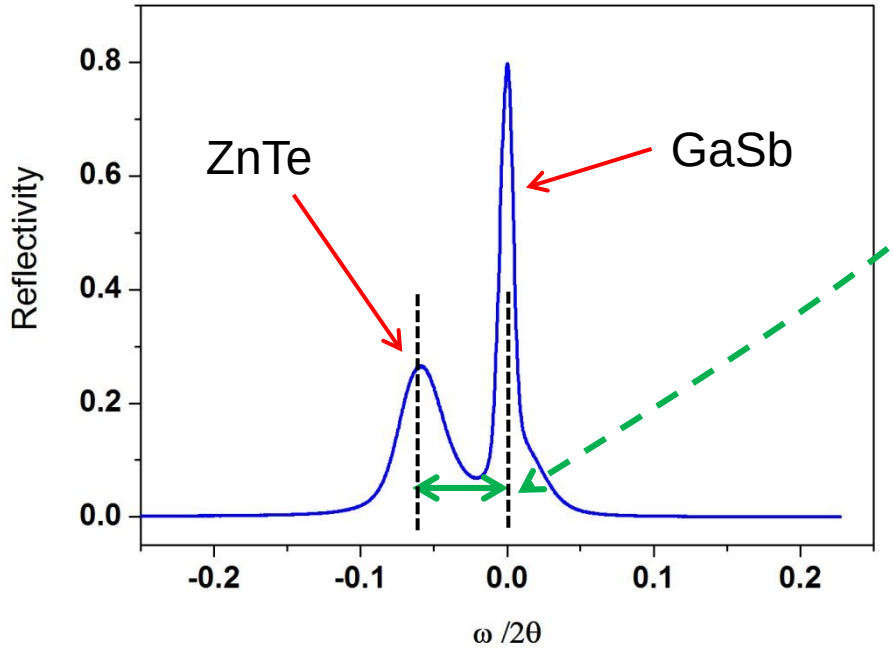

High-resolution reciprocal space map (RSM)

line scan in RSM at $\omega_{offset}=0°$

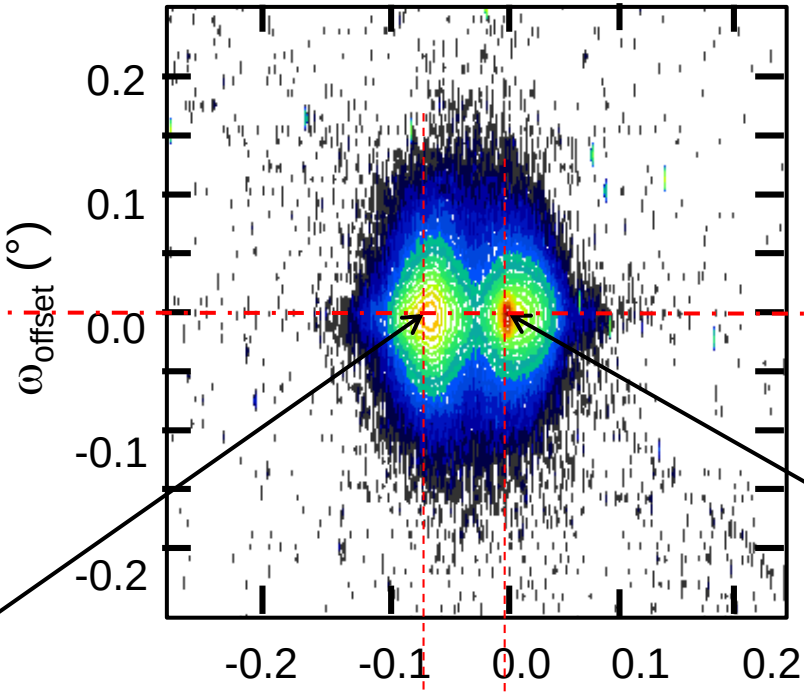

ZnTe layers

GaSb layers + GaSb substrate

HRXRD curve

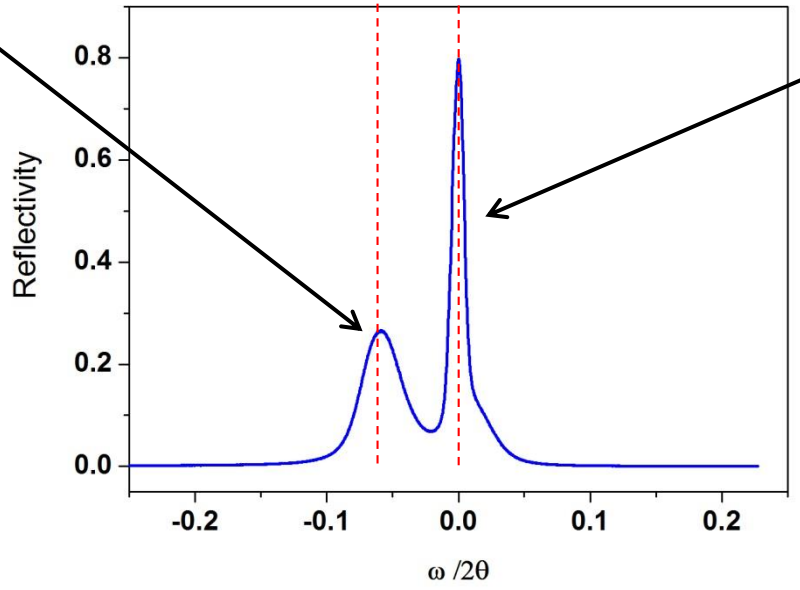

2D intensity maps around reciprocal lattice points

peak shape in reciprocal space maps for epitaxial films of ideal and mosaic structure

ideal interface between heterostrucure and substrate

the same interface lattice parameter

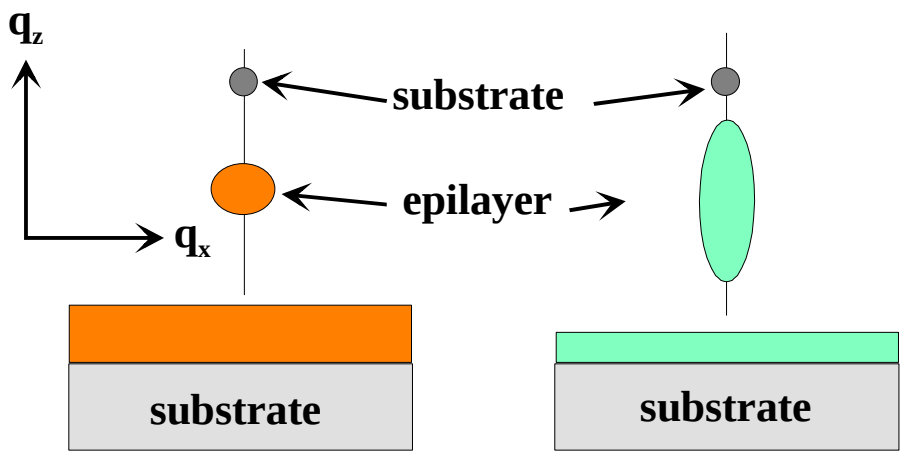

thick epitaxial film of ideal structure

thin epitaxial film of ideal structure

imperfect interface between heterostrucure and substrate

defect (dislocations, clusters) formation at interface due to different lattice parameters and strain relief ($\rightarrow$ mosaicity)

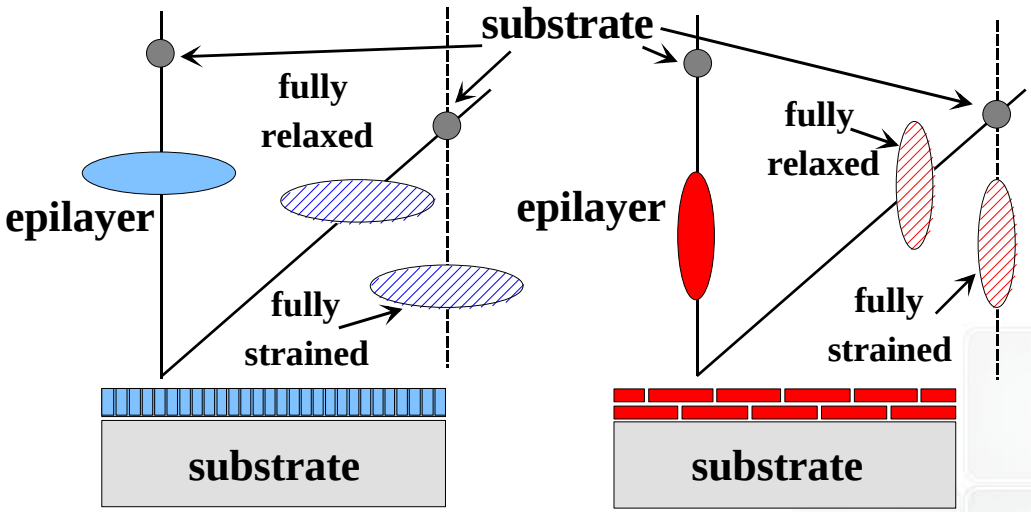

mosaic epitaxial film columns

mosaic epitaxial film discs (platelets)

Recording of reciprocal space maps (RSM)

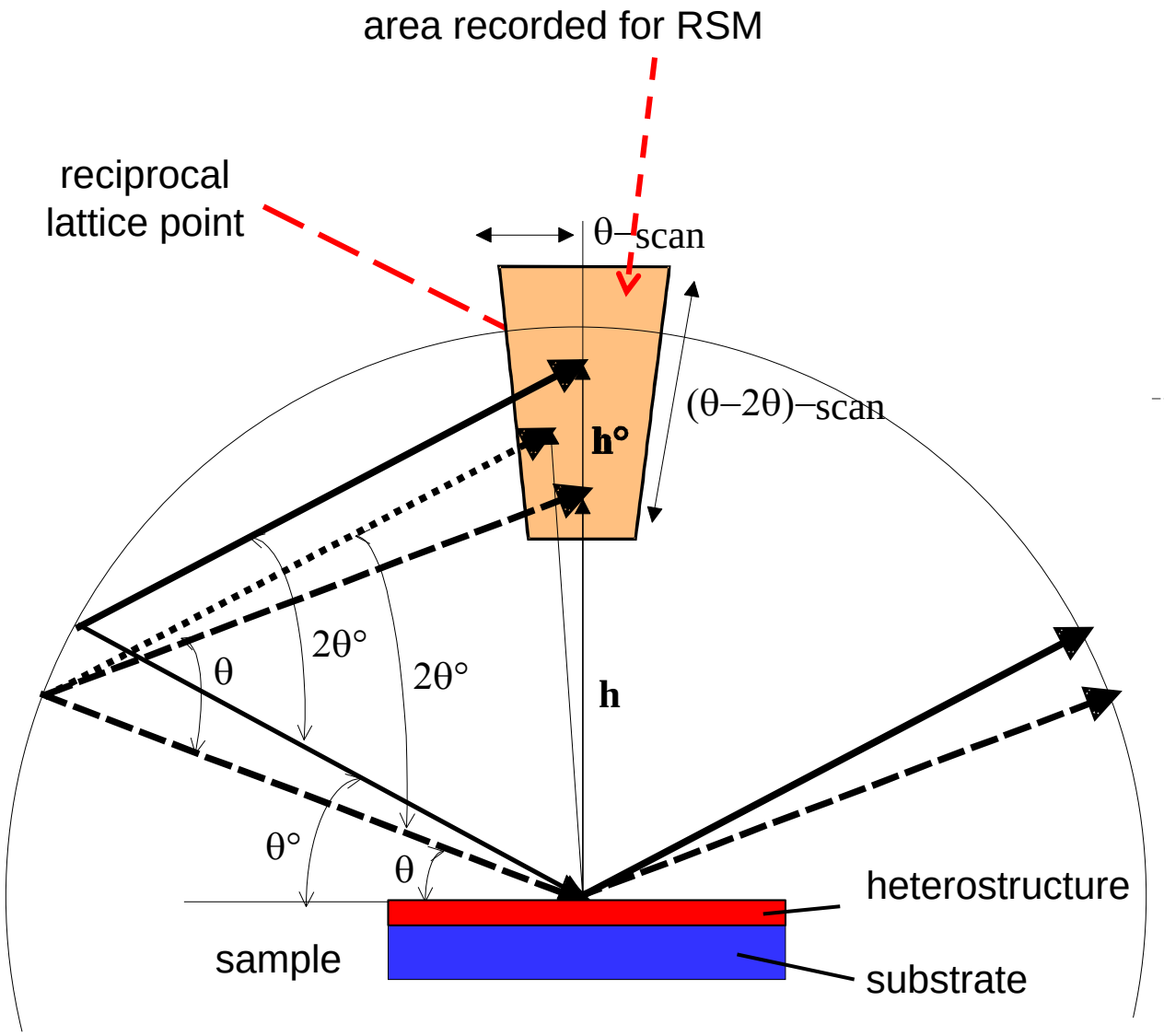

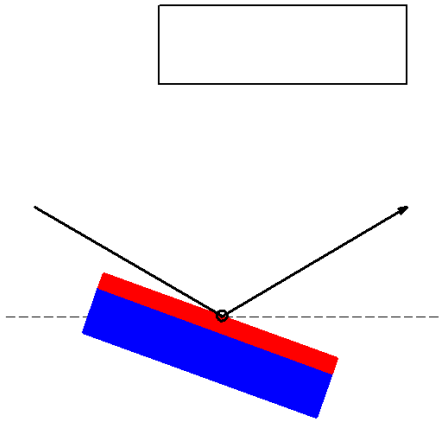

RSM measurement by acquisition of single (θ-2θ) line scans with different offset angles

Qualitative analysis of RSM and parameter contributions

peak shape in reciprocal space maps for epitaxial films of mosaic structure (columnar structure)

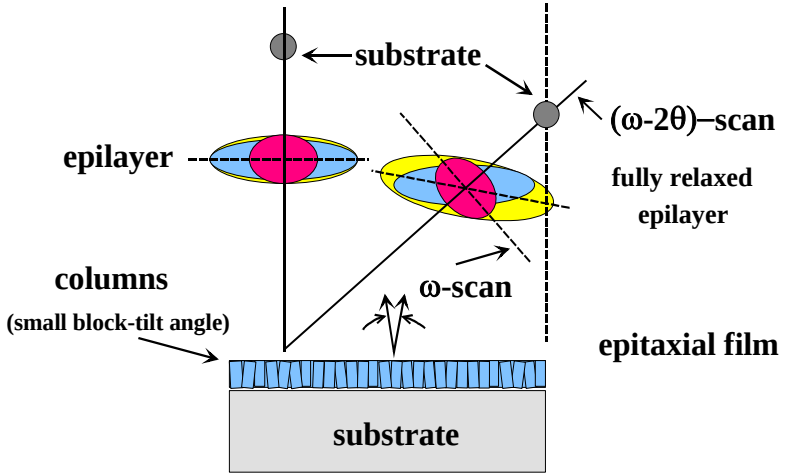

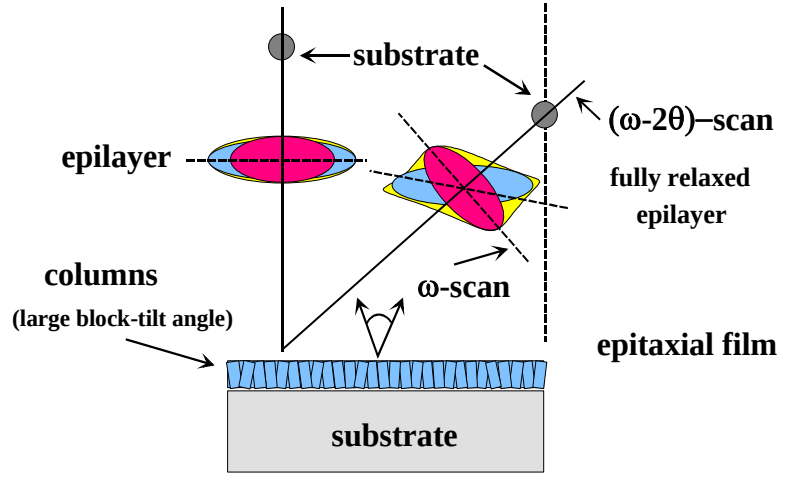

peak shape in reciprocal space maps for epitaxial films of mosaic structure (mosaic block structure:platelets/discs)

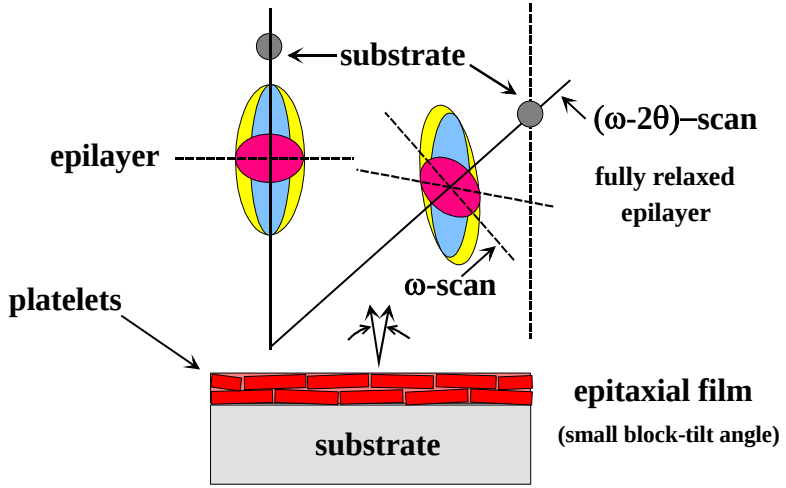

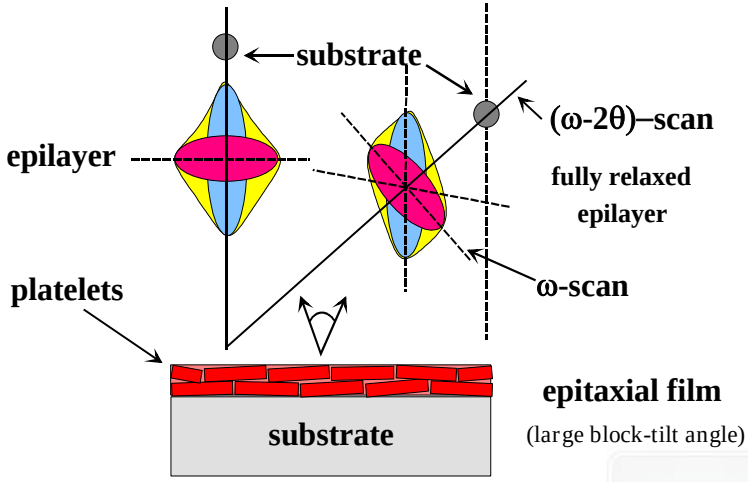

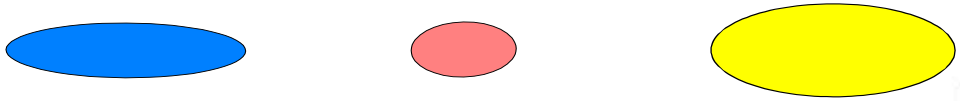

contribution of correlation lengths

contribution of angular tilt

sum of all contributions

Interpretation and qualitative analysis of RSM

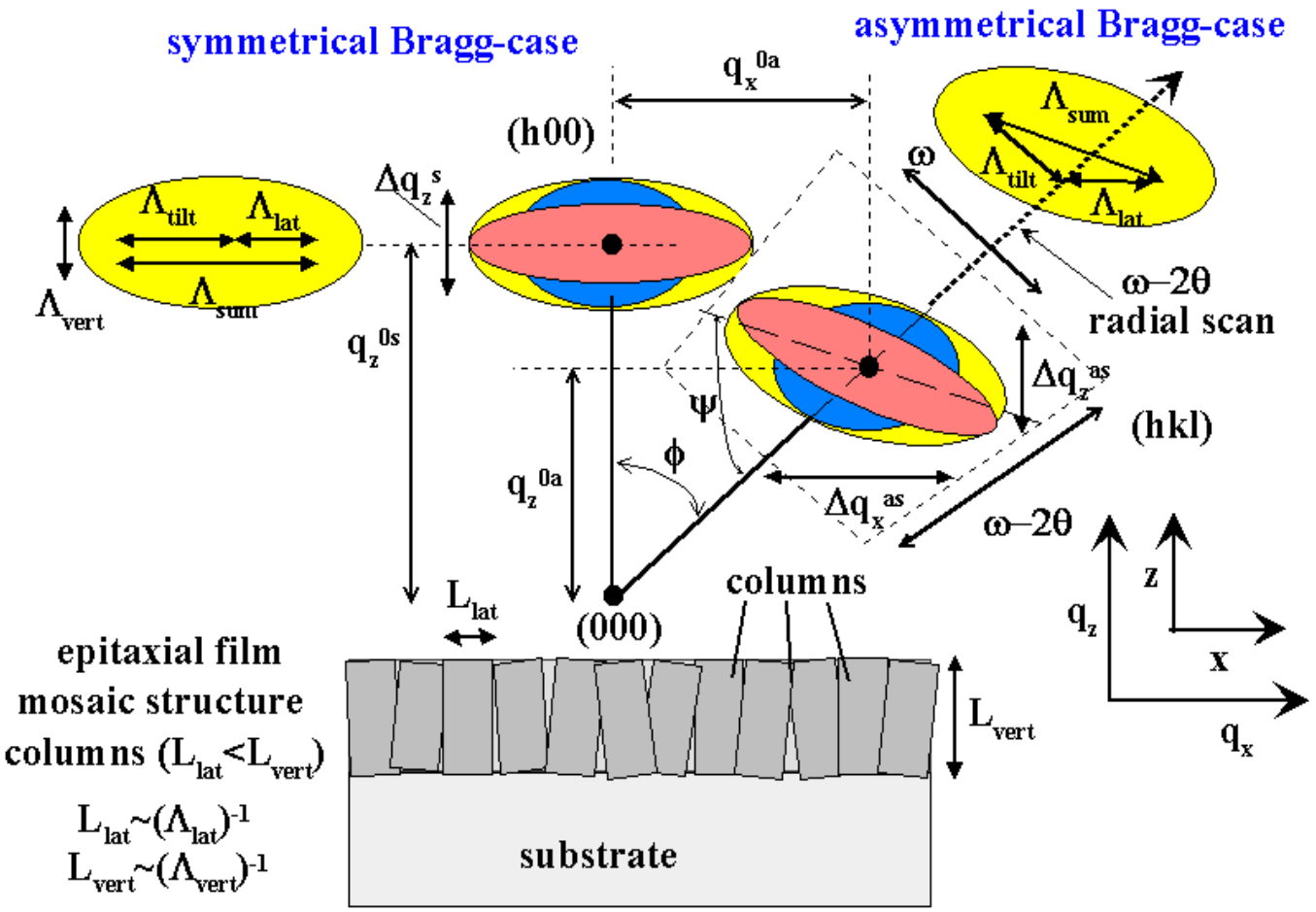

- strain state (lattice relaxation)
- lateral extension (lateral correlation length)
- vertical extension (vertical correlation length)
- lattice tilt angle

Example: RSM of nanowires (NWs) grown on semiconductor surfaces

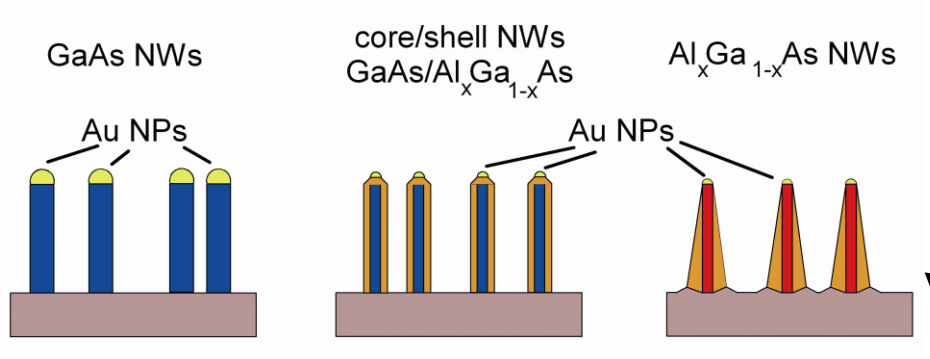

FESEM micrographs

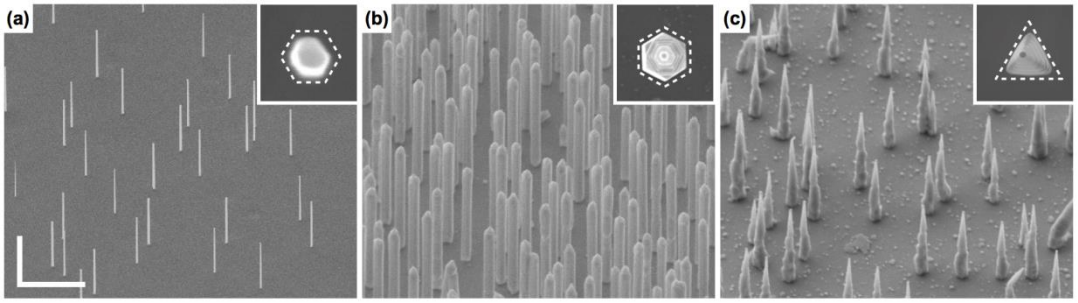

different shape of the NWs

⇓

Recorded RSMs

close to the (400) rlp

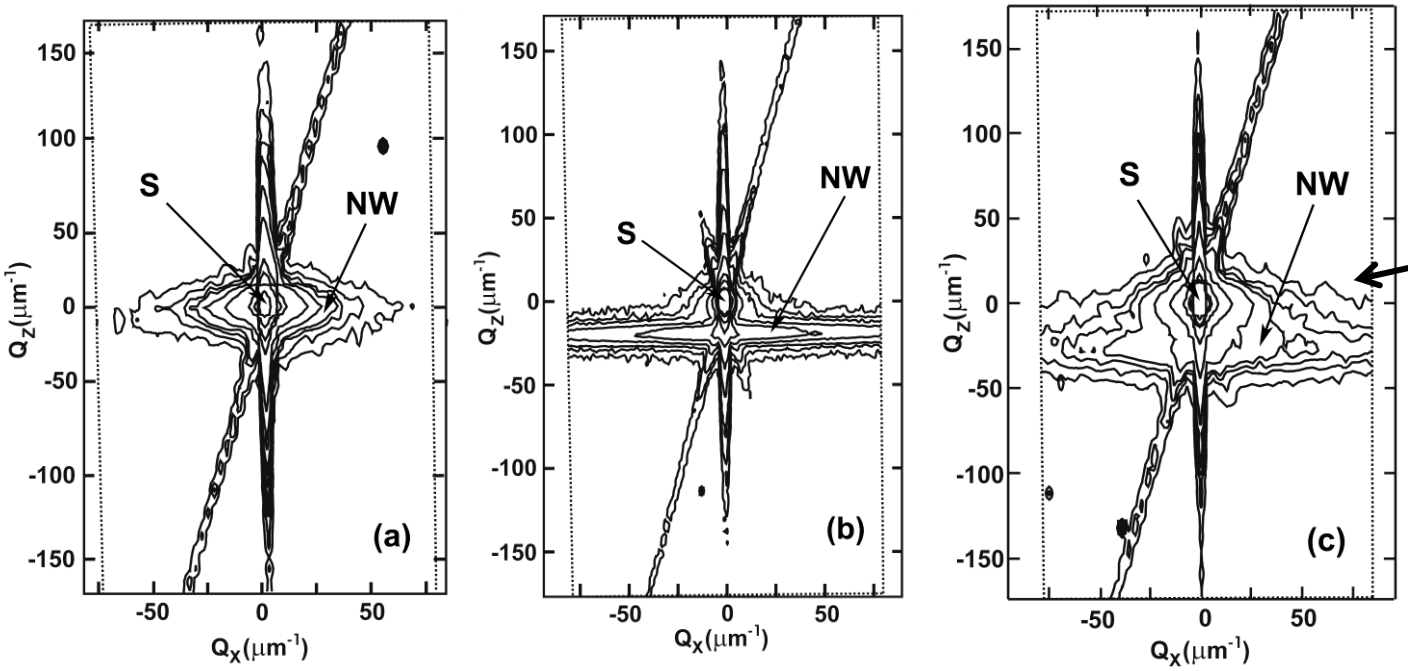

different features, shape, intensity distribution of the RSMs

RSM of nanowires grown on semiconductor surfaces

RSMs recorded close to the (400) rlp

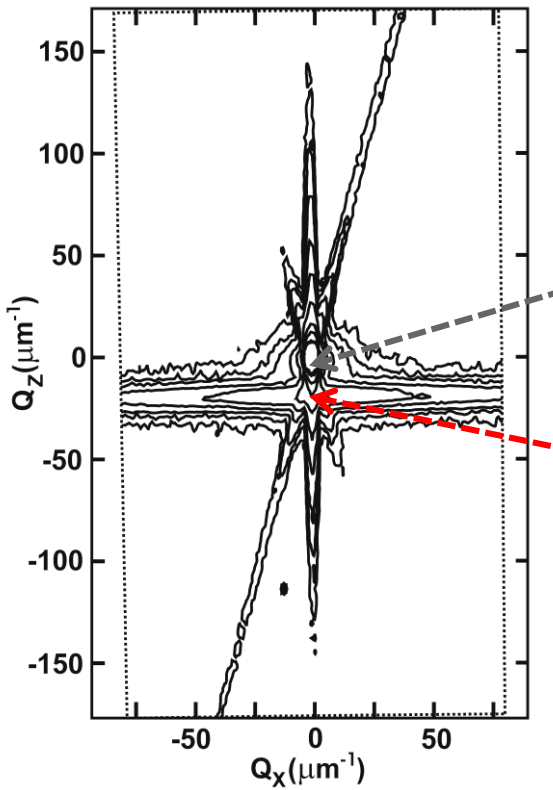

GaAs substrate

core/shell NWs

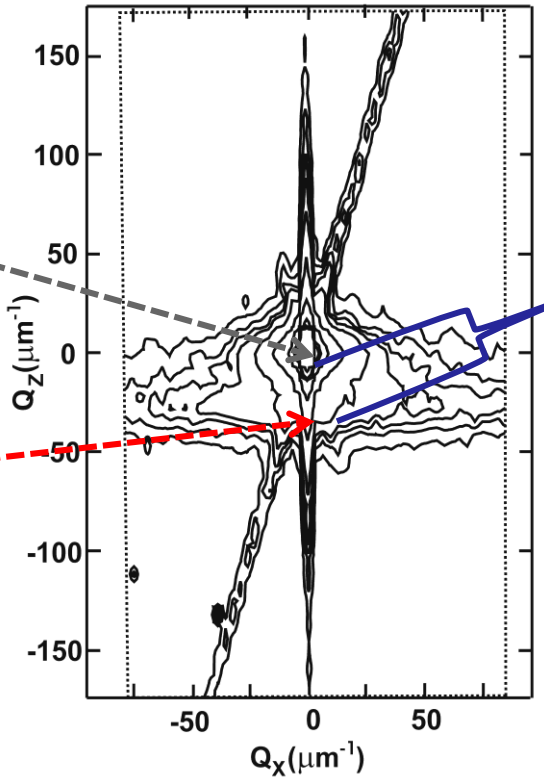

angular distance
⇓
lattice mismatch
⇓
Al mole fraction

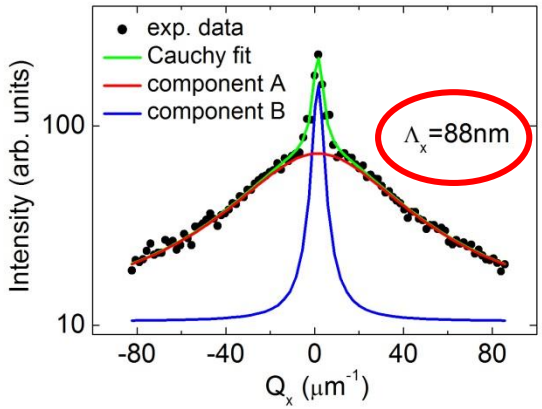

line scan along the Q_x-direction taken from the RSMs

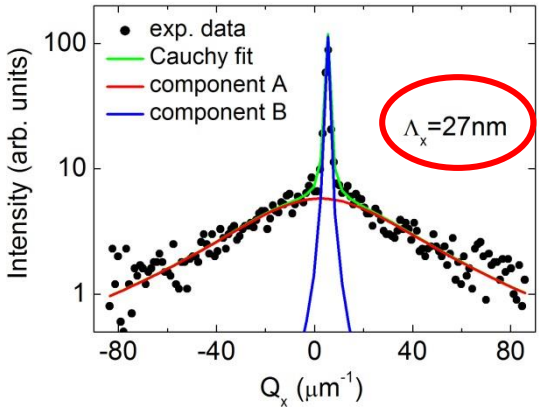

$D=\Lambda_{||}$

Q_x line profile
⇓
fwhm
⇓
NW diameter D

X-ray specular reflectivity (XSR)

Optical Theory of the X-Ray Reflectivity

Refraction index for X-ray radiation $n = 1 - \frac{r_0 \lambda^2}{2\pi} N_{at}(f_1 + i f_2) < 1$

Classical electron radius $r_0 = e^2/4\pi\varepsilon_0 m_e c^2$

Refraction index of the vacuum $n = 1$

Snell's law $n_A \cos\theta_r^A = n_B \cos\theta_r^B$

Snell's law (vacuum/material) $\cos\theta = n_M \cos\theta_M$

Critical angle $\cos\theta_c = n_M$

$$1 - \frac{\theta_c^2}{2} \approx n_M = 1 - \frac{r_0 \lambda^2}{2\pi} N_{at}(f_1 + i f_2) \Rightarrow \theta_c^2 \approx \frac{r_0 \lambda^2}{\pi} N_{at}(f_1 + i f_2)$$

Experimental Configuration for X-ray reflectivity measurements

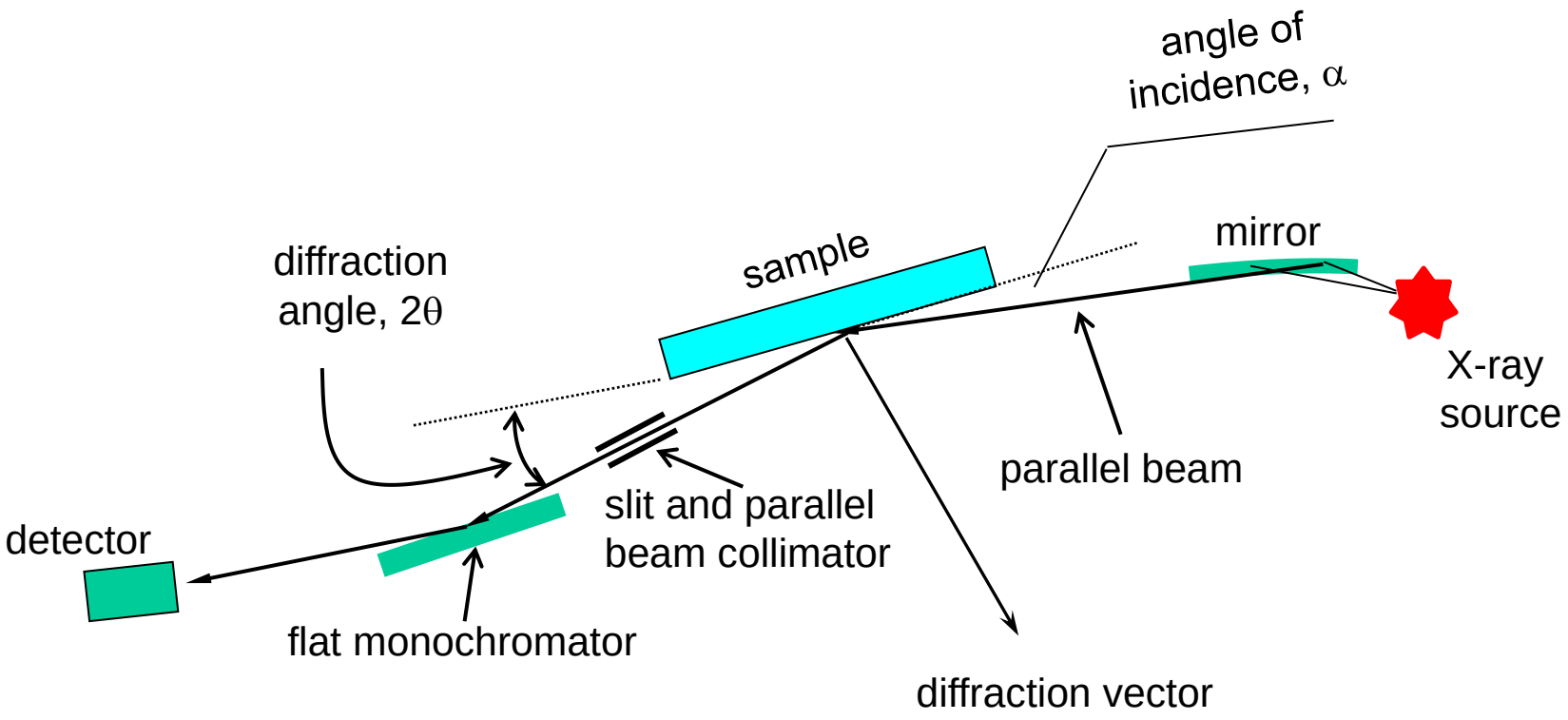

Refraction Index for X-ray Radiation

$$n = \frac{\cos\theta}{\cos\theta'} = \frac{\lambda}{\lambda'}$$

$$n\cos\theta' = \cos\theta$$

$$n < 1 \Rightarrow \cos\theta_c = n \quad \text{bei} \quad \theta' = 0$$

$$n = \cos\theta_c \approx 1 - \frac{\theta_c^2}{2}$$

$$\theta_c^2 \approx 2(1-n) = 2(\delta - i\beta)$$

$$n = 1 - \frac{r_e\lambda^2}{2\pi} N_e (f_0 + f' - if'')$$

vacuum: n = 1

$n \approx 1-\delta-i\cdot\beta < 1$

Gold (Au):

$\delta = 4.6409\times10^{-5}$

$\beta = -4.5823\times10^{-6}$

$n = 0.99995 - 4.58\times10^{-6}\, i$

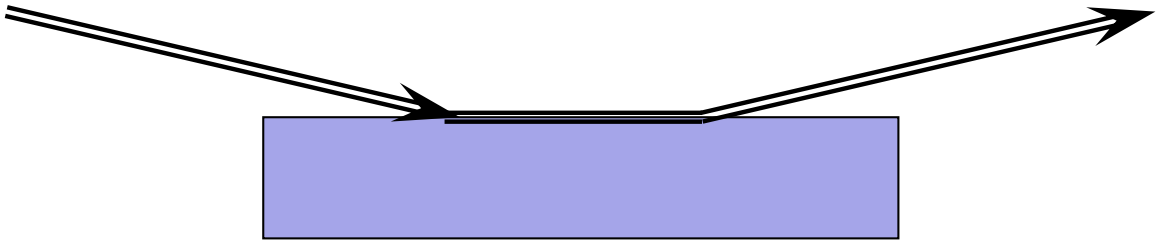

total external reflection (TER)

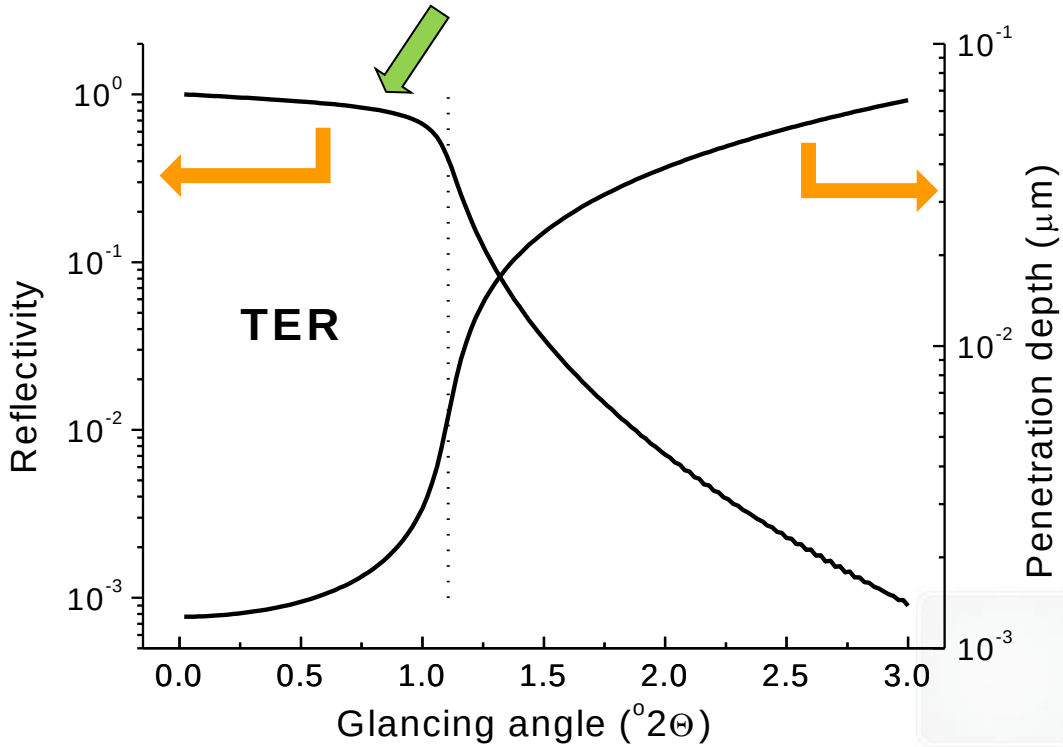

X-ray penetration depth at small incidence angle (optical reflection)

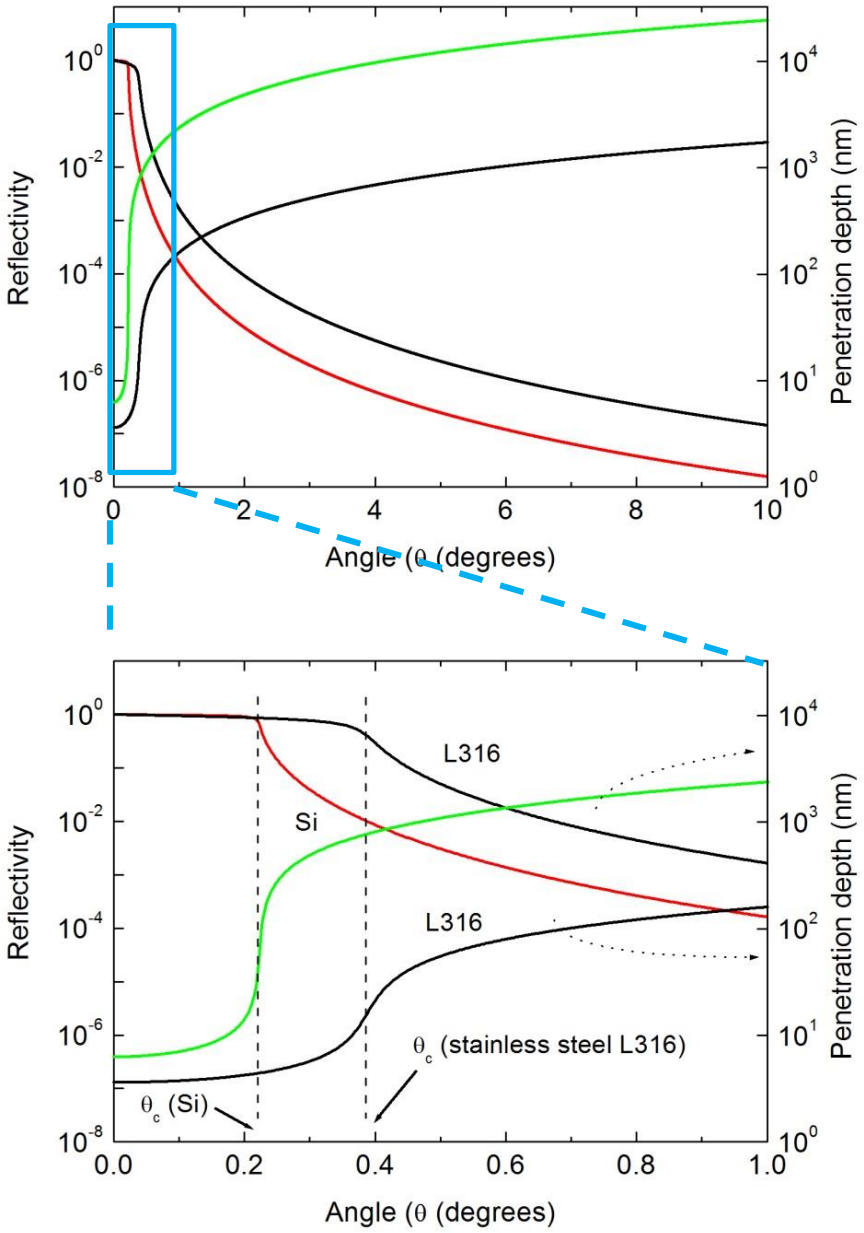

the critical angle θ_c depends (at the same X-ray wavelength) on the following materials parameters:

- mass density
- atomic mass
- electric susceptibility

silicon
$\Theta_c = 0.223°$

polycarbonate (PC)
$\Theta_c = 0.165°$

silicon dioxide (SiO_2)
$\Theta_c = 0.235°$

polystyrene (PS)
$\Theta_c = 0.147°$

stainless steel (L316)
$\Theta_c = 0.385°$

X-ray reflcetivity and penetration depth (thin polymer films on substrates)

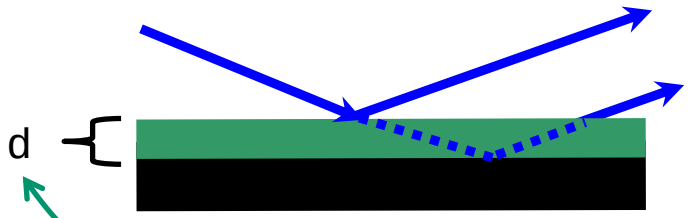

Polystyrene polymer layer on Si

film thickness d is related to the distance between interference fringes (Kiessig fringes)

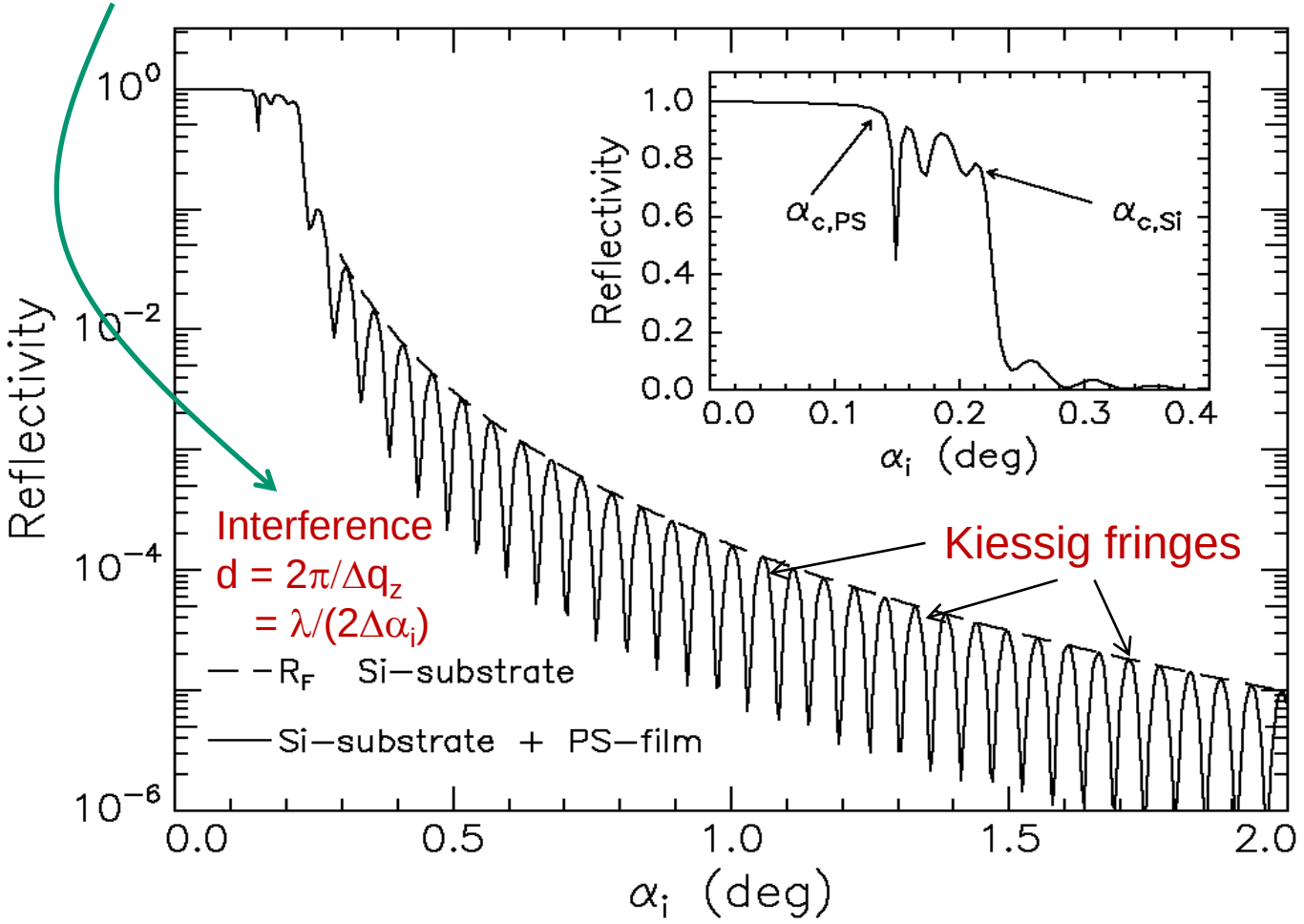

Roughness: surface and multiple interfaces

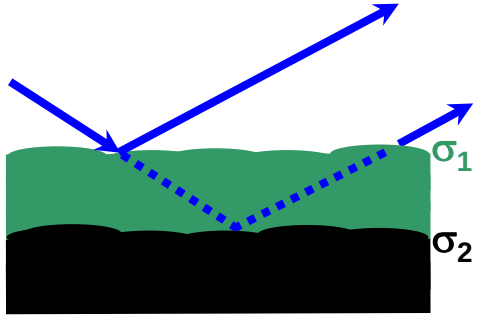

Interference:

$d = 2\pi/\Delta q_z = \lambda/(2\Delta\alpha_i)$

Damping:

roughness σ_1 , σ_2

surface , interfaces

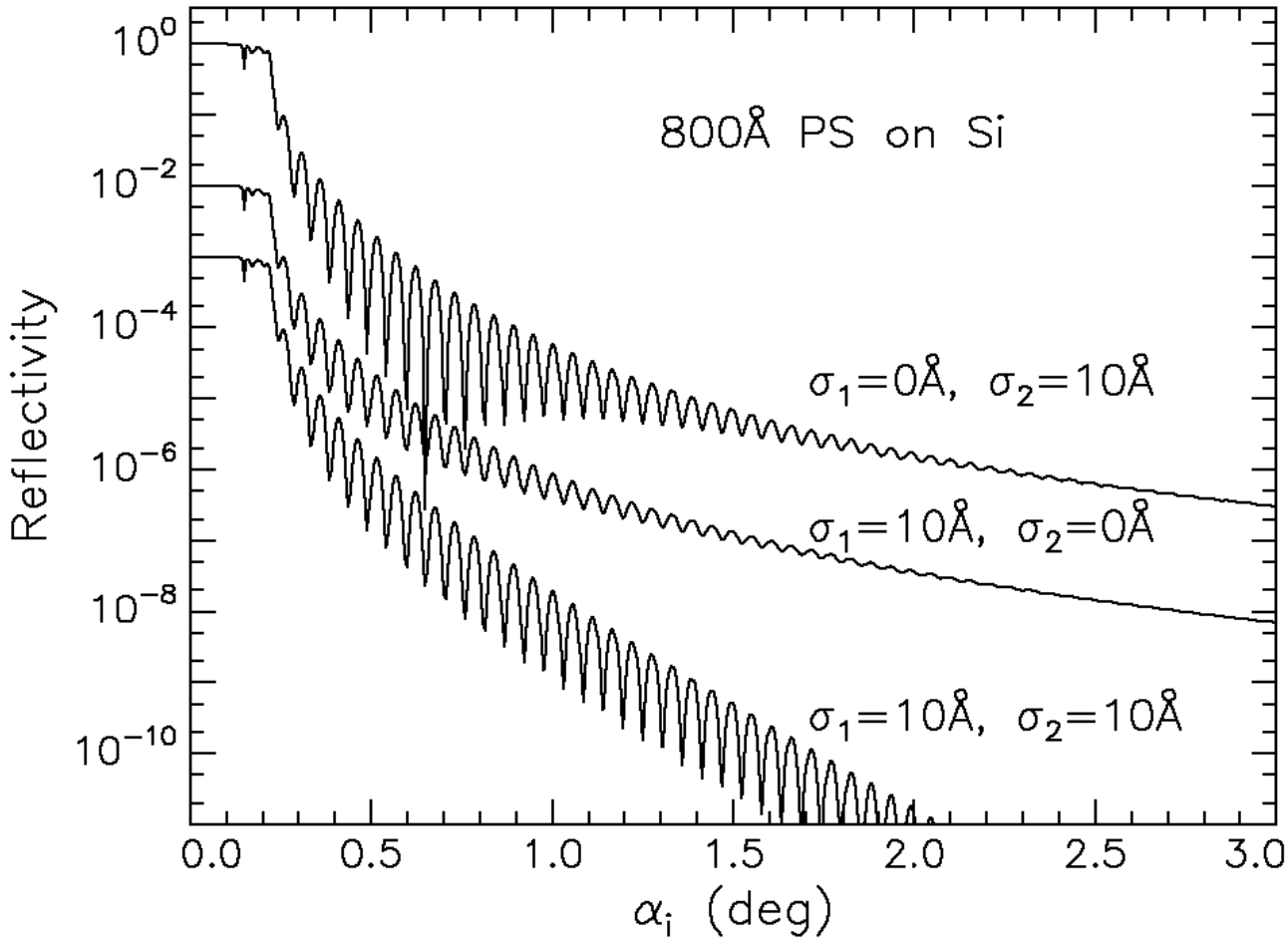

Scans in Reciprocal Space (q_x, q_z) - RSM close to the (000) rlp

The region below the solid line is inaccessible for in-plane scattering (beam or detector below the sample).

In-Plane Scattering Geometry and reciprocal space map measurements

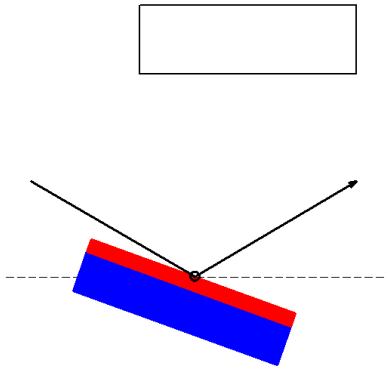

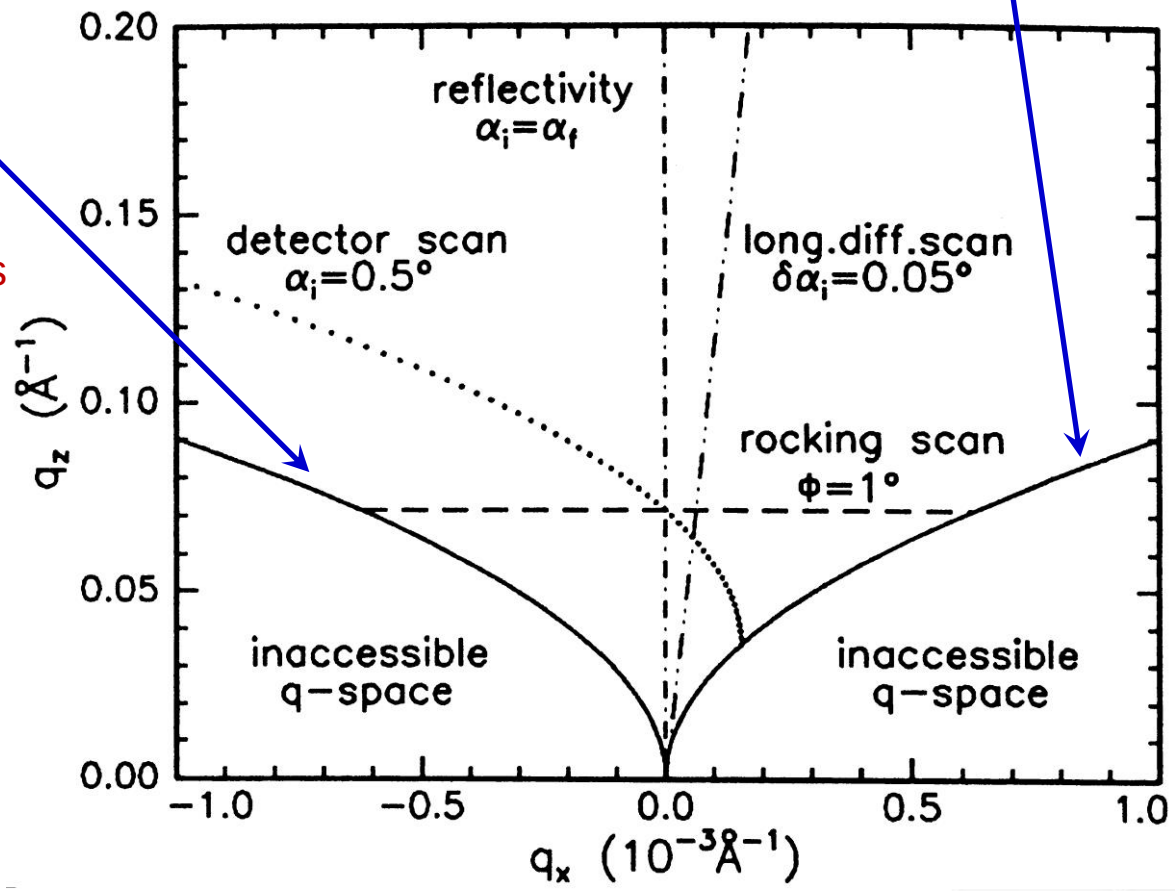

Dashed line: transverse scan (rocking scan).
Dashed-dotted line: specular reflectivity.
Inclined dashed-dotted line: longitudinal diffuse scan (reflectivity with offset $\delta\alpha_i$).
Dotted line: detector scan

Langmuir-Blodgett multilayer analyzed by X-ray reflectivity

chemical structure: long chain ammonium salt of 12-phosphomolybdate ($PMo_{12}O_{40}^{3-}$)

the LB unit cell is divided into 3 parts:

- upper and lower aliphatic chains of different thickness
- a lamella containing 2 clusters of $PMo_{12}O_{40}^{3-}$

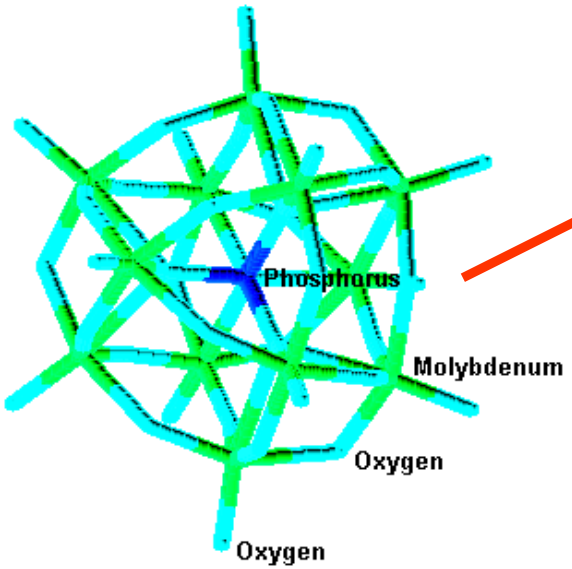

$PMo_{12}O_{40}^{3-}$

cluster size: 10-11 Å

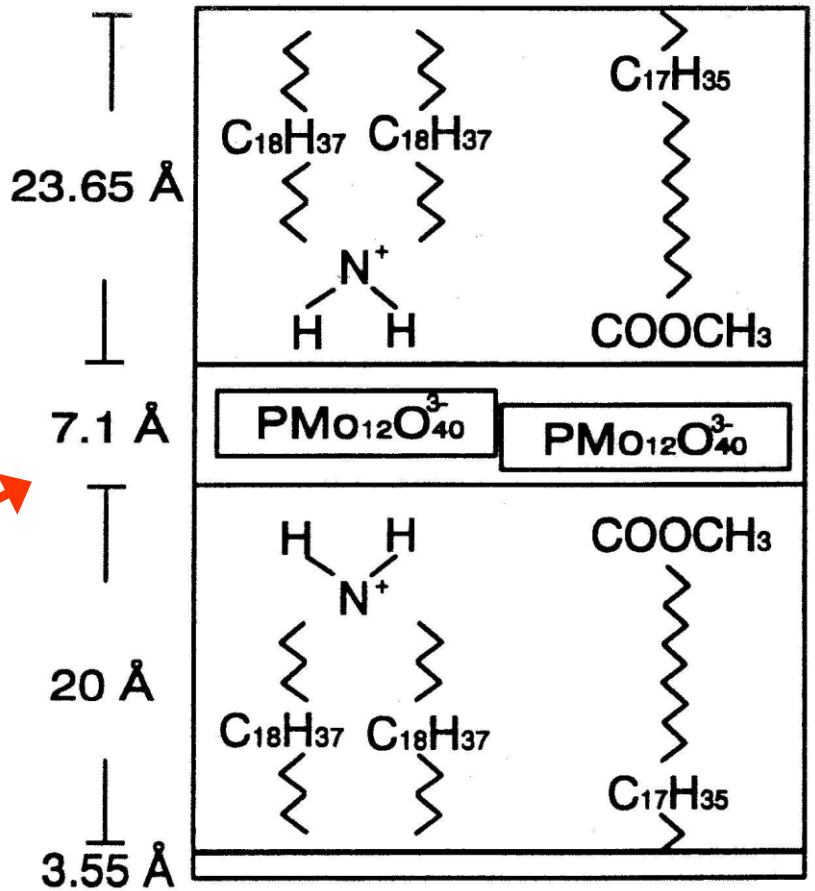

$PMo_{12}O_{40}^{3-}$ LB multilayers (21 monolayers)

long chain ammonium salt of
12-phosphomolybdate ($PMo_{12}O_{40}^{3+}$)

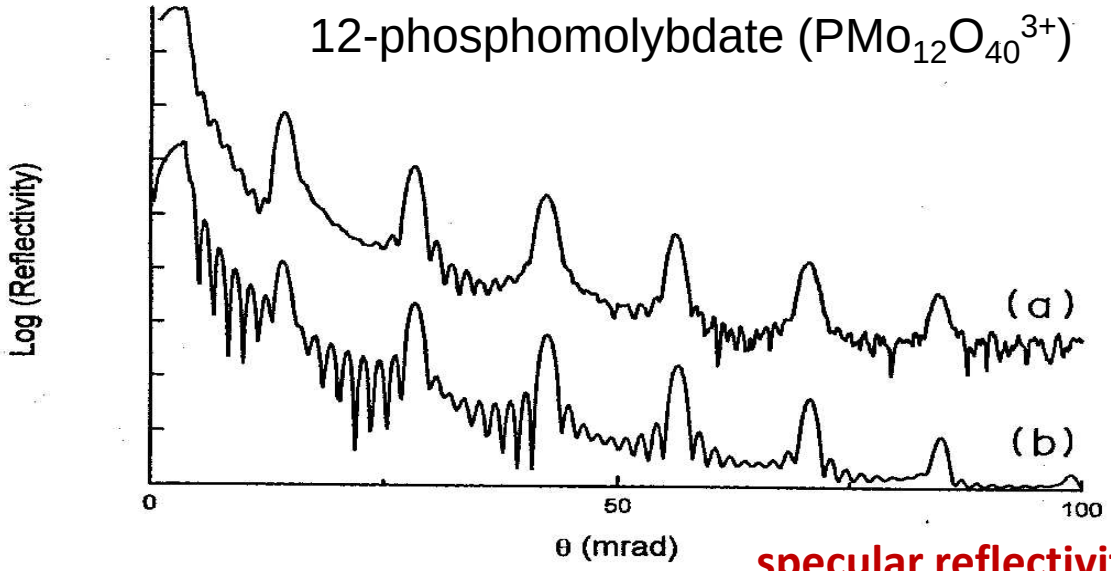

specular reflectivity

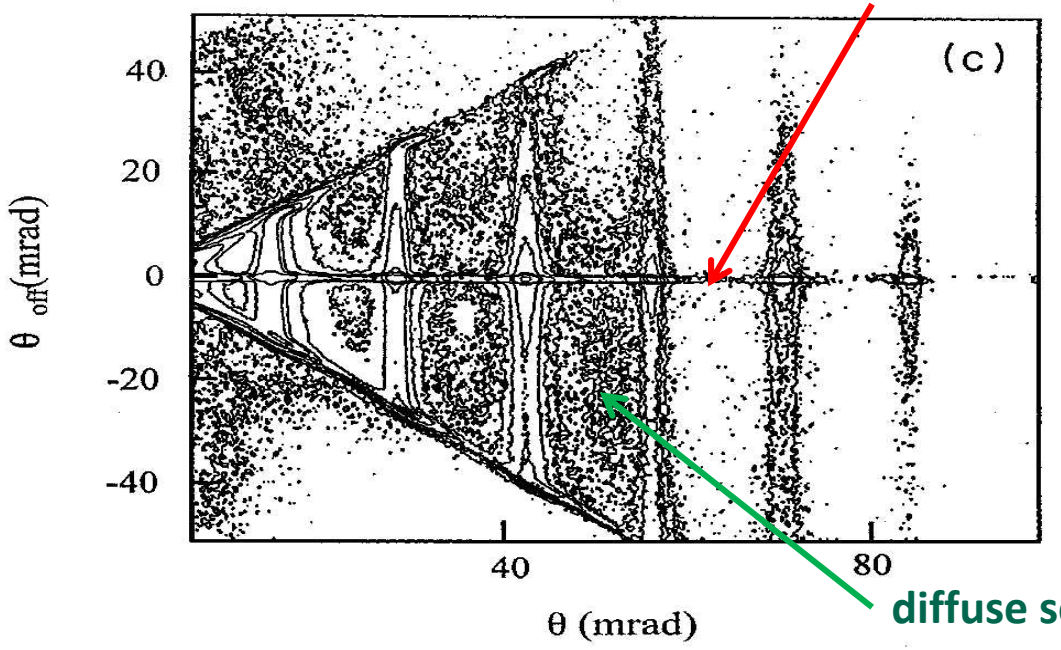

diffuse scattering

X-ray specular reflectivity

SL periodicity:
Λ=55±2nm
interface roughness:
σ=1.2Å

reciprocal space mapping (RSM) - diffuse scattering

interface roughness:
high correlation (bands)
LB structure:
uniform in thickness
good molecular packing
height fluctuation:
D=120±20Å

SAXS and WAXS

Small angle x-ray scattering (SAXS) – experimental configuration

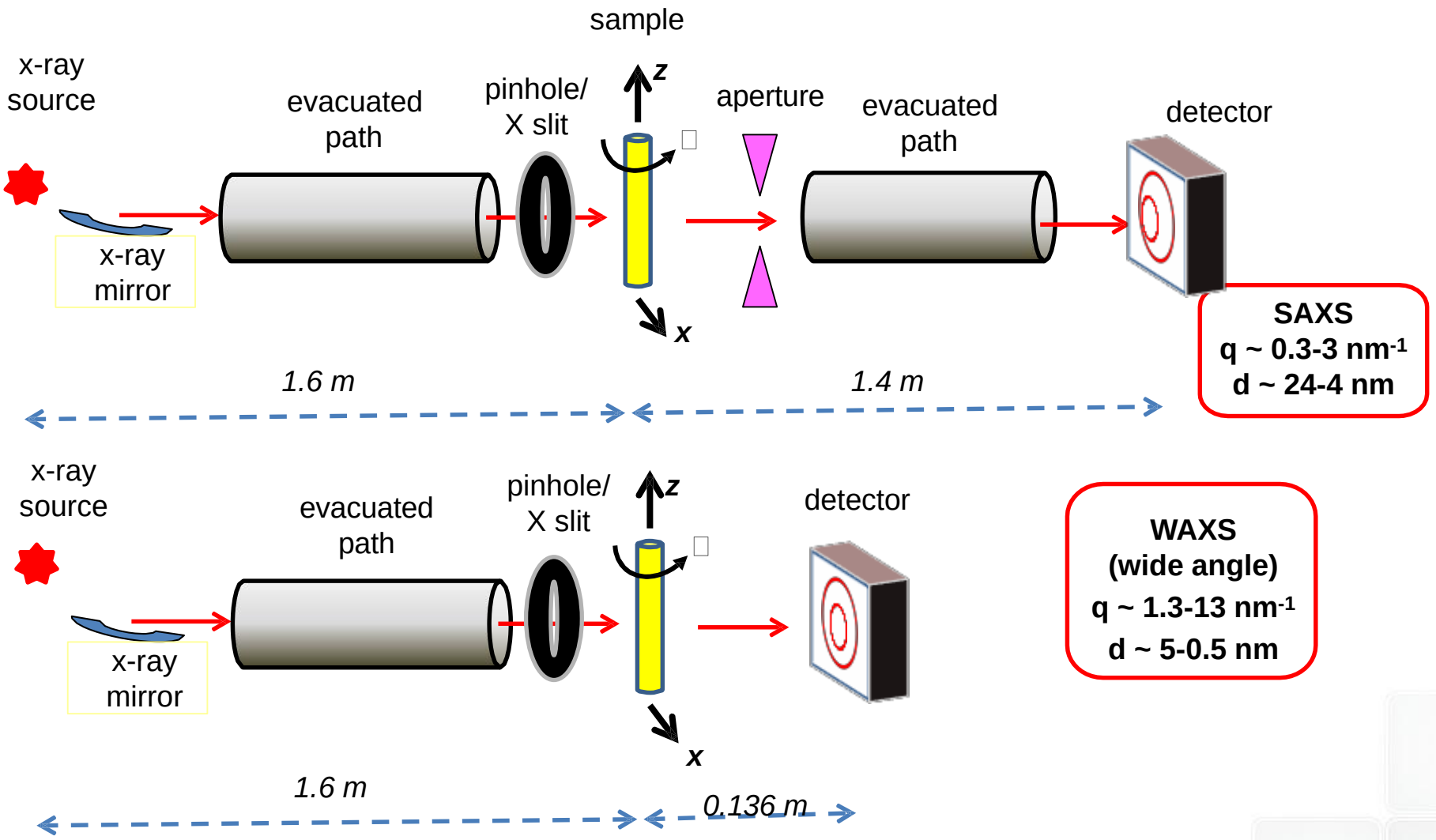

Intensity rings (Debye rings) of different intensity and broadening, depending on the structure of the sample are observed on a image plate / CCD camera.

⇒ for **amorphous materials**, such as for polymers, the Debye rings are rather large;
⇒ for **crystalline materials** the rings become narrower and intense.

SAXS applications

Materials:

- Nanoparticles
- Membranes
- Lipids
- Proteins
- Food and nutrients
- Pharmaceuticals
- Solutions
- Nanocomposites
- Polymers
- Thin films
- Bio materials
- …

Analysis:

Crystalline structure

Degree of crystallinity and orientation

Particle shape and structure

Particle size and distribution

Particle molecular weight

Surface roughness and correlation

Length scale of SAXS and WAXS

For elastic scattering: $\left|\vec{k}_i\right| = \left|\vec{k}_f\right| = k = \frac{2\pi}{\lambda}$, $\left|\vec{Q}\right| = 2k\sin\theta$

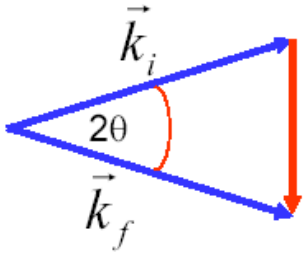

$\vec{Q} = \vec{k}_f - \vec{k}_i$

For small angles: $d = \frac{2\pi}{Q} = \frac{2\pi}{\frac{4\pi}{\lambda}\sin\theta} = \frac{\lambda}{2\sin\theta} \approx \frac{\lambda}{2\theta}$

Scattering experiments probe length scales $\lambda/2\theta$.

Example: λ = 1 nm, θ = 1° yields d = 1nm/2x0.0175 =28.6 nm

1) small angle scattering (SAXS) — Length scale ~ 0.1 – 100 nm

2) wide angle scattering (WAXS) — information about the structure, 3-dimensional structure, Length scale ~ Å

very small angles are required for the study of large objects!

Peculiarities of the method and the objects (samples) analyzed

Peculiarities for “small-angle”:

- Typically >10nm (from 0.1nm to several hundreds of nm)-
- Samples: nano-scale size features
- Models: ignore atoms
- Data: no sharp peaks; fitting curves
- Experimental setup: usually in transmission (2D detector), primary beam blocked

Independent objects

- Objects are in a uniform, featureless matrix (e.g. solvent) which is ignored.
- Assume dilute enough so scattering independently
- Assume randomly oriented in all directions

“Objects” may be:

  - Globular proteins or clusters
  - Micelles
  - Random polymer chains in melt/solution
  - Inorganic nanoparticles (colloids)
  - nanopores

Typical 2D SAXS pattern

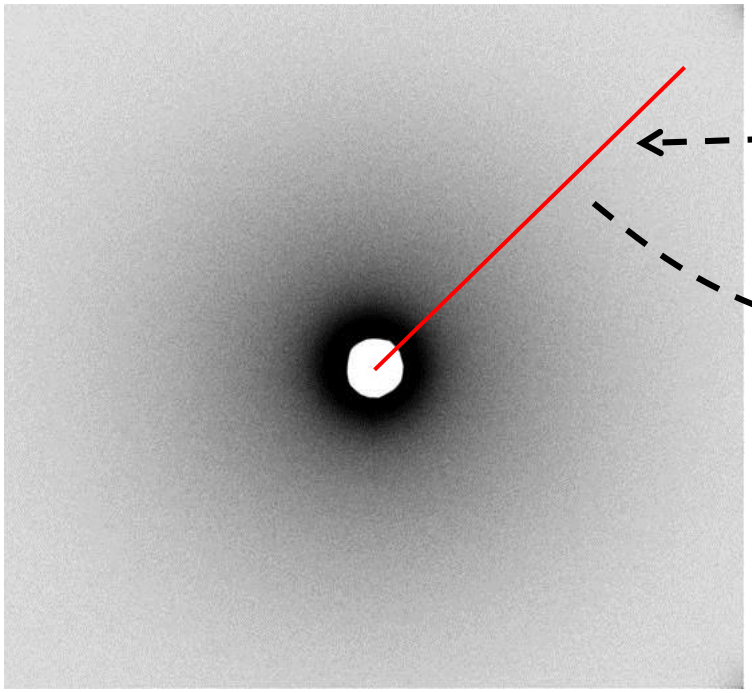

Radial intensity distribution at small angle scattering

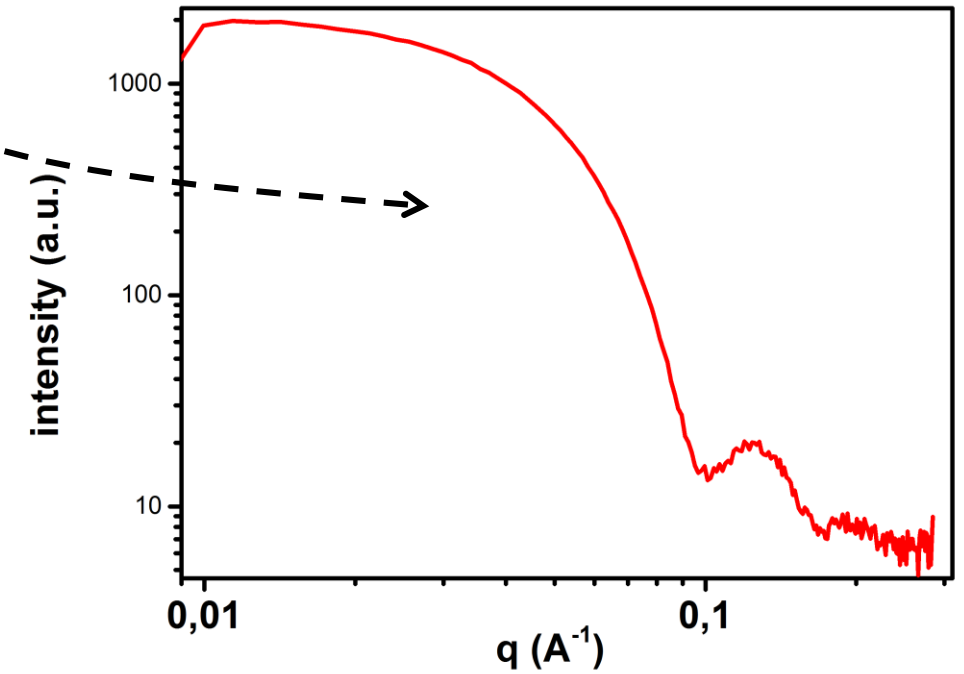

radial profile (..because isotropic)…

Title

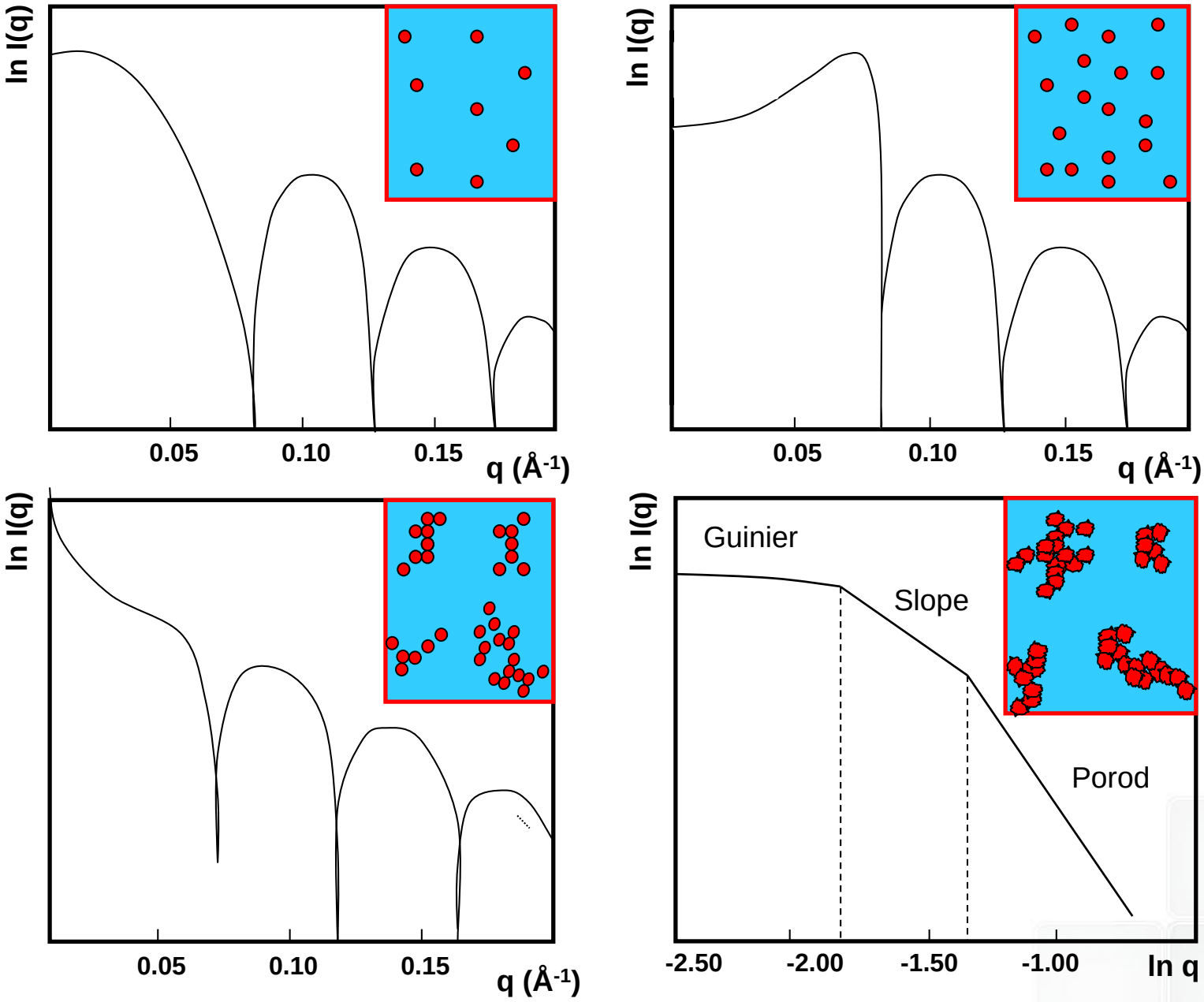
ln I(q)
0.05
0.10
0.15
q (Å-1)
ln I(q)
0.05
0.10
0.15
q (Å-1)
ln I(q)
0.05
0.10
0.15
q (Å-1)
ln I(q)
Guinier
Slope
Porod
-2.50
-2.00
-1.50
-1.00
ln q

SAXS – regions

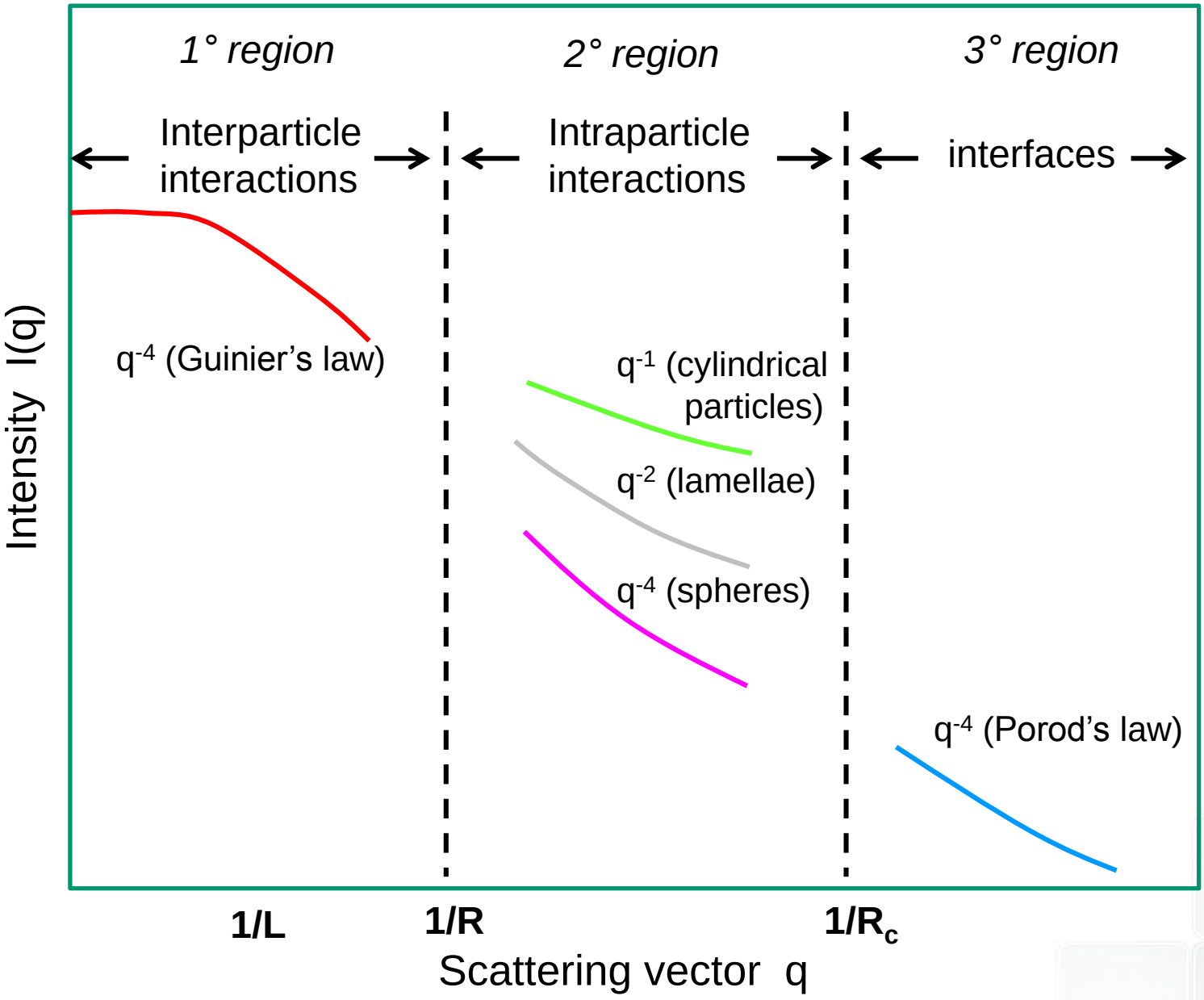

Guinier and Porod limits for mono-dispersed spheres

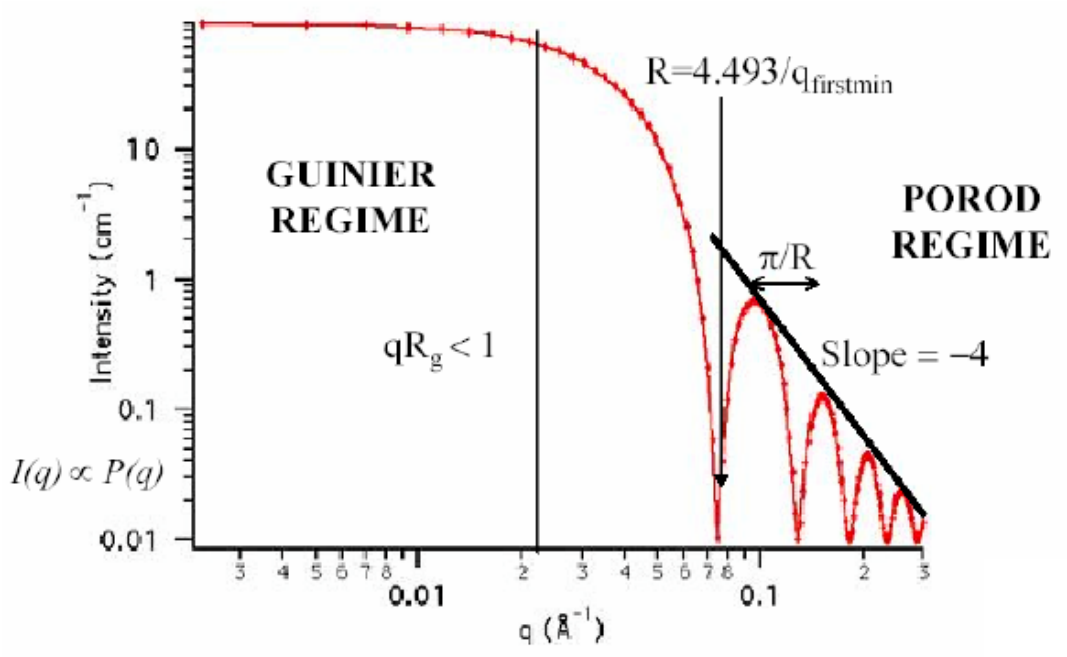

for the Porod limit:
the scattered intensity is proportional to the surface area per unit volume.

slope = - 4 is valid for a sharp interface

the Porod limit is independent on the geometry of the scattering particles and will not give any structural information.

for isolated particles (no interaction between particles) the scattered intensity depends by the radius of gyration R_G and is described by Guinier's law (valid for small scattering vectors, $qR_G<1$)

the intensity is independent from the shape of the particles

If the shape of particles is known, their size can be determined from the radius of gyration

Example:
precursor molecules dispersed in polymers & nanoparticle formation

Precursors dispersed in polymer

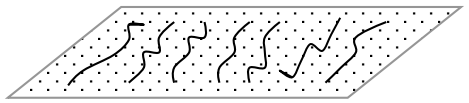

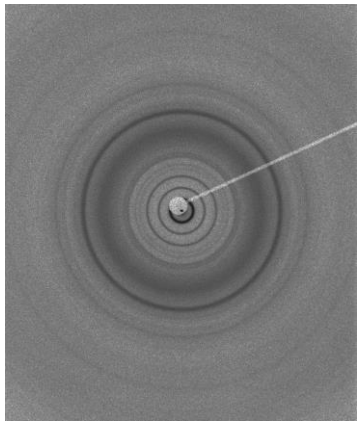

Nanoparticles of CdS dispersed in polymer

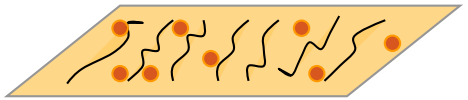

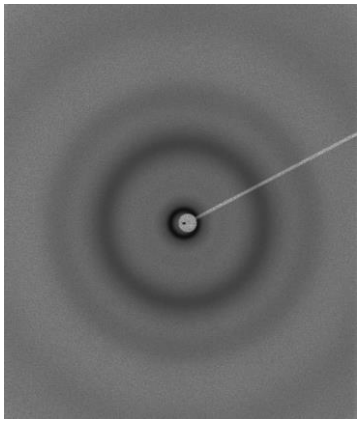

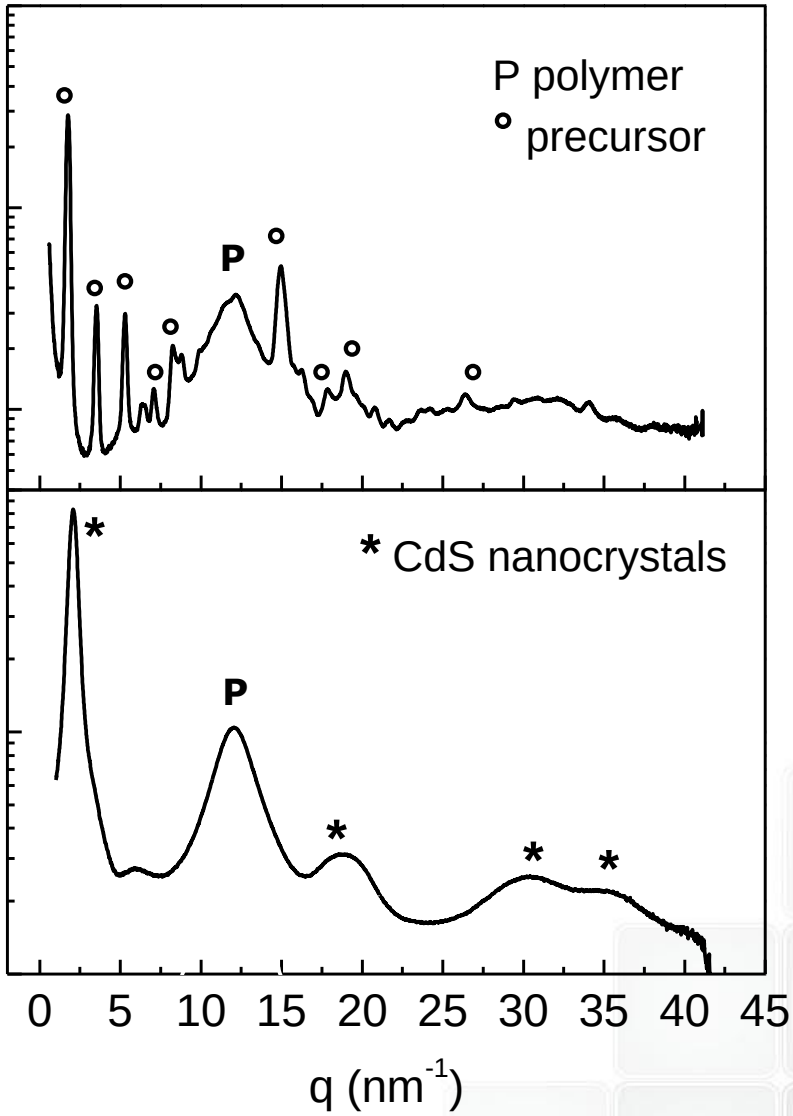

Example:
precursor molecules dispersed in polymers & nanoparticle formation

SAXS

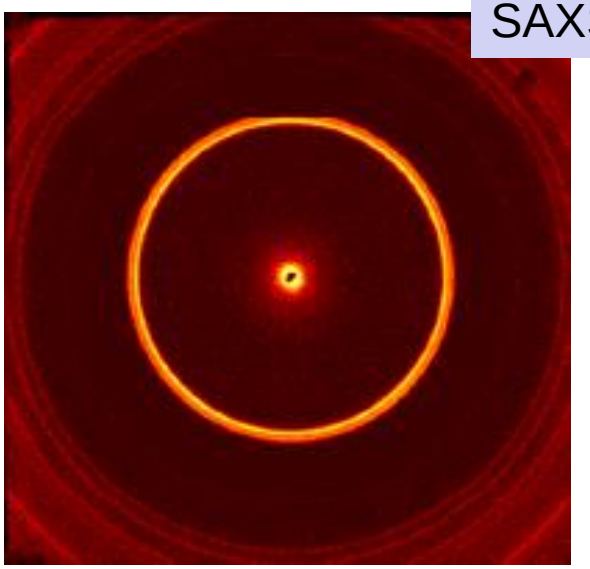

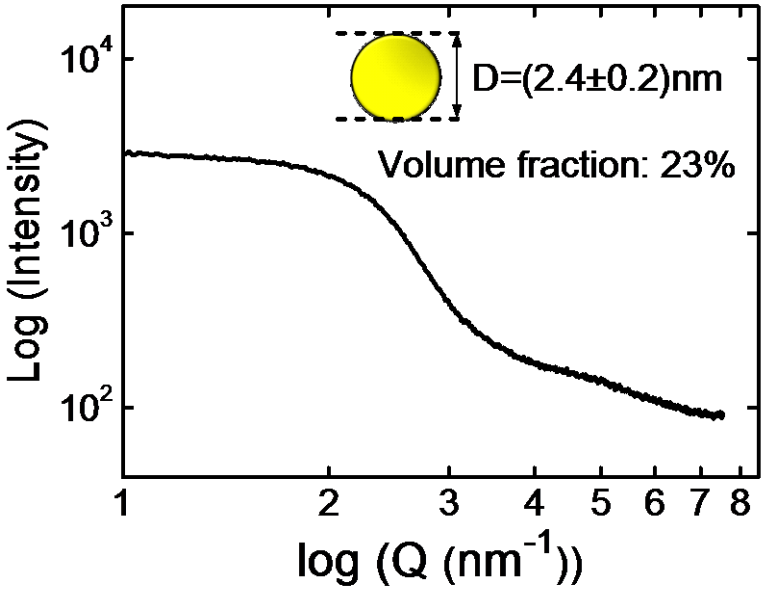

WAXS

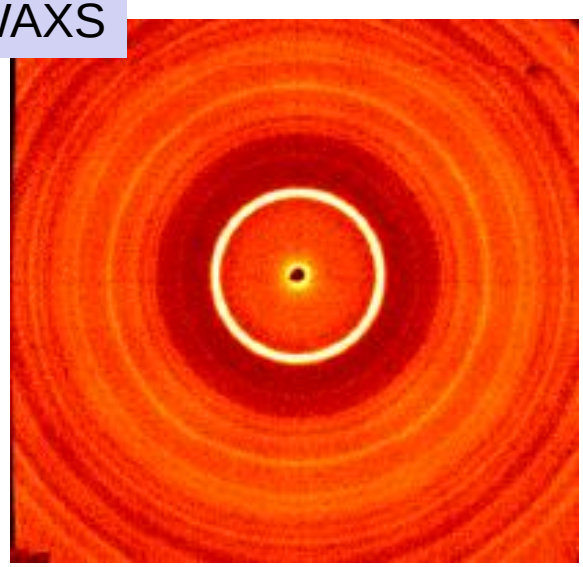

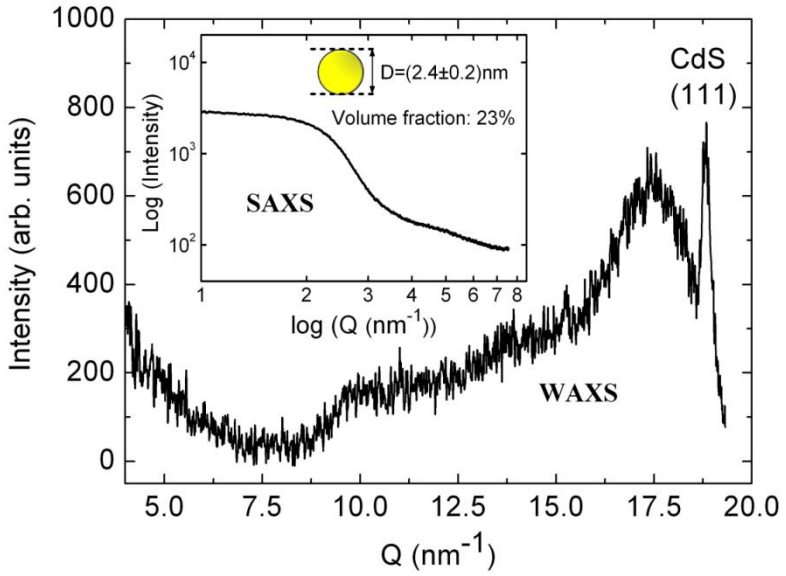

Distribution of chemical precursors (molecules or molecular chains) in polymers

Chemical structure of the precursors

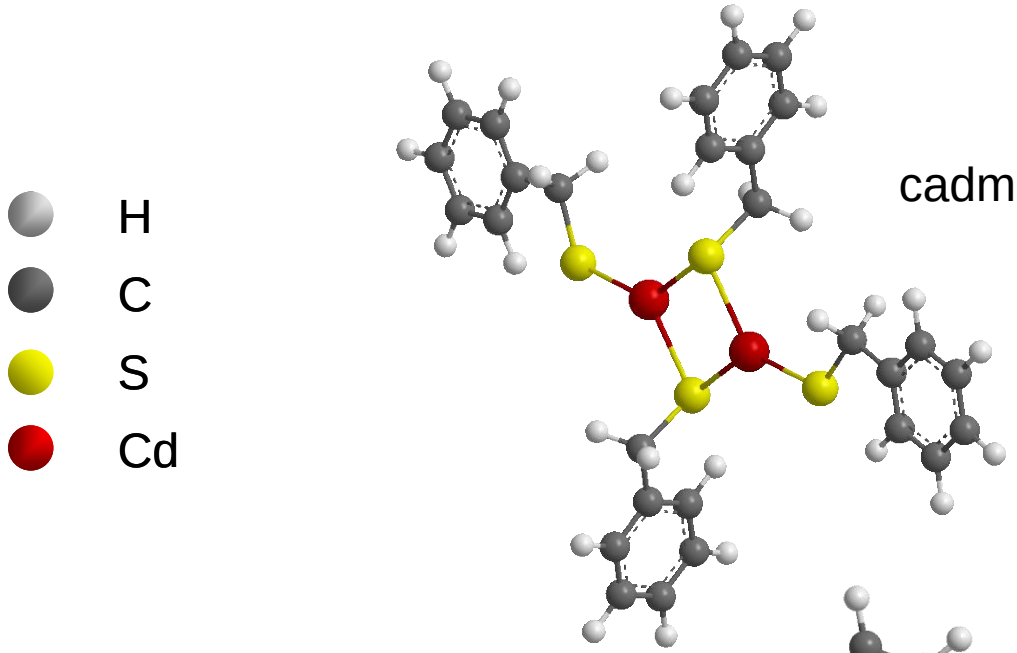

cadmium-*bis*(benzylthiolates), $Cd(SBz)_2$

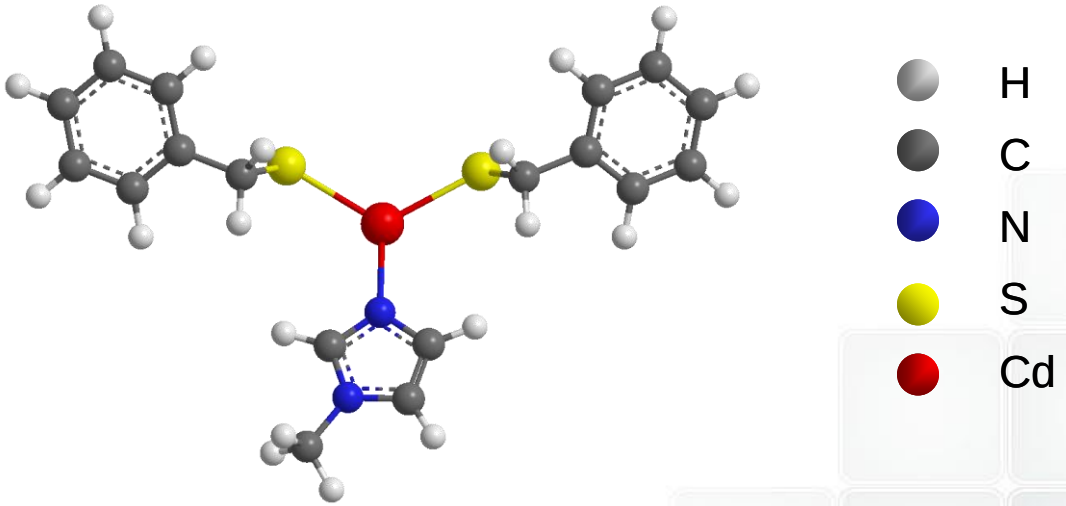

methyl imidazole (MI) added $Cd(SBz)_2$, $[Cd(SBz)_2]_2 \cdot MI$

WAXS - Arrangement of the precursors molecules in PMMA

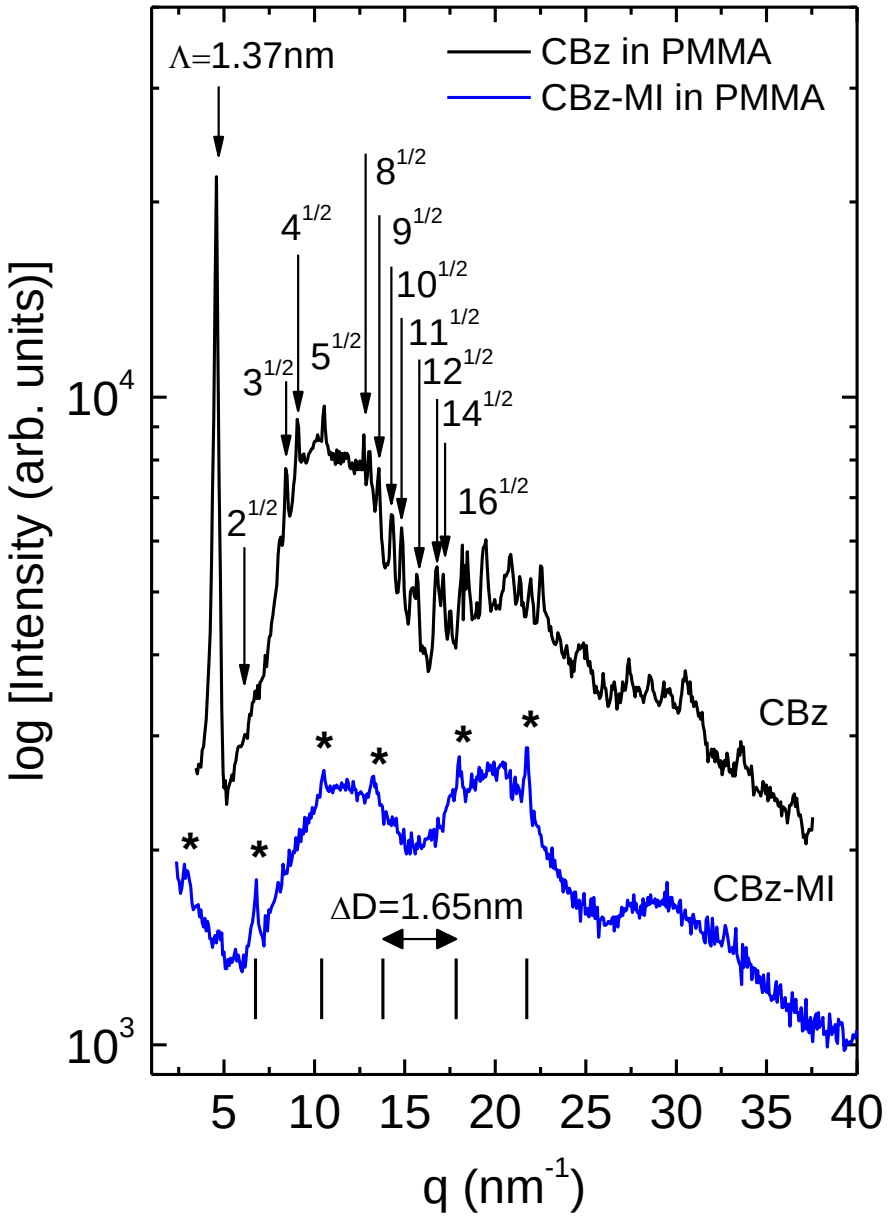

WAXS patterns of PMMA bulk like samples added with $Cd(SBz)_2$ (upper curve) and $[Cd(SBz)_2]_2 \cdot MI$ (lower curve) precursors, respectively, before the annealing processes.

The amorphous PMMA peak is located at $q=11\ nm^{-1}$.

The sharper Bragg-like peaks are due to the periodic and regular ordering of the precursor molecules within the PMMA polymer matrix.

For the CBz sample, the q-positions and the indexing of the Bragg peaks allows us to identify the Bravais lattice as a primitive cubic lattice, being the first and most intense Bragg peak, located at $q=4.56\ nm^{-1}$, the (100) peak that yields a lattice constant $\Lambda=1.37nm$.

The pattern of the CBz-MI sample shows equidistant Bragg peaks indicating a superlattice order of periodicity $\Delta D=1.65nm$

Arrangement of the $[Cd(SBz)_2]_2 \cdot MI$ precursor in PMMA

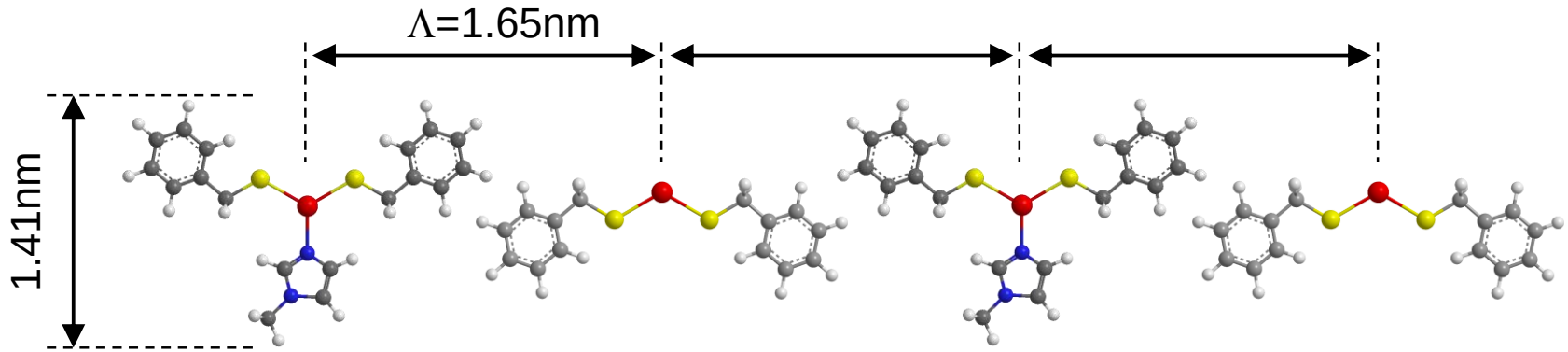

Superlattice (SL) ordering of the $[Cd(SBz)_2]_2 \cdot MI$ precursor in PMMA polymer before the annealing process. Two superlattice configurations are possible having all a SL period length Λ=1.65nm

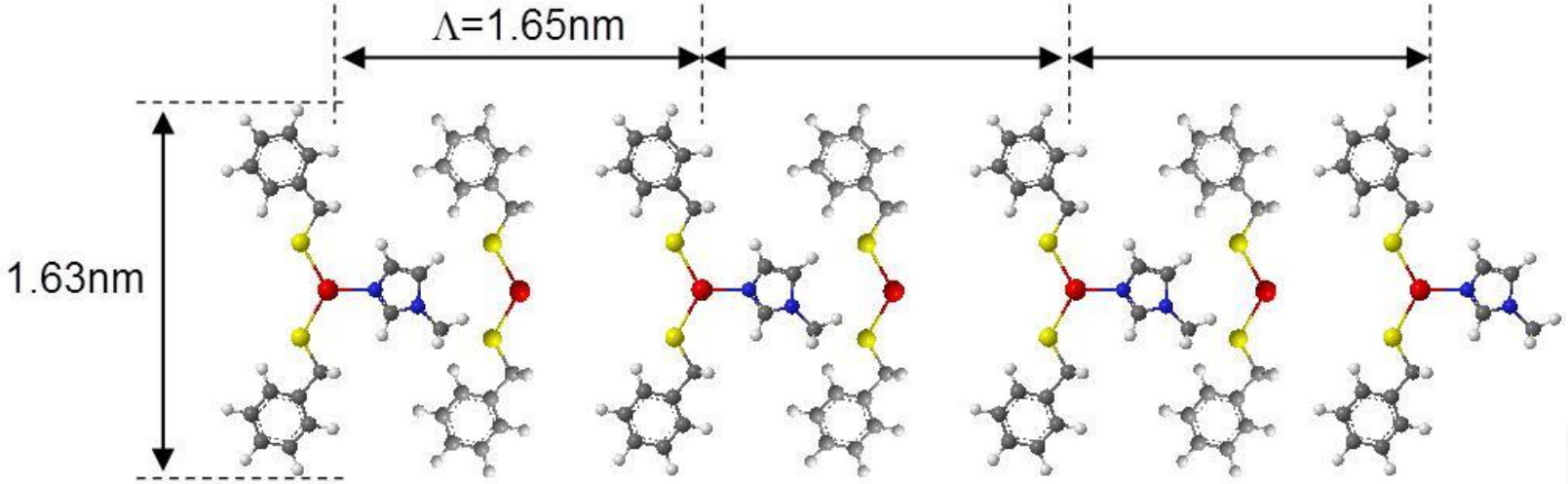

Here, a regular order of the $Cd(SBz)_2 \cdot MI$ and $Cd(SBz)_2$ molecules is assumed in accordance with the measured stoichiometric values. This hypothesis allows to consider and to interpret the measured superlattice period length.

Arrangement of the $[Cd(SBz)_2]_2$ precursor in PMMA

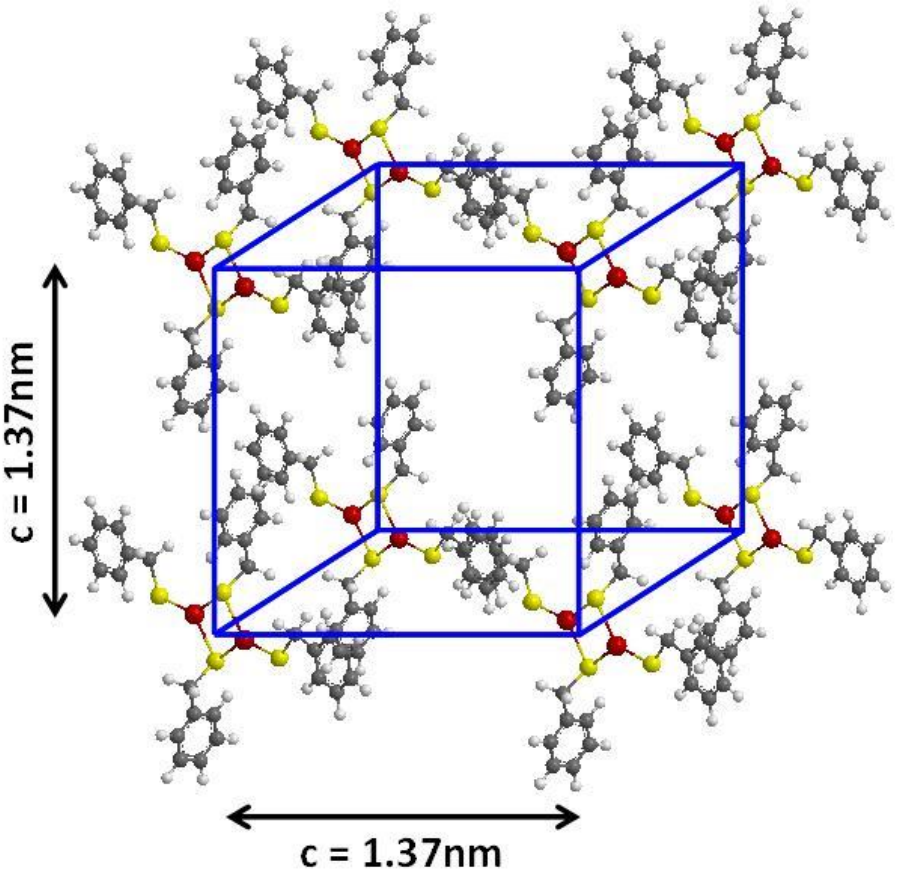

Spatial ordering of the $Cd(SBz)_2$ precursor molecules within the PMMA matrix before the annealing process, in accordance with the WAXS results.

The unit cell, i.e. the primitive cubic lattice, of lattice parameter 1.37nm is highlighted. The molecules are placed on the edges of the cubic lattice

Nucleation and growth process - precursor decomposition and nanocrystal formation

I

homogeneous distribution of precursor molecules in polymer matrix

II

diffusion of neighbor molecules and nucleation

III

initial growth process and nanocrystal formation

IV

nanocrystal growth and saturation

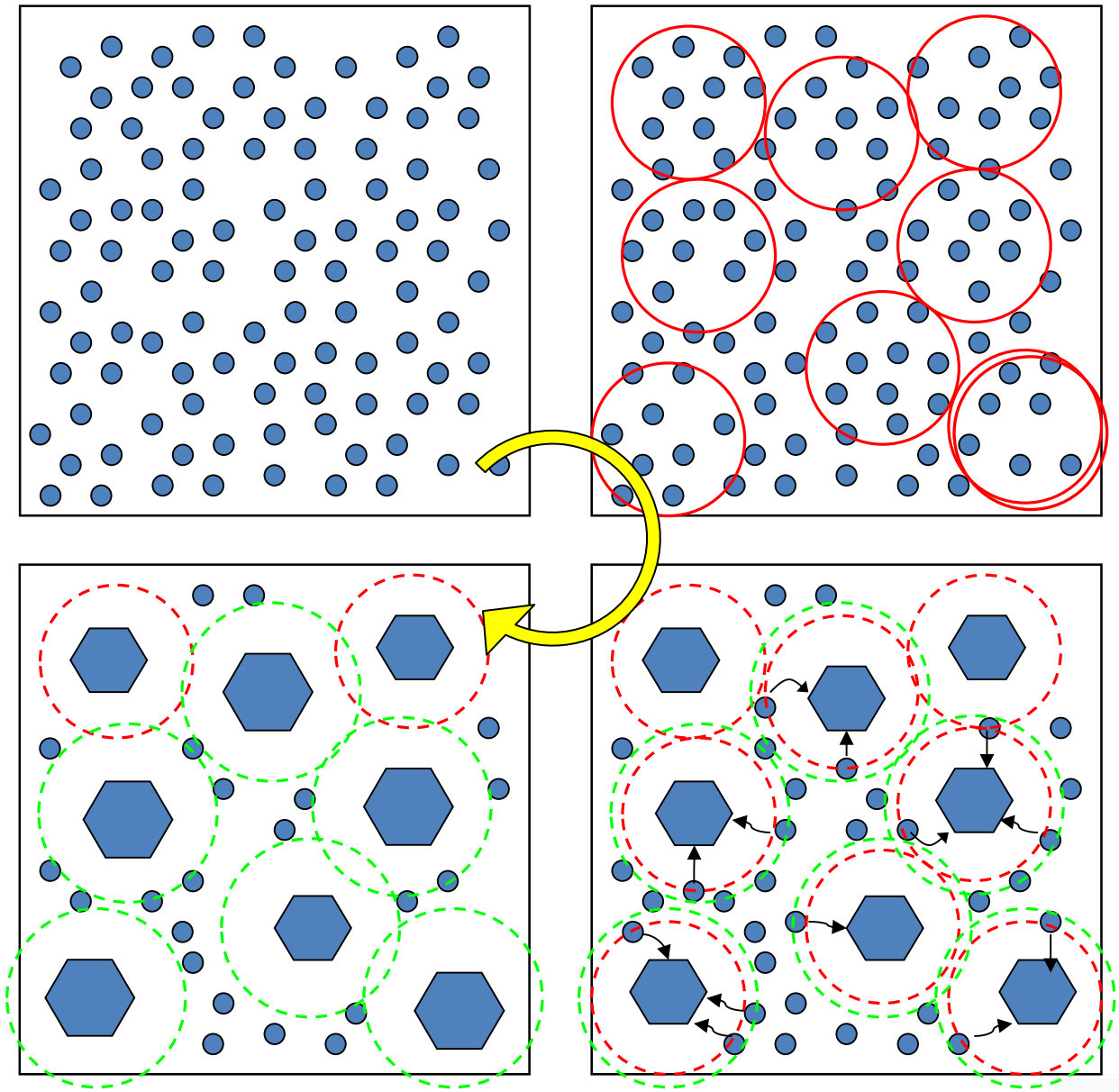

Comparison of X-ray techniques with other characterization tools ……and peculiarities

Comparison with other techniques

	X-ray analysis methods	Other techniques
Sample preparation and vacuum compatibility	❖ No vacuum compatibility required (except XRF, XSW on vacuum). ❖ "Any" sample size (depends on the goniometer size/weight capability). ❖ Rough surfaces acceptable (parallel beam configuration). ❖ No sample preparation required (preparation recommended for the detection of unknown phases or elements in XRD/XRF).	❖ Surface analysis and electron microscopy techniques will require vacuum compatibility and in many cases sample preparation. ❖ Optical spectroscopy techniques will do analysis on air.
Composition and impurity determination and quantification	❖ ~ 0.1 w % (XRF > ppm); may require standards ❖ XRD: also phase information and % of crystallinity. ❖ Data averaged over large lateral area.	❖ XPS: > 0.01 – 0.1 at % (may require depth profiling). ❖ SIMS: > 1 ppm (requires sputtering depth profiling). ❖ EDS: > 0.1 – 1 w % over small volume 1μm^3. ❖ Little with phase information; averages over small lateral areas (< 100 μm).
Lattice constants	❖ Better than within 10^{-5}	❖ TEM: estimates ~ 10^{-3} / ~ 10^{-4}
Thickness in thin films	❖ HRXRD or XRR: direct measurement (no modeling for single or bi-layers) ❖ requires flat surfaces	❖ RBS: > 10 nm (requires modeling). ❖ Ellipsometry: requires modeling. ❖ TEM: requires visual contrast between layers.
Grain size	❖ Measures Crystallite Size. ❖ Typically ~ 1-2 nm – microns, requires size/strain assumptions/ modeling. ❖ "Volume average" size	❖ SEM: grain size distribution averaged over small area. ❖ TEM/SEM: "number average" size.

Comparison with other techniques

	X-ray analysis methods	Other techniques
Texture	❖ Type and distribution averaged over large sample volume.	❖ EBSD: within grain sizes dimensions, better sensitivity at the surface.
Residual Stress	❖ 10MPA, averaged over large sample volume (large number of grains) ❖ Needs crystallinity. ❖ Measures strain and obtains stress from Hooke's law. ❖ Averages macro and micro stresses over large area of a layer.	❖ Wafer curvature: No need for crystallinity. Direct measurement of stress, but only interlayer stress between film and substrate (macrostress).
Depth dependent information	❖ Phase, grain sizes, texture and stress "depth profiling" – requires x-ray information depth modeling	❖ Surface analysis depth profiling: compositional depth profiles.
Surface or Interface roughness	❖ XRR: interface roughness 0.01 – 5 nm, including buried interfaces	❖ SPM: top surface only; rsm~ 0.01-100 nm.
Defects	❖ Misfit dislocations (HR-XRD). ❖ Point defects (diffuse scattering with model). ❖ Extended defects (powder XRD with model). ❖ Average over larger sample area (> mm).	❖ TEM: accurate identification of defects and their densities; average over small sample area. Sample preparation may introduce artifacts.

adapted from M. Sardela

Title